



South Eastern Australian Climate Initiative

South-Eastern Australia Climate Initiative

June 2007 End of Project Reports



Prepared for

South-Eastern Australian Climate Initiative Steering Committee

Prepared by

CSIRO Bureau of Meteorology

Editorial team

Mr Craig Macaulay, Mr Paul Holper, Dr Bryson Bates, Dr Francis Chiew, Dr Ian Smith, Ms Mandy Hopkins, CSIRO; Dr Harry Hendon, Dr Bertrand Timbal, Bureau of Meteorology

© Copyright Commonwealth Scientific and Industrial Research Organisation ('CSIRO') Australia 2007

November 2007

Important Notice

All rights are reserved and no part of this publication covered by copyright may be reproduced or copied in any form or by any means except with the written permission of CSIRO.

The results and analyses contained in this Report are based on a number of technical, circumstantial or otherwise specified assumptions and parameters. The user must make its own assessment of the suitability for its use of the information or material contained in or generated from the Report. To the extent permitted by law, CSIRO excludes all liability to any party for expenses, losses, damages and costs arising directly or indirectly from using this Report.

Use of this Report

The use of this Report is subject to the terms on which it was prepared by CSIRO. In particular, the Report may only be used for the following purposes –

- this Report may be copied for distribution within the Client's organisation;
- the information in this Report may be used by the entity for which it was prepared ("the Client"), or by the Client's contractors and agents, for the Client's internal business operations (but not licensing to third parties);
- extracts of the Report distributed for these purposes must clearly note that the extract is part of a larger Report prepared by CSIRO for the Client. The Report must not be used as a means of endorsement without the prior written consent of CSIRO. The name, trade mark or logo of CSIRO must not be used without the prior written consent of CSIRO.

Address and contact details:

CSIRO Marine and Atmospheric Research
Private Bag 1, Aspendale, Victoria 3195 Australia
Ph (+61 3) 9239 4400; Fax (+61 3) 9239 4444
e-mail: enquiries@csiro.au

Table of contents

Compare documented climate changes with those attributable to specific causes	4
Calibration of statistical downscaling models	23
Reanalysis archive intercomparison.....	36
Develop improved regional projection techniques for MDB and the CMA regions of Victoria using multi-model weighted approach.	46
Simulation and potential predictability of SE Australia rainfall and temperature from the national dynamical seasonal prediction model.....	70
Review of techniques to bridge/calibrate dynamical seasonal predictions with focus on south eastern Australia.....	82
SEACI publications.....	90



South Eastern Australian **Climate initiative**

Final report for **Project 1.1.2**

**Compare documented climate changes with those
attributable to specific causes**

Principal Investigator: **Dr. Bertrand Timbal**,

Centre for Australian Weather and Climate Research (CAWCR),

Bureau of Meteorology

b.timbal@bom.gov.au,

Tel: 03-9669-4697, Fax: 03-9669-4660,

GPO Box 1289, Melbourne 3001

Co-Authors:

Drs. Bradley Murphy and Karl Braganza

(National Climate Centre, BoM)

Drs. Harry Hendon and Matt Wheeler

(Centre for Australian Weather and Climate Research, BoM)

Mr. Clinton Rakich

(NSW Regional Office, BoM)

Completed: 18 November 2007

Project Abstract - Executive summary

Initial Project objectives

- Compare recent observed climate changes to variability associated with modes of climate features using up to date knowledge on the role of key large-scale modes of variability gathered as part of project 1.1.1
- Attribute the recent changes to possible external forcing with a focus on cold season rainfall decline in the south and warm season rainfall decline in the north and increased heat waves.

Proposed methodology

- Benefit from the review of the existing scientific literature on the climate of south-east Australia and the analysis of the importance of various large-scale modes of variability to focus on the most likely contributor to observed rainfall decline.
- Compare recent observed climate change to variability associated with the Southern Annular Mode (SAM) and evaluate the likelihood that the SAM has contributed to the observed rainfall decline directly or through the influence on local MSLP.
- Investigate the causes of the changes of MSLP surrounding southern Australia and its role in relation to the rainfall decline in south-east Australia.
- Investigate the role of MSLP changes in explaining recent heat wave using as a case study the April 2005 Murray-Darling Basin wide heat wave.

Summary of the findings

- The autumn rainfall decline (60% of the total rainfall decline) in south-east Australia (SEA) is a combination of autumn to early winter in the south and summer to autumn in the north. In the south, the decline started in the early 1990s but is only apparent since 2000 in the north. The two areas can be broadly separated by the location of the Sub-Tropical Ridge (STR).
- In the south-western part of eastern Australia (SWEA), the Southern Annular Mode (SAM) has a negative impact on rainfall during a six month period from May to October, which is when most of the total rainfall is encountered. In autumn as a whole, the SAM influence on rainfall in SEA cancels out and is negligible overall. The modes of variability generated in tropical oceans (ENSO and IOD) are also unlikely to have contributed to the rainfall decline as if anything, their influence on the local rainfall is rather small and diminishing during the last the two decades.
- The SAM index has been trending upward. There is a positive trend in the 1980s and 1990s across summer and autumn but it does not translate into a rainfall decline. Arguably, the trend extends to early winter (May to July) when the series is extended back in time to the 1960s and 1970s; this trend could have resulted in a rainfall decline of about 5% in those decades, but did not.
- The SAM rainfall relationship is mostly felt through the local MSLP. The main control of MSLP over southern Australia is the intensity and location of the STR. The intensity of the STR has been trending upward since the 1970s and that can be translated into a sizeable rainfall decline (about 70% of the observed decline in autumn to early winter: from March to July, which in itself represents 71% of the total decline) using the correlation between the STR intensity and rainfall in SEA.
- The intensity of the STR also peaked in the 1940s at the time of the previous dry decade in the south-east. By and large during the 20th century, the long-term evolution of the intensity of the STR follows the curve of the global temperature of the planet.

This relationship gives a high likelihood that the current rainfall deficit is linked to the global warming of the planet, through the intensification of the STR.

- On the northern side of the STR, the rainfall relates well to a north-south MSLP gradient along the east coast (the Gayndah-Deniliquin Index or GDI). This index suggests a combination of long-term trends and decadal variability as the most likely explanation for the current rainfall deficit.
- Weather patterns do not explain the heat wave observed in April 2005, while the long term lower tropospheric warming trend appears as an important contribution. However, it does not appear to be the only explanation.

Technical details

Flow-on effects from project 1.1.1

The specifics of the rainfall decline across the south-east of Australia in the last 10 years were described in Murphy and Timbal (2007) as part of the Project 1.1.1. Key results emerging from this in-depth analysis is that although the rainfall decline is not unprecedented in the historical record, its consequences on the ground are, in particular in term of water resources. By comparing a series of numbers (Table 1, in appendix 1) between the current dry decade (since 1997) and the driest decade on record (1936 to 1945), three reasons for this “*amplification*” were proposed:

- (1) About 60% of the rainfall decline is concentrated in autumn (71% in the five month period from March to July); this precedes the largest run-off during the year. During the previous dry decade the autumn decline was less than one third of the total rainfall decline.
- (2) The year to year variability (measured by the standard deviation in each period) has been lower during this decade than the previous dry decade. This result, underlining the absence of any year markedly in excess of the long-term average, is likely to have exacerbated the impact on river systems and reservoirs.
- (3) The on-going warming is likely to have increase the evaporation and reduce the amount of water available for run-off. The current decade occurred with maximum day-time temperatures about 0.7 °C higher. This is a very significant warming (about 1.5 times the standard deviation over the long-term means).

The focus on autumn is somewhat misleading and a better understanding of the regional pattern of the decline across SEA is captured by projecting on the annual cycle of the total rainfall. In the southern part of SEA, most of the rainfall occurs during the cold months from the autumn break to spring. There the largest decline (in absolute term) is in late autumn to early winter as rainfall in early autumn is negligible. On the contrary, in the northern part of SEA where more rainfall falls during the warmer month, the decline is most noticeable in summer to autumn (C. Rakich and P. Wiles, personal communication). A convenient way to separate between the two regions is to use the location of the Sub-Tropical Ridge (STR). The STR has a marked annual cycle; during autumn it vary rapidly between a mean summer position of 38°S and a mean winter location of 31°S and sits around 35°S (Drosdowsky, 2005).

Also as part of Project 1.1.1, the current state of the science regarding the climate of SEA was reviewed (Murphy and Timbal, 2007) and preliminary analyses of the importance of several large-scale modes of variability were conducted (Timbal and Murphy, 2007). It showed that in that particular time of the year, there is very little influence from remote large-scale modes of variability on the local rainfall whereas most of the rainfall decline could be related directly to regional MSLP trends.

All the findings listed above and coming from the first project of the SEACI were used to help focus this project. Rainfall trends were studied separately between the South-West of Eastern Australia (SWEA) and a large area on the other side of the STR. The focus on autumn was tuned to early winter in SWEA and warm season rainfall further north. Amongst the large-scale mode of variability, only the role of the SAM was investigated further as it appears that the strength of the teleconnections between tropical SSTs in both the Pacific (linked to ENSO) and the Indian Ocean (linked to IOD) and the rainfall in SEA is relatively weak overall. They tend to vary with time and in the case of the SWEA have been declining in the last 20 years (Timbal et al., 2008b). This finding suggests that the rainfall decline in most of the SEA (at least in the southern winter-rainfall dominated area) is unlikely to be explained by the time-evolution of these tropical modes of variability as, if anything, their influence on the local rainfall is rather small and diminishing in last the two decades. It was also noted that in the SWEA the on-going rainfall trend is consistent with future projections (Timbal and Jones, 2007).

Past trends in the Southern Annular Mode and their role on rainfall and MSLP

The Southern Annular Mode (SAM) describes a naturally occurring oscillation of pressure between the mid-latitudes of the southern hemisphere and the southern polar region. The high-phase of SAM is characterised by higher than normal pressure over the southern mid-latitudes and lower than normal pressure over Antarctica. Conversely, the low-phase of SAM is characterised by lower than normal pressure over the mid-latitudes and higher than normal pressures over the pole.

The importance of the Southern Annular Mode (SAM) on Australian temperature and rainfall has been documented (Hendon et al., 2007). Subsequently, the same analysis was redone across the SEACI domain using high resolution gridded rainfall (Fig. 1 in appendix 2). It reveals that rainfall on and south of the Great Dividing Range across Victoria is more related to SAM than previously thought. This could be an important result as this mountainous area is a high rainfall area and is important to generate run-off for most of the Eastern part of Victoria. Comparison of the monthly and seasonal interactions shows that the SAM-rainfall relationship is much more robust on seasonal timescales. Month to month relations are less statistically reliable due to the small number of days in each phase and do not confirm a possible role in SAM to explain the month to month variability in rainfall decline: large in April, May and July but not in June (Murphy and Timbal, 2007).

The seasonal relationship calculated by Hendon et al. (2007) was adapted to match the key seasons for SWEA: early winter (May-Jun-July), where observed rainfall has declined and SAM index is trending upward, and late winter (August-September-October), where rainfall has not declined and SAM is not trending upward. It was found that a rainfall decline of 5% in MJJ could be attributed to the SAM trend using the Marshall (2003) SAM index from

1959 onward (this is well below the observed decline in this region of about 11% at this time of the year (Timbal et al., 2008a). In ASO, there is hardly any rainfall decline attributable to SAM (below 1%) since the index has hardly any trend since 1959. Taken at face value, these estimates indicate that almost 50% of the total decline in rainfall could be attributable to the SAM increase. However closer inspection of the timing of SAM changes, and rainfall changes, indicate that the relationship is perhaps more complex. While the SAM increased during the 1960s and 1970s, the rainfall decline has occurred only since the mid-1990s.

The work of Hendon et al. (2007) was adapted for MSLP. It shows that, for all seasons, increasing SAM is associated with increasing pressure above SEA, with the largest signal in the observations occurring in MJJ. Using the Marshall SAM index, the observed trend on SAM index can be translated into a MSLP rise of 0.5 hPa in the vicinity of SEA. This is a significant amount up to one third of the observed MSLP increase in MJJ. Even higher number were obtained using NCEP based SAM index but the result in this case are more doubtful as the NCEP SMA index is questionable prior to 1979. As for rainfall, there is a timing issue as most of the MSLP increase above the eastern part of Australia has happen since the 1970s (Timbal et al., 2008a).

Future trends in the SAM and their role on rainfall and MSLP

Climate models are very consistent in predicting that global warming will lead to a more permanent high-phase of the Southern Annular Mode. Models are also very consistent in projecting a winter-time rainfall reduction affecting southern Australia, including the SWEA. Hendon et al. (2007) analysis was adapted and applied to a series of climate simulations with the CSIRO Mk3.5 global climate model: a 2000-year long control simulation (i.e. no external forcings such as greenhouse gas increases) used to obtain statistical significance of the results under 'natural' climate variability, a simulation of the 20th century with all known external natural and anthropogenic forcings and a projection for the 21st century forced with anthropogenic forcings according to the SRES A2 emission scenario.

Figure 2, in the appendix, provide a global perspective for the contribution of SAM to rainfall in the Southern Hemisphere from the CSIRO model. This is the pattern of rainfall changes one would expect from an increasingly positive SAM index. The model appears to perform very well since the results are consistent with the observations across Australia, in particular the rainfall reductions in the south-east of the continent, as well as the south west. This change is most likely associated with increases in local pressure, and a southerly shift in the storm systems that bring wintertime rainfall to these regions.

Trends in the SAM are analysed for various 30-year periods from all CSIRO simulations and compared to the observations (Table 2). In order for all the SAM indices to be comparable we used MSLP based index as it is the case with the Marshall index. This is because surface pressure is a variable that is more easily obtainable from climate model simulations. The SAM index estimated from NCEP reanalysis of surface pressure shows larger positive changes in winter and spring than the Marshall index. In comparison the CSIRO model underestimates the observed trends during the 20th century. The future projected trends for the 21st century are very comparable to the modelled trends for the 20th century.

Then the model SAM signal is translated into a rainfall signal using Hendon et al. (2007) to project SAM related rainfall and pressure changes in a future, warmer world and to compare these estimates to the total rainfall and pressure projections in the future climate scenario. The rainfall changes for the south-east of the continent expected from future changes in SAM using the CSIRO model are quite sizeable for both 30-year periods: 2031-2060 and 2061-2090 relative to pre-industrial climate (Table 3.1). The underlying SAM-rainfall relationship for south east Australia is calculated from the model by considering multiple 30 year samples from the 2000 year control simulation. Similarly uncertainty in the underlying SAM-rainfall relationship is calculated from the distribution of 30 year samples. The SAM related rainfall change accounts for around 60% (2031-2060) and 30% (2061-2090) of the total predicted trend in MJJ rainfall in the CSIRO climate change projections.

Similarly, the SAM-pressure signal accounts for between 60% and 95% of future MJJ and JJA pressure changes (Table 3.2). For the periods 2031-2060 and 2061-2090, for autumn and winter months, the SAM related changes in pressure account for a much higher proportion of total pressure changes in the CSIRO climate projections when compared to rainfall. A caveat to this result is that SAM related changes account for much more of the total pressure changes in the model compared to the observed for the 20th century.

In general, the SAM-pressure correlations are more robust than those for rainfall. This result perhaps reflects the fact that rainfall has a much higher level of variability or climate noise compared with pressure. In particular the signal to noise ratio of the SAM-pressure relationship in the long control simulation is much higher than that for the SAM-rainfall relationship. Changes in pressure associated with SAM may therefore be a more robust way to characterise future SAM related climate change for southern Australia.

It is plan to continue this analysis by applying it to a selection of IPCC-AR4 climate models in order to compare with these results based on the CSIRO model and investigate the consistency amongst models of this triangular relationship: SAM index, MSLP and rainfall above the SEA.

The role of the sub-tropical ridge on south-east Australian rainfall

The role of the STR on SWEA revealed that up to 80% of the MJJ rainfall decline could be related to the strengthening of the ridge since the 1970s (Timbal et al., 2008b). It is worth noting that the timing of the increase of the STR intensity corresponds better to the rainfall decline than the SAM related rainfall decline mentioned earlier (in the 1960s and 1970s). It is worth noting that during that earlier period the STR intensity was relatively low compare to the previous dry decades of the 1940s and 1950s and that might have compensate the expected SAM related decline.

We have extended the analysis of the role of STR across the entire SEA region and across the months for which the rainfall decline is largest: from March to July. Across SEA, rainfall in March-April-May-June-July has decreased from a mean of 262 mm.year⁻¹ from 1950 to 1980 to a mean of 201 mm.year⁻¹ since 1997 (a 23% decline which account for 71% of the total rainfall decline). Although, the relationship between MSLP and rainfall is strongest in winter, it remains significant in autumn and overall quite high over the entire MAMJJ period (Table 4). Correlations with the STR intensity are higher than with direct MSLP and in MAMJJ explain up to 35% of the inter-annual variability (Fig. 3).

The long-term evolution of the intensity of the STR in MAMJJ was compared to the average surface temperature of the globe (data from the Climatic Research Unit, University of East Anglia, UK). For both variables, 21-year running annual means were calculated (Fig. 4) centred on the 20th century (to have a mean of zero on the graph) and using different Y-axes (on the left for the STR and on the right for global temperature). The long-term co-evolution of both variables is remarkable. The previous high values of the STR correspond to the 1940s to 1950s when the global temperature reaches a maximum before decreasing until the 1960s and then rising again after the 1970s as does the global temperature. Using the slope of the relationship (-35 mm.hPa^{-1}) it is possible to translate the intensification of the STR from the low values between 1950 and 1980 to the record high since 1997 into a rainfall signal equivalent to 43 mm.year^{-1} . This amounts to 70% of the observed decline. This amount is comparable, albeit lower than the similar role of the STR for the MJJ rainfall decline in SWEA where the same calculation indicated that up to 80% of the observed decline could be linked to the STR intensification (Timbal et al., 2008b). It shows that although, the role of STR intensification is strongest in the south-west of the SEACI domain, where winter rainfall dominates it can be felt across the entire domain.

North of the sub-tropical ridge: the role of MSLP gradient on rainfall

In complement to diagnosing the role of the STR on rainfall and of the role of the SAM, south of the STR, a further analysis has been conducted on the relationship between rainfall in the northern part of the SEA and large-scale forcing using a newly developed MSLP index: the Gayndah-Deniliquin Index or GDI (Rakich et al., 2007). This index represents the variability in the trade wind flow over eastern Australia bringing moisture inland from the surrounding Tasman Sea and relates particularly well with warm season (summer and autumn) rainfall (correlation of 0.76) in NSW (Fig. 5). This index exhibits large decadal variability corresponding to abrupt changes in rainfall over vast areas of the eastern Australian continent where warm season rainfall dominates.

An analysis of the relative contributions of each pole of the index (Fig. 6) reveals that until 1946, the MSLP variations at the two locations were roughly synchronized, leading to a relatively stable GDI. In contrast, during the late 1940s and early 1950s, a strong rise in Deniliquin MSLP combined with a fall in MSLP at Gayndah resulted in a rapid rise in the GDI at the time when most of SEA started to experience its wettest 30-years period on record. Since the 1970s, MSLP at the northern pole (Gayndah) has been rising, slowly regaining levels seen prior to 1947. The recent sharp decline in the GDI has resulted from this continued rise of summer MSLP at Gayndah, combined with a sudden decline of summer MSLP at Deniliquin since 2000 at a time where the protracted drought which was already well underway in SWEA started to extend to the rest of Eastern Australia

The GDI was found to be complimentary to the ENSO in summer and autumn, when the south-easterly trade winds affect eastern Australia and the SOI-rainfall relationship is at its weakest. Of interest, it was found that the relationship between the GDI and the SOI was asymmetric as is the ENSO-rainfall relationship: an asymmetry between positive and negative phases (see Power et al., 2006 in the case of ENSO) which as a consequence generates a inter-decadal variability of the strength of the relationship during El Niño dominated and La Niña dominated epochs (see Power et al., 1999 in the case of ENSO). Similarly the GDI-rainfall exhibits multi-decadal variability in the strength of the

relationship. That suggests that although complimentary, the relationship between the GDI and warm season rainfall over eastern Australia is not independent of ENSO.

Can the heat wave of April 2005 be attributed to global warming?

It is usually acknowledged that it is difficult to attribute a single extreme event to climate change; on the other hand, it is possible, if the frequency of particular extreme events is observed to increase, to attempt to attribute such increases. In the case of hot temperature and heat waves, a number of records have been established in the last decade or so and there has been some attempt to attribute this increase to on-going global warming. In this study, we have decided to investigate a single extreme event (rather than the frequency of occurrence) with large and severe impacts: the heat waves of April 2005. On a national scale, April 2005 saw the most extreme temperature anomalies ever recorded for Australia (NCC, 2005). The Australian mean temperature was 2.58°C above the 1961-90 average, nearly 1°C above the previous April record (1.73°C in 2002), and well above the largest anomaly previously recorded for any month (2.32°C in June 1996). Averaged across the Murray-Darling Basin, the anomaly was spectacular: 4°C (almost 1.5°C above the previous record in 2002).

The Bureau of Meteorology Statistical Downscaling Model (SDM) has been used to examine the role of day-to-day meteorological conditions in producing the extreme temperatures across the MDB. The large-scale mean sea level pressure (MSLP) and temperature at 850 hPa (T_{850}) have been used to see whether the heat waves can be explained by natural variability in the atmospheric circulation or whether global warming is a major contributor. The model takes analogues from a “pool” of MSLP and/or T_{850} fields from 1958-2004 to reproduce the situation in April 2005.

First the ability of the SDM to reproduce the observed temperature inter-annual variability and trend over the entire 1958 to 2004 period was evaluated. The T_{850} predictor was able to reproduce much of the year-to-year variations in stations surface maximum temperatures and had more skill than the MSLP predictor. This skill generally improved when the two predictors were used together. It was found that changes in MSLP patterns in April should have resulted in cooling temperature trend at MDB stations, whereas the T_{850} patterns produced no trend when averaged across MDB stations. However, combining both large-scale circulation and temperature produces a positive, but weaker than observed, temperature trend. This result is difficult to interpret; it suggests that part of the surface temperature trend across the basin can be accounted for by changes in synoptic situations combined with warmer air aloft, thus emphasising the importance of mid-tropospheric warming to explain the surface trends. However, the absence of trend when MSLP is used as a single predictor clearly demonstrates that the on-going warming across the basin cannot be explained by changes in synoptic situations.

Then the SDM was applied in a cross-validated mode to try to reproduce the heat wave of April 2005. The T_{850} patterns reproduce about half of the observed hot anomaly in April 2005 across the MDB while MSLP reproduces very weak and generally negative anomalies (Figure 7). When the two predictors are combined, the anomalies are in most cases smaller. The results show that the April 2005 heat wave cannot be accounted for by anomalous synoptic situation (i.e. it was not due to a series of anomalous meteorological situations). On the contrary the warming of the troposphere appears critical and explains about half of observed surface heat wave.

Acknowledgement: This work was funded by the South Eastern Australia Climate Initiative.

Additional information

Outputs from this project

Publications:

- (1) Hendon, H.H., D.W.J. Thompson, and M.C. Wheeler, 2007: Australian rainfall and surface temperature variations associated with the Southern Annular Mode. *J. Climate*, **20**, 2452-2467
- (2) Rakich, C., N. Holbrook and B. Timbal, 2008: An index to capture moisture transport affecting rainfall over Eastern Australia. *Geo. Res. Let.*, (submitted)
- (3) Timbal, B. and D. Jones, 2007: Future projections of winter rainfall in southeast Australia using a statistical downscaling technique. *Climatic Change*, (in press)
- (4) Timbal, B., Hope, P. and R. Fawcett, 2008: On the relationship between rainfall in the southwest and the southeast of Australia. Part I: Variability on daily and longer time-scales, *J Climate*, submitted
- (5) Timbal, B., Wheeler, M. and P. Hope, 2008: On the relationship between rainfall in the southwest and the southeast of Australia. Part II: Possible causes of recent declines, *J Climate*, submitted

Conference papers:

- (1) B. Murphy., B. Timbal and D. Jones, 2007: "A Tool for Attribution of Climate Anomalies", *Australian Meteorological and Oceanographic Society 14th National Conference*, Adelaide, February 2007.
- (2) B. Timbal and P. Hope, 2006: "On the relationship between South West and South East Australian winter rainfall", *17th Australian New-Zealand Climate Forum*, Canberra, September 2006.
- (3) B. Timbal. 2007: "Winter rainfall in Southern Australia: Past and future trends", *International Union of Geodesy and Geophysics General Assembly*, Perugia, Italy, July 2007.
- (4) B. Timbal. 2007: "Observed climate changes in the south-east of Australia: detection and possible attribution", *Hydrological consequences of climate change*, Canberra, November 2007.

References

- Drosowsky, W., 2005: The latitude of the subtropical ridge over eastern Australia: the L index revisited. *International Journal of Climatology*, **25**, 1291-1299
- Hendon, H.H., D.W.J. Thompson, and M.C. Wheeler, 2007: Australian rainfall and surface temperature variations associated with the Southern Annular Mode. *J. Climate*, **20**, 2452-2467
- National Climate Centre, 2005: An exceptionally warm April and dry start to 2005. *Special Climate Statement*, **5**, April 2005
- Murphy, B.F. and B. Timbal, 2007: A review of recent climate variability and climate change in south eastern Australia. *Int. J. Clim.* (in press)
- Power, S., F. Tseitkin, V. Mehta, B. Lavery, S. Torook, and N. Holbrook, 1999: Decadal climate variability in Australia during the twentieth century, *International Journal of Climatology*, **19**, 169-184
- Power, S., M. Haylock, R. Colman, and X. Wang, 2006: The predictability of interdecadal changes in ENSO activity and ENSO teleconnections, *Journal of Climate*, **19**, 4755-4771
- Rakich, C., N. Holbrook and B. Timbal, 2008: An index to capture moisture transport affecting rainfall over Eastern Australia. *Geo. Res. Let.*, (submitted)
- Timbal, B., Hope, P. and R. Fawcett, 2008a: On the relationship between rainfall in the southwest and the southeast of Australia. Part I: Variability on daily and longer time-scales, *J Climate*, submitted
- Timbal, B., Wheeler, M. and P. Hope, 2008b: On the relationship between rainfall in the southwest and the southeast of Australia. Part II: Possible causes of recent declines, *J Climate*, submitted
- Timbal, B. and D. Jones, 2007: Future projections of winter rainfall in southeast Australia using a statistical downscaling technique. *Climatic Change*, (in press)
- Timbal, B. and B.F. Murphy, 2007: Observed climate change in South-East of Australia and its relation to large-scale modes of variability. *BMRC Research Letter*, **6**, 6-11

Project Milestone Reporting Table

To be completed prior to commencing the project				Completed at each Milestone date	
Milestone description ¹ (up to 33% of project activity)	Performance indicators ²	Completion date ³	Budget ⁴ for Milestone (\$)	Progress ⁵ (1- 3 dot points)	Recommended changes to workplan ⁶
1. Review literature on SEA climate variability	Review prepared	01/10/2006	15 k	A review (Murphy and Timbal) has been completed. It has accepted by the <i>International Journal of Climatology</i> subject to revision.	None
2.Document Australian rainfall and temperature variations associated with the SAM	Scientific paper prepared	01/01/2007	15 k	A scientific paper (Hendon et al.) on a broad Australian perspective is in press (<i>Journal of Climate</i>). Some additional calculations using high resolution gridded data have been performed for SEA.	None
3. Assess other modes of variability and their role in climate change in SE	4 pages report prepared	01/07/2007	25 k	A report has been prepared. A more extensive scientific article focusing on the similarities between rainfall decline in SEACI and IOCI and including results from this milestone is currently underway (Timbal et al., 2 parts article)	None
4. Study recent record heat waves across south-eastern states	Scientific paper prepared	01/07/2007	25 k	Results were presented at the AMOS meeting. The importance of circulation changes in recent heat waves has been analysed. A scientific paper is being prepared (Murphy, Timbal and Jones).	None

Appendix: 1: Tables

Period vs. Variables	1997-2006		1936-1945		1961-1990	
	Mean	Std	Mean	Std	Mean	Std
Total Rain (mm)	511	90	494	106	595	120
Autumn Rain (mm)	98	32	116	36	149	51
Tmax (°C)	20.4	0.27	19.7	0.47	19.9	0.48
Murray Inflow (GL)	4872	2722	5855	4406	9437	5541

Table 1: Mean and standard deviation for total rainfall, autumn rainfall, annual temperature and Murray River modelled inflow for three period: 1997-2006, 1936-1945 and 1961-1990.

Season	Observed	CSIRO GCM	CSIRO GCM
	1971-2006	1971-2000	2001-2030
DJF	0.81	0.61	-0.11
MAM	1.92	-0.06	0.13
MJJ	1.71	0.41	0.79
JJA	1.51	0.74	1.03
SON	0.20	0.22	0.00

Table 2: Trend in SAM expressed as units of standard deviation from Observations and for future climate model projections. The trends are expressed as 30 Year trends using 11 year low pass filtered data. Projections indicate a tendency toward a high-phase in the months May through to August.

	2031-2060		2061-2090	
	SAM-Forced Rainfall Trend	% of total projected rainfall trend	SAM-Forced Rainfall Trend	% of total projected rainfall trend
DJF	0.91	-4.39	0.89	-3.35
MAM	2.15	-21.89	2.36	-12.12
MJJ	-7.47	62.67	-9.45	30.89
JJA	-6.43	38.28	-9.25	28.61
ASO	0.06	-1.16	0.21	-0.62
SON	1.17	-51.99	3.17	-10.23

Table 3.1: Future projected changes in rainfall (mm) due to changes in the Southern Annular Mode under global warming (SRESA2) emissions scenario. The GCM SAM-Forced rainfall amounts represent the implied change in rainfall due to future SAM.

	2031-2060		2061-2090	
	SAM-Forced Pressure Trend	% of total projected Pressure trend	SAM-Forced Pressure Trend	% of total projected Pressure trend
DJF	4.48	31.97	4.38	-10.69
MAM	40.26	71.90	44.21	42.51
MJJ	115.00	68.86	145.55	65.27
JJA	96.00	94.12	138.00	91.39
ASO	19.42	-176.51	64.22	91.74
SON	15.48	110.55	41.88	62.51

Table 3.2: Future projected changes in pressure (hPa) due to changes in the Southern Annular Mode under global warming (SRESA2) emissions scenario. The GCM SAM-Forced rainfall amounts represent the implied change in rainfall due to future SAM.

	SEA rainfall		
	MAM	MAMJJ	MJJ
MSLP	-0.29	-0.53	-0.68
STR-I	-0.42	-0.59	-0.70

Table 4: *Pearson correlation between MSLP or the intensity of the sub-tropical ridge (STR-I) and the rainfall averaged across the SEA region for several period: autumn, March to Jul and early winter (May to July). The bold correlation is used to infer a rainfall reduction linked to the STR intensification across SEA.*

Appendix: 2: Figures

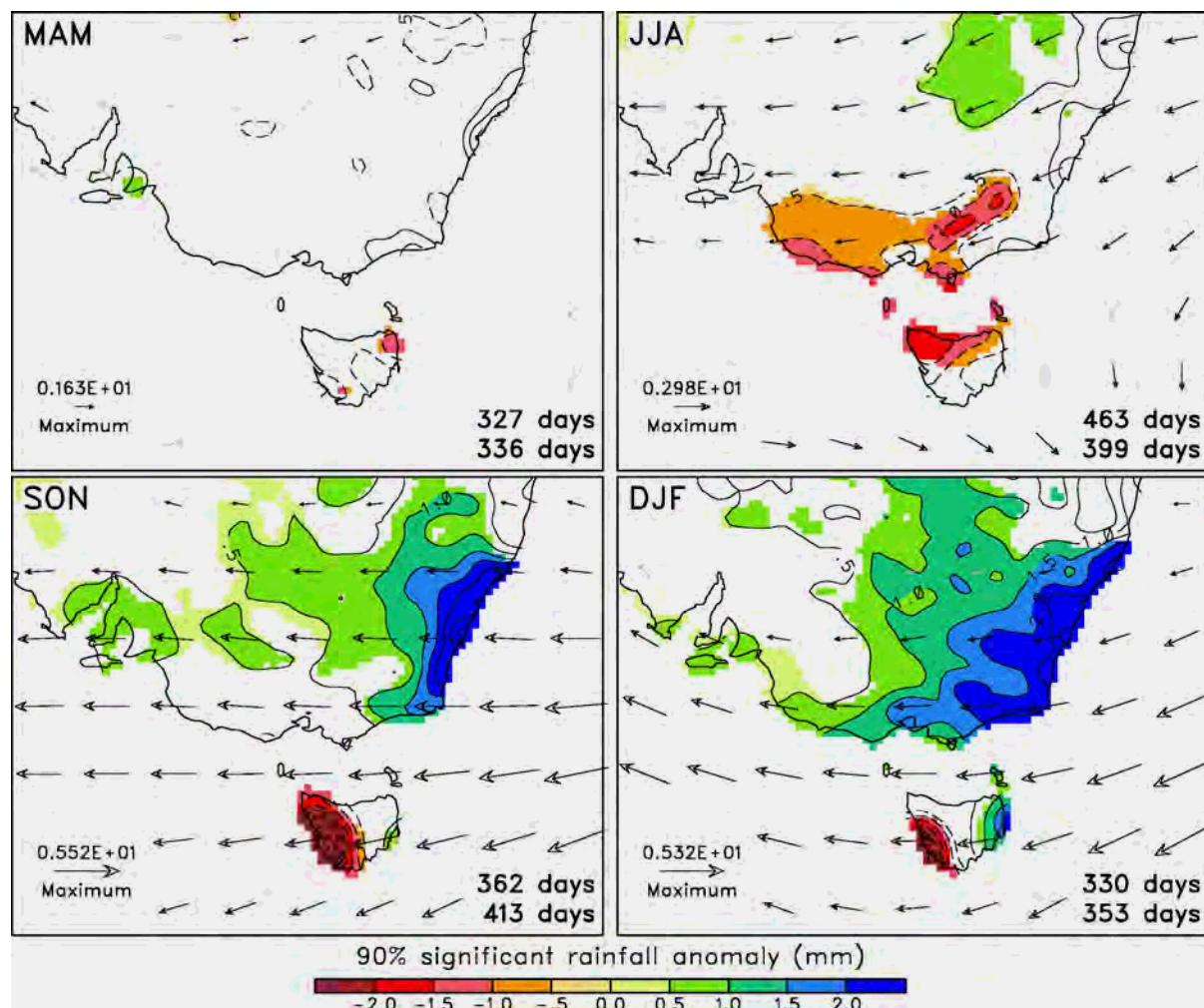


Figure 1: Composite daily rainfall (contours and shading) and 850 hPa winds (maximum vector shown in lower left corner of each panel) for high minus low polarity of the SAM index for MJJ (left) and ASO (right), using daily data (1979 to 2004). Significant differences at the 90% level are shaded. The number of days in the high and low index polarity of the SAM is listed in each panel.

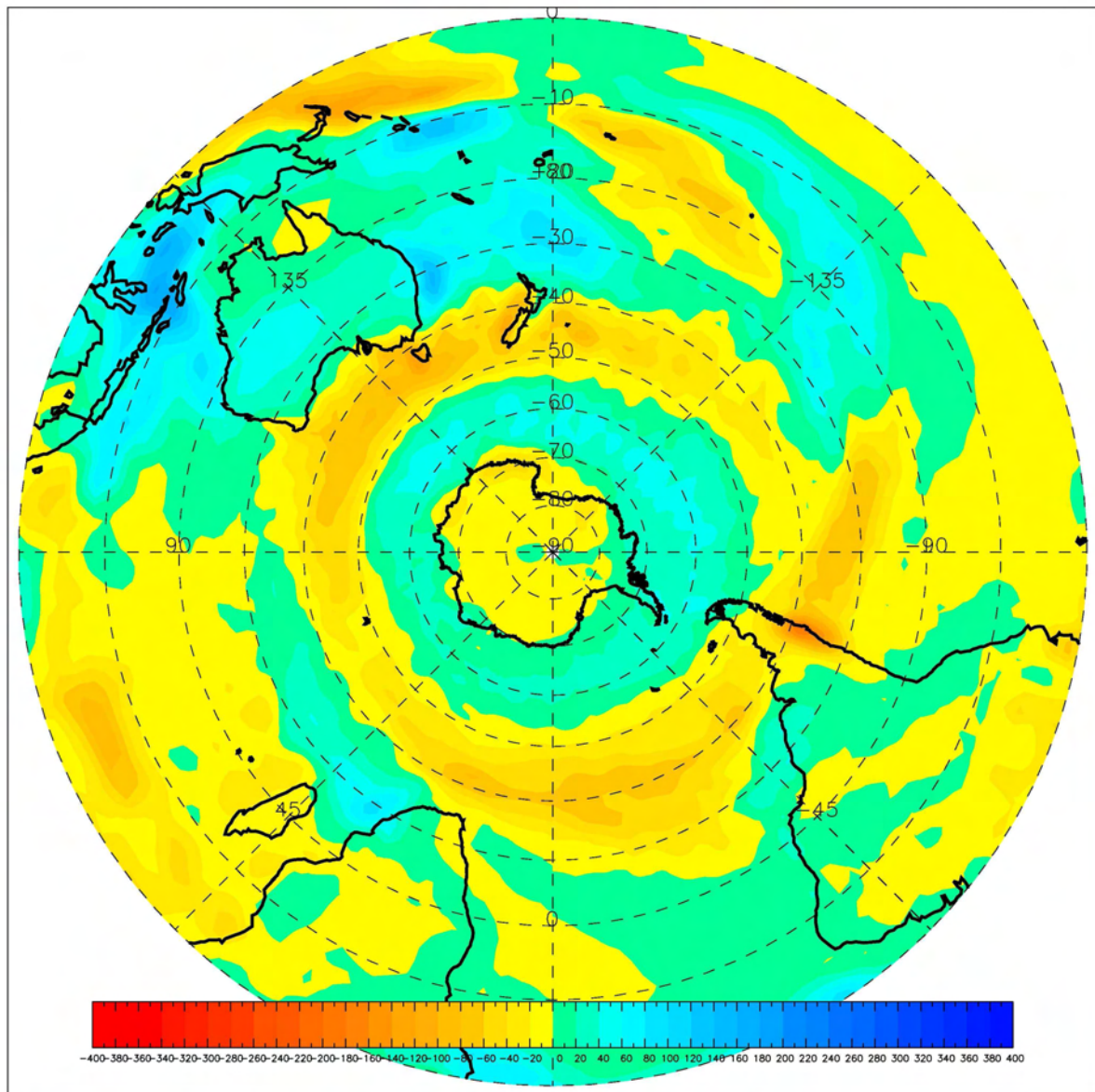


Figure 2: Mean Composite Rainfall difference for seasonal (MJJ) SAM high-low phase events. Negative values indicate a net rainfall reduction for that region associated with high-phase SAM. South west Western Australia and south eastern Australia are regions associated with reduced rainfall during high phase SAM.

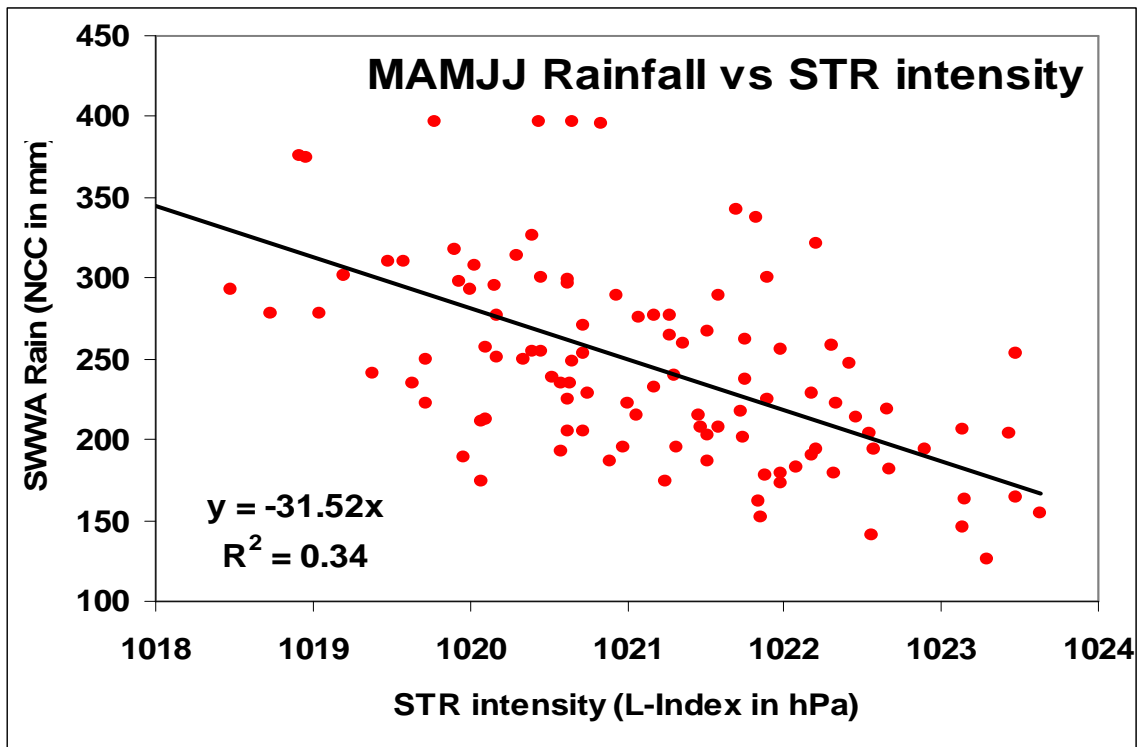


Figure 3: Five-year moving averages of both the warm season (Oct-Mar) NSW state-wide average rainfall (solid line) and the summer GDI (dashed line).

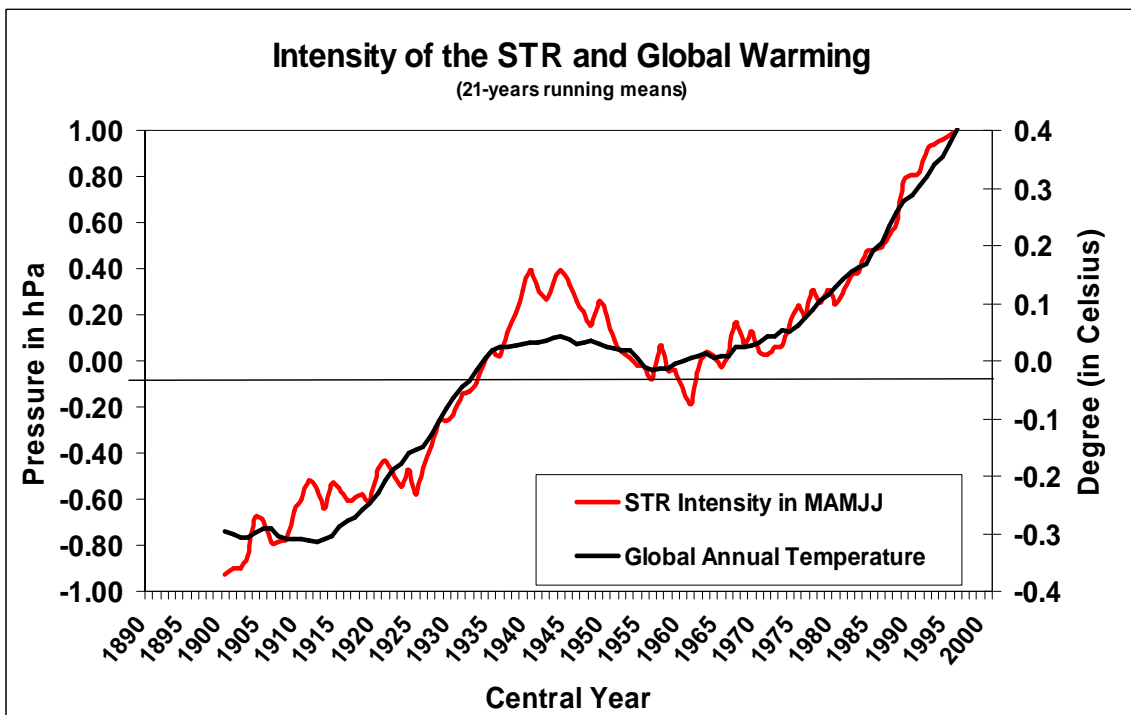


Figure 4: Five-year moving averages of both the warm season (Oct-Mar) NSW state-wide average rainfall (solid line) and the summer GDI (dashed line).

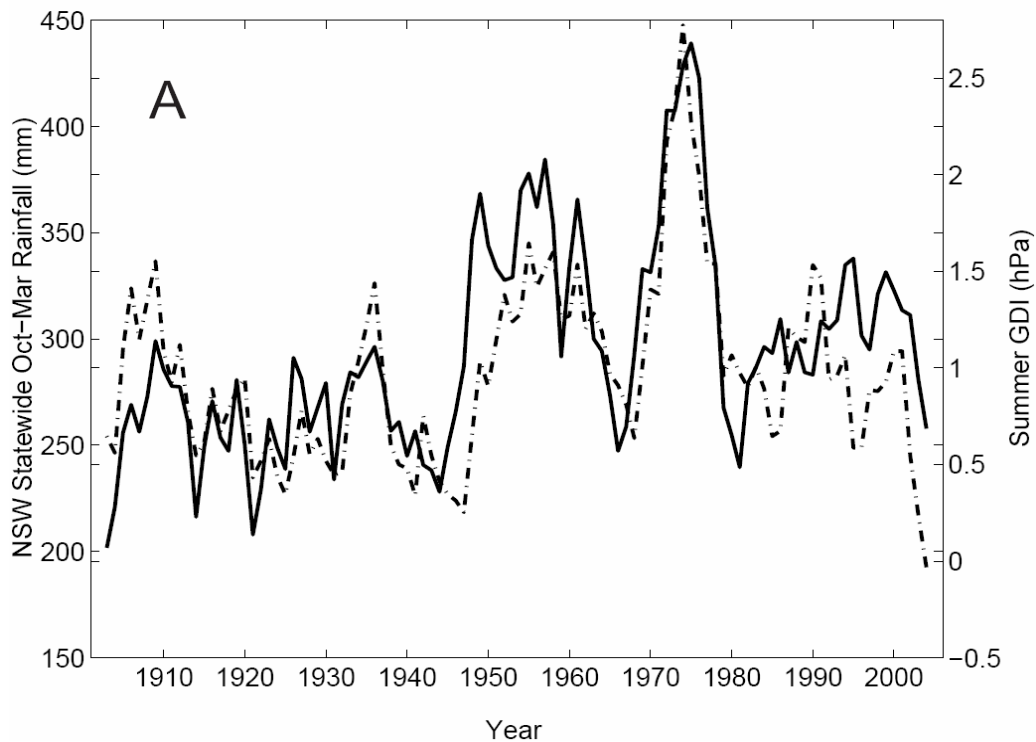


Figure 5: Five-year moving averages of both the warm season (Oct-Mar) NSW state-wide average rainfall (solid line) and the summer GDI (dashed line).

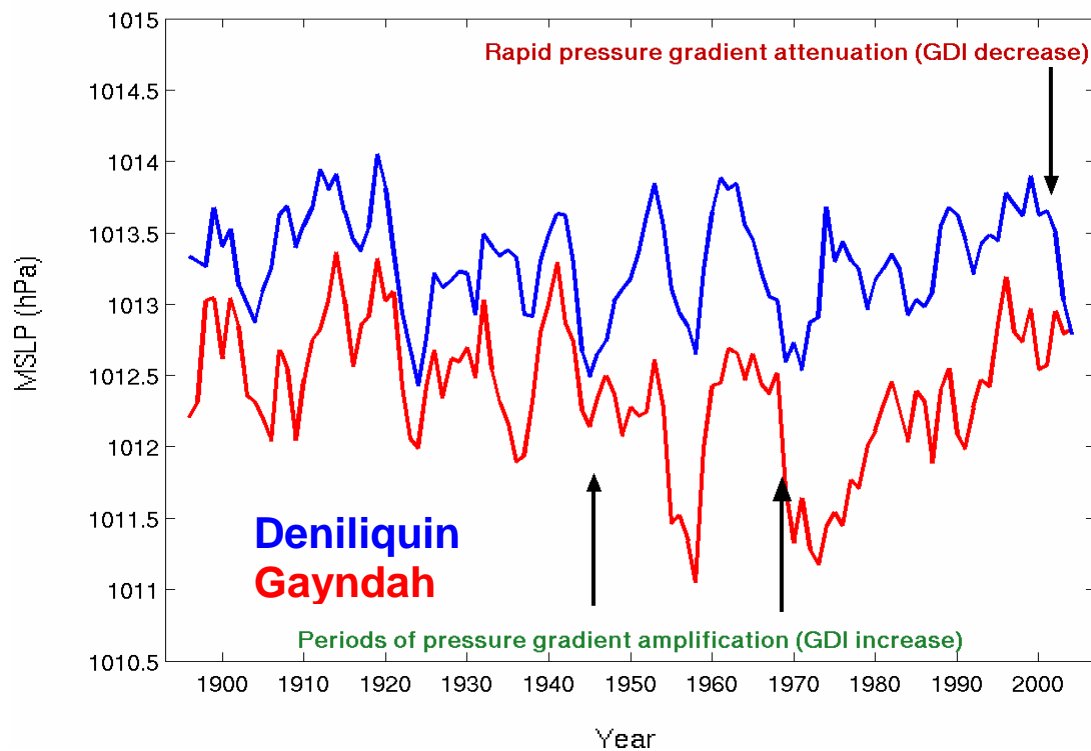


Figure 6: Five-year moving averages of summer (DJF) MSLP at Gayndah, QLD (red line) and Deniliquin, NSW (blue line) showing periods of rapid pressure gradient amplification (e.g. late-1940s and late-1960s) and rapid pressure gradient attenuation (e.g. mid-1960s and 2000-2006).

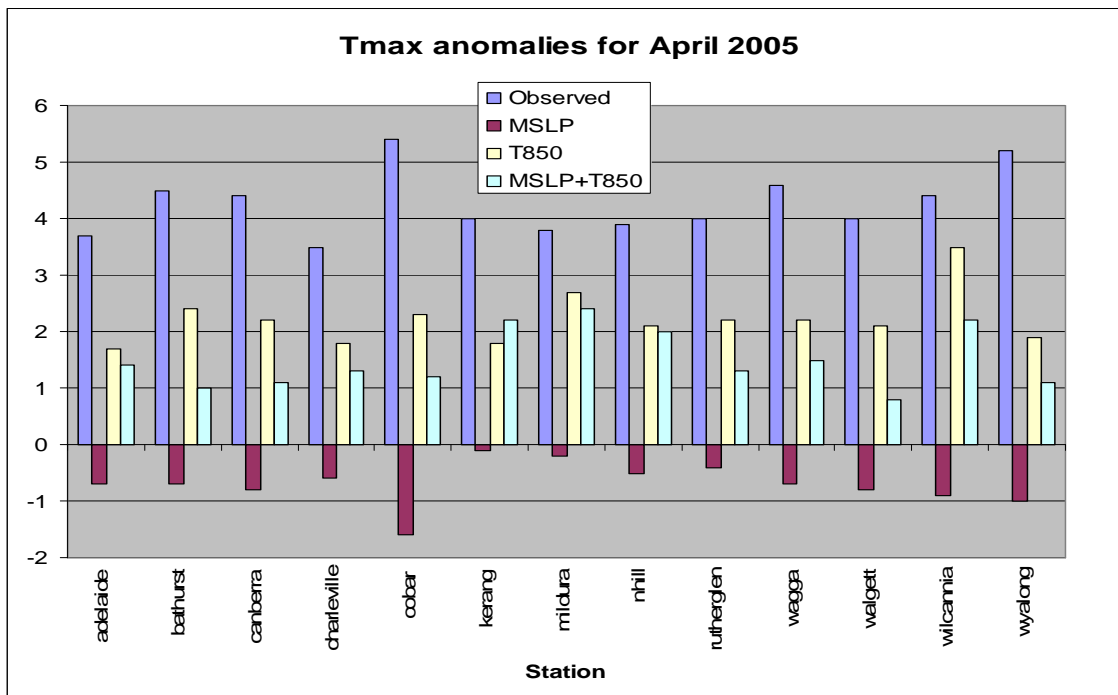


Figure 7: Mean maximum temperature anomalies for April 2005 observed and as simulated by downscaling model with MSLP, T_{850} and MSLP/ T_{850} as predictors.



South Eastern Australian **Climate initiative**

Final report for Project 1.3.4

Calibration of Statistical Downscaling Models

Principal Investigator: Steve Charles

CSIRO Land and Water, Private Bag 5, Wembley WA 6913

Steve.Charles@csiro.au

Tel: 08 9333 6795

Fax: 08 9333 6499

Co-Authors:

Guobin Fu

CSIRO Land and Water, Private Bag 5, Wembley WA 6913

Guobin.Fu@csiro.au

Completed: 29 June 2007

Abstract

Statistical downscaling allows us to bridge the gap between the coarse spatial scales of GCMs and the regional and local scales where climate impacts are experienced and analysed. Within SEACI, the Nonhomogeneous Hidden Markov Model (NHMM) statistical downscaling model will be used in a range of projects investigating the historical relationships between regional rainfall and synoptic scale circulation, assessing the ability of GCMs to reproduce key atmospheric processes at the synoptic scale, and using GCM projections to produce regional precipitation projections suitable for use in impacts assessment (such as hydrological models). Confidence in NHMM performance for current and future climates is founded on obtaining parsimonious NHMMs through rigorous calibration and assessment, as undertaken here. The selected NHMMs are shown to perform well, reproducing key properties of observed multi-site daily rainfall, and thus providing a physically realistic linkage between atmospheric processes at the synoptic scale and regional rainfall patterns.

Significant research highlights, breakthroughs and snapshots

- NHMMs were successfully fitted (1986 – 2005) and validated (1958 – 1984) for a 30 station network for summer (November-March) and winter (April-October).
- The selected models simulate the full range of natural climate variability experienced during the 1958 to 2005 period.
- The selected models produce physically consistent and plausible weather state (i.e. multi-site rainfall occurrence) patterns.

Statement of results, their interpretation, and practical significance against each objective

Objective 1: Calibrate Nonhomogeneous Hidden Markov Models (NHMMs) for the south-east Murray Darling Basin (MDB).

The statistical downscaling technique employed relates multi-site, daily rainfall patterns to synoptic-scale atmospheric predictors (Hughes *et al.* 1999; Charles *et al.* 1999). The model (nonhomogeneous hidden Markov model, NHMM) selects a small set of atmospheric predictors that relate to a discrete set of “weather states” associated with particular multi-site daily precipitation occurrence patterns (e.g., wet everywhere, wet in the north and dry in the south, etc.). The sequence of daily transitions from state to state is a function of the selected atmospheric predictors. Characteristics of these states are examined by constructing composite plots of their precipitation occurrence patterns and associated atmospheric predictor fields.

NHMMs were successfully fitted and validated for a 30 station network, shown in Figure 1 and Table 1. Fitting was on an approximately half year basis, with summer defined as November-March and winter as April-October. This season demarcation was selected based on the relationship between atmospheric predictors and multi-site rainfall as determined in the precursor Project 1.3.3 ‘*Atmospheric Predictor Selection for Statistical Downscaling*’.

The fitting period used was 1986 to 2005, with the earlier 1958 to 1984 data reserved for out-of-sample validation. It was not possible to investigate earlier periods due to the unavailability of sufficient quality atmospheric data prior to 1958. The daily rainfall data for the selected 30 station network is of very high quality for the fitting period, as previously determined in Project 1.3.2 ‘*Station Networks and Data for Statistical Downscaling*’. However, for the

earlier validation period data quality degrades for some stations due to missing periods of record or an increased incidence of untagged accumulations. This may bias the validation of the NHMM performance for this period.

Objective 2: Determine the performance of the selected NHMMs in terms of reproduction of key statistics of daily multi-site rainfall occurrence and amounts.

The selected downscaling models produce physically consistent and plausible weather state patterns. The summer model has 6 weather states (see Figure 2) and 3 predictors: mean sea level pressure (MSLP), 700 hPa dew-point temperature depression (DT_d), and East – West 500 hPa geopotential height (GPH) gradient. The winter model has 5 weather states (see Figure 3) and 4 predictors: North – South MSLP gradient, 700 hPa and 850 hPa DT_d , and North – South 700 hPa GPH gradient. Brief descriptions of these weather states and their mean frequencies are presented in Tables 3 and 5, for summer and winter respectively. The probabilities of the daily transitions between weather states are presented in Tables 4 and 6, for summer and winter respectively.

Figures 5 to 7 (for Summer) and 8 to 10 (for Winter) evaluate the reproduction of mean seasonal precipitation probabilities, log-odds ratios (measures the correlation in binary series, i.e. daily rainfall occurrence as ‘1’ wet or ‘0’ dry, for all station pairs), and Spearman rank correlations for calibration and validation periods. These confirm that the calibrated NHMMs can reproduce, in turn, the correct frequency of wet days, inter-site correlations in rainfall occurrence, and inter-site correlation in rainfall amounts. For the out-of-sample validation period, there is evidence of increased bias however the previously noted degradation in observed precipitation quality for this period may mean that the observed statistics are biased.

At-site spell lengths and amounts distributions were also well reproduced for the validation period (not shown for reasons of space, available on request). Overall the selected models appear to perform well across the full range of natural climate variability experienced during the 1958 to 2005 period.

Objective 3: Identifying deficiencies requiring further research and development.

One area of relatively deficient performance is poor reproduction of long dry spells in summer for some stations (not shown for reasons of space, available on request). Other NHMM parameterisations will be investigated in the subsequent Project 1.3.5 ‘*Further development of statistical downscaling methodology*’ to determine whether these limitations can be improved upon.

Summary of methods and modifications (with reasons)

- A network of 30 high quality rainfall stations was selected, encompassing the majority of the catchments of the south-east MDB. This station network is not definitive, as future research and client needs can modify the extent of the network. This initial calibration will provide a baseline to which any future NHMMs that use different (potentially lower quality) rainfall station networks can be compared to.
- NHMMs have been calibrated for the selected station network for two seasons (‘summer’ November to March and ‘winter’ April to October).
- For each season, a unique NHMM (in terms of number of weather states and atmospheric predictor set used) has been selected based on calibration criteria.

- The performance of these selected NHMMs has been quantified, by assessing reproduction of key statistics of daily multi-site rainfall occurrence and amounts, for calibration and validation periods.

Summary of links to other projects

Project 1.4.3 '*Comparison of Observed and Reanalyses Downscaled Synoptics and Precipitation*' will use the NHMMs selected here to investigate the weather state time-series properties and relate these to the time-series of the atmospheric predictors and observed seasonal rainfall. The ability to reproduce observed properties will provide confidence in using these downscaling models to produce climate change projections in Project 2.1.3 '*Drive Statistical Downscaling Models with GCM Predictor Sets*'. Evaluation of the downscaled rainfall simulations suitability for use in hydrological models will be a key component of these next stage projects.

Publications arising from this project

None to date.

Acknowledgement

The NHMM was originally developed by Professor Jim Hughes, University of Washington, Seattle, USA. His assistance is gratefully acknowledged.

Recommendations for changes to work plan from your original table

None.

References

- Charles SP, Bates BC, Hughes JP. 1999. *A spatio-temporal model for downscaling precipitation occurrence and amounts*. Journal of Geophysical Research 104: 31657-31669.
- Hughes JP, Guttorp P, Charles SP. 1999. *A non-homogeneous hidden Markov model for precipitation occurrence*. Applied Statistics 48: 15-30.

Project Milestone Reporting Table

To be completed prior to commencing the project				Completed at each Milestone date	
Milestone description ¹ (brief) (up to 33% of project activity)	Performance indicators ² (1- 3 dot points)	Completion date ³ xx/xx/xxxx	Budget ⁴ for Milestone (\$) (SEACI contribution)	Progress ⁵ (1- 3 dot points)	Recommended changes to workplan ⁶ (1- 3 dot points)
1. Develop calibration data sets	30 station network selected Seasons for NHMM calibration selected NHMM input files created	1/3/2007	10	Completed	None
2. Calibrate NHMMs	NHMMs calibrated Occurrence NHMMs selected Amounts models calibrated	1/5/2007	15	Completed	None
3. Assess calibrated NHMMs	Occurrence and amounts statistics assessed for calibration period Assessment repeated for validation period Report on final model selection (4-6 pages)	30/6/2007	15	Completed. This report is the report on final model selection.	None

Table 1. Stations shown in Figure 1.

Number	BoM No.	BoM Name	Latitude (°S)	Longitude (°E)
1	49048	BALRANALD (TILLARA)	-34.64	143.05
2	70014	CANBERRA AIRPORT	-35.3	149.2
3	70028	YASS (DERRINGULLEN)	-34.74	148.89
4	70054	COOMA (KIAORA)	-36.2	149.06
5	72019	HOLBROOK (GLENFALLOCH)	-35.66	147.56
6	72023	HUME RESERVOIR	-36.1	147.03
7	72150	WAGGA WAGGA AMO	-35.16	147.46
8	73007	BURRINJUCK DAM	-35	148.6
9	73051	MURRINGO (WINDERMERE)	-34.21	148.55
10	74008	GRONG GRONG (BEREMBED)	-34.86	146.82
11	74025	BURRUMBUTTOCK (HOLYROOD)	-35.85	146.78
12	74087	URANA (NOWRANIE)	-35.33	146.03
13	75012	WAKOOL (CALIMO)	-35.42	144.6
14	75049	MAUDE (NAP NAP)	-34.45	144.17
15	75054	CONARGO (PUCKAWIDGEE)	-35.28	145.21
16	75067	CARRATHOOL (UARDRY)	-34.47	145.3
17	76044	NYAH	-35.18	143.37
18	77001	QUAMBATOOK (BARRAPORT NORTH)	-35.98	143.65
19	80044	PATHO WEST	-36	144.42
20	80053	TANDARRA	-36.43	144.25
21	81019	NAGAMBIE (GOULBURN WEIR)	-36.72	145.17
22	82002	BENALLA (SHADFORTH STREET)	-36.55	145.97
23	82018	UPLANDS (GIBBO RIVER PARK)	-36.77	147.69
24	82127	PEECHELBA EAST	-36.14	146.25
25	83010	EUROBIN	-36.64	146.86
26	83038	TAWONGA	-36.66	147.13
27	88011	CAMPBELLTOWN	-37.22	143.96
28	88042	MALMSBURY RESERVOIR	-37.2	144.37
29	88060	KINGLAKE WEST (WALLABY CREEK)	-37.45	145.21
30	88131	NARBETHONG	-37.5	145.68

Table 2. Selected atmospheric predictor sets.

Atmospheric predictor	NCEP/NCAR Reanalysis Grids (refer to Figure 2)
Summer <i>MSLP</i> DT_d^{700} East – West <i>GPH</i> ⁵⁰⁰	$(B2+B3+B4+C2+C3+C4)/6$ $(C2+C3+C4+D2+D3+D4)/6$ $(C3+C4+D3+D4)-(E3+E4+F3+F4)/4$
Winter North – South <i>MSLP</i> DT_d^{700} DT_d^{850} North–South <i>GPH</i> ⁷⁰⁰	$(A5+B5+C5+D5)-(A4+B4+C4+D4)/4$ $(B2+B3+B4+C2+C3+C4+D2+D3+D4)/9$ $(A3+A4+B3+B4+C3+C4)/6$ $(A5+B5+C5)-(A4+B4+C4)/4$

Table 3. Summary of Summer weather state patterns

State		Description
No.	%Freq.	
1	58	Rainfall: dry everywhere Synoptics: high pressure centred over SE Australia; warm, dry continental airflow
2	5	Rainfall: wet only in the most southerly stations Synoptics: high moving into the Australian Bight; southerly moist maritime airflow
3	6	Rainfall: wet everywhere Synoptics: low trough over SE Australia; southerly moist maritime airflow
4	15	Rainfall: wet in the northeast Synoptics: weak low trough over SE Australia.
5	11	Rainfall: moderately wet everywhere Synoptics: low trough over SE Australia; southerly moist maritime airflow
6	5	Rainfall: north (dry) to south (wet) rainfall gradient Synoptics: moderate low trough over SE Australia; southerly moist maritime airflow

Table 4. Weather state TPM[#] for Summer NHMM.

	1	2	3	4	5	6
1	0.76	0.04	0.02	0.09	0.04	0.04
2	0.48	0.22	0.03	0.06	0.11	0.10
3	0.15	0.03	0.25	0.20	0.33	0.04
4	0.46	0.02	0.04	0.34	0.11	0.04
5	0.26	0.04	0.16	0.24	0.26	0.05
6	0.20	0.06	0.16	0.11	0.24	0.22

[#] Transition Probability Matrix. * e.g., 4% probability of being state 2 today if previous day was state 1.

Table 5. Summary of Winter weather state patterns

State		Description
No.	%Freq.	
1	48	Rainfall: dry everywhere Synoptics: high pressure centred over region; dry continental air
2	12	Rainfall: wet everywhere Synoptics: low pressure trough; moist southerly maritime airflow
3	10	Rainfall: moderately wet everywhere Synoptics: weak low pressure trough; moist system over region
4	18	Rainfall: wet in the south predominantly Synoptics: weak low pressure trough; moist southerly maritime airflow
5	12	Rainfall: wet everywhere, moderate in northwest Synoptics: low pressure trough further east than in State 2; moist southerly maritime airflow

Table 6. Weather state TPM[#] for Winter NHMM.

	1	2	3	4	5
1	0.72	0.04	0.07	0.13	0.04
2	0.09	0.27	0.13	0.21	0.30
3	0.30	0.22	0.31	0.11	0.07
4	0.36	0.12	0.06	0.30	0.15
5	0.22	0.17	0.05	0.29	0.27

[#] Transition Probability Matrix. * e.g., 22% probability of being state 2 today if previous day was state 3.

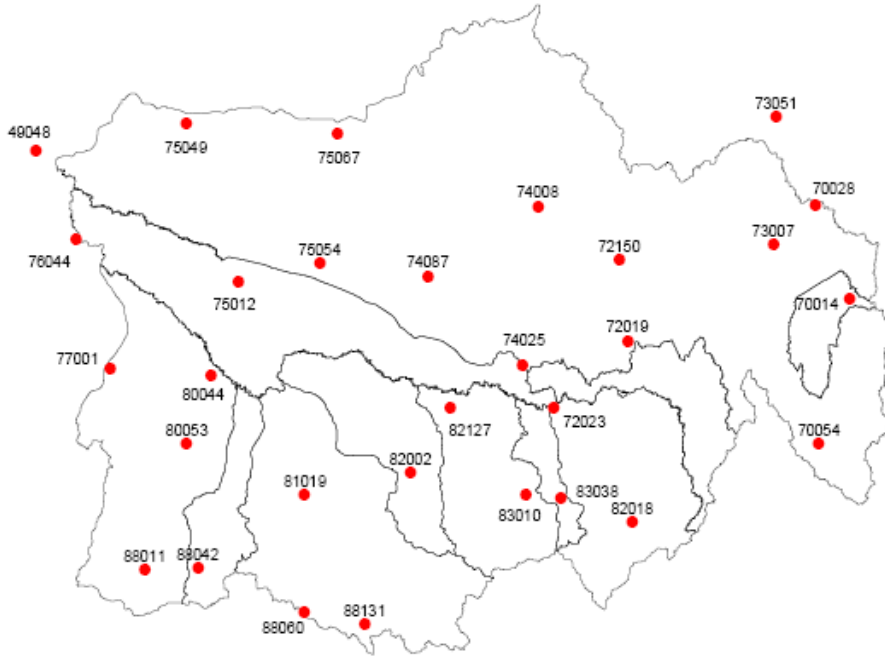


Figure 1. Location of 30 stations in Table 1.

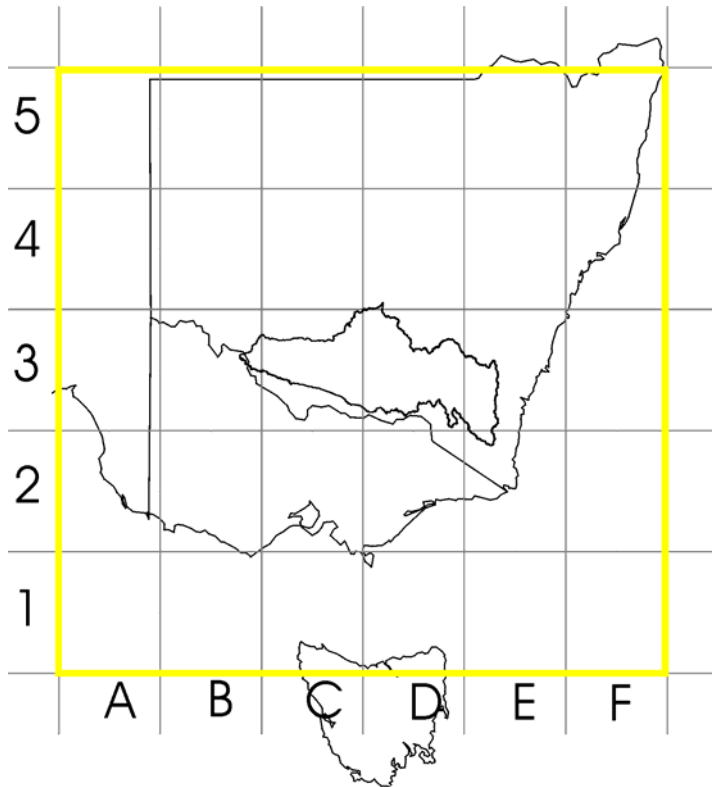


Figure 2. Reanalysis atmospheric data grid, showing coordinates (A to F, 1 to 5) used in Table 2. (outline of Murrumbidgee shown for reference).

SEACI End of Project Reports June 2007

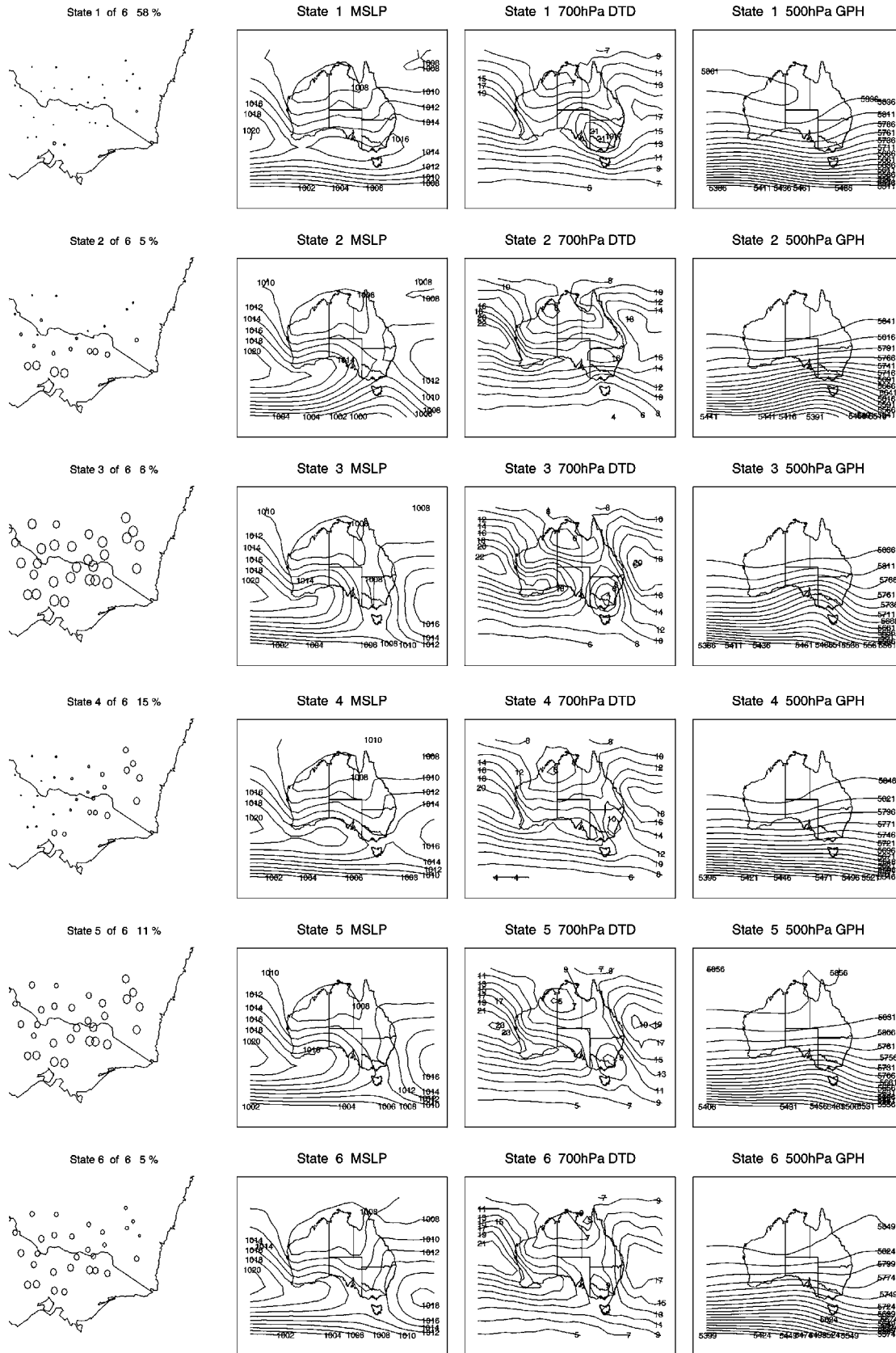


Figure 3: Weather states of the summer NHMM: precipitation occurrence probabilities, diameters of circles proportional to probability of a wet-day with the largest circle 1.0; composite MSLP (hPa); 700 hPa DTD (K); 500 hPa GPH (m).

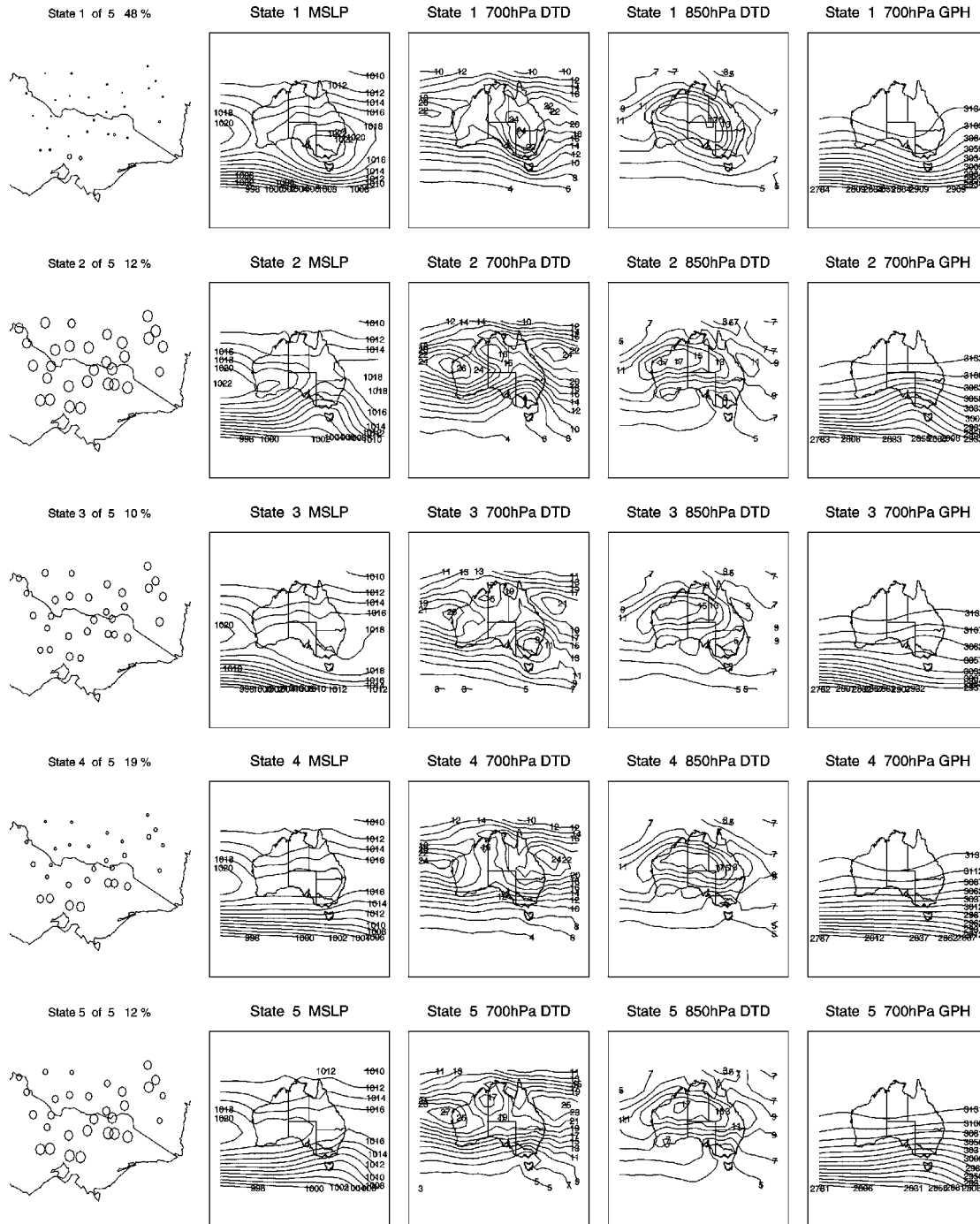


Figure 4: Weather states of the winter NHMM: precipitation occurrence probabilities, diameters of circles proportional to probability of a wet-day with the largest circle 1.0; composite MSLP (hPa); 700 hPa DTd (K); 850 hPa DTd (K); 700 hPa GPH (m).

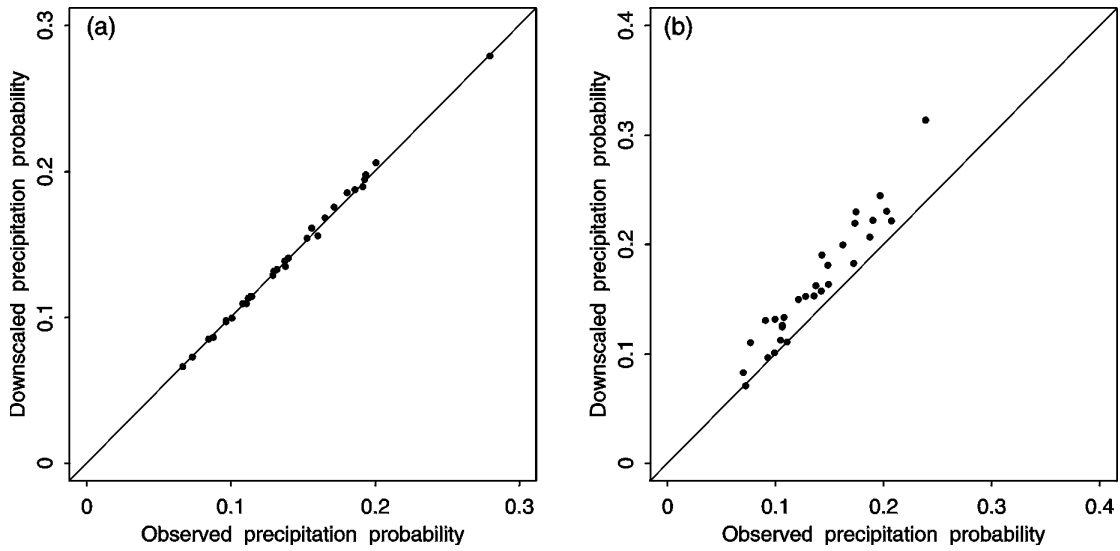


Figure 5: Summer NHMM precipitation probabilities (a) fitting period verification and (b) out-of-sample validation.

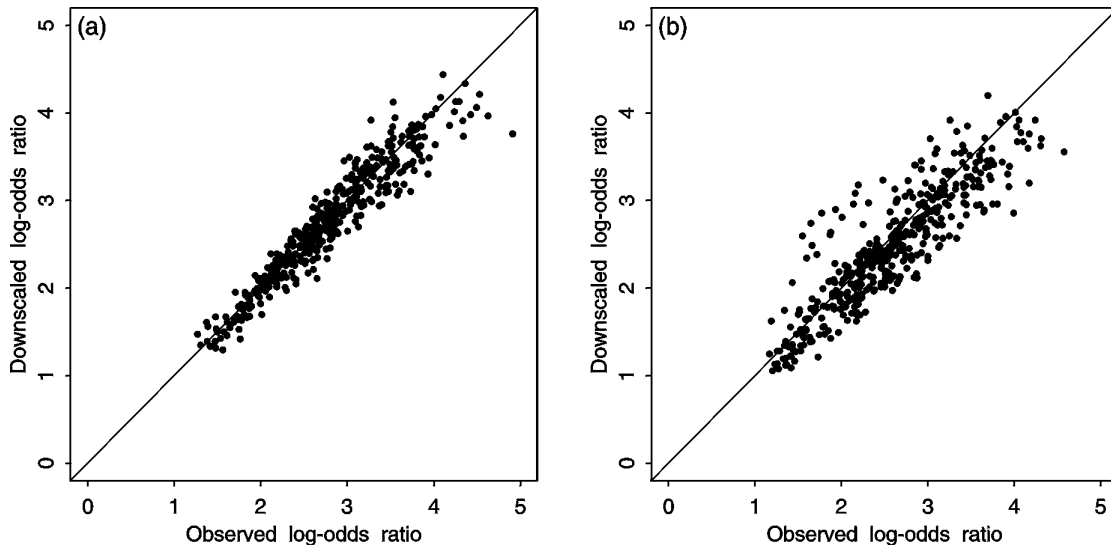


Figure 6: Summer NHMM log-odds ratios (a) fitting period verification and (b) out-of-sample validation.

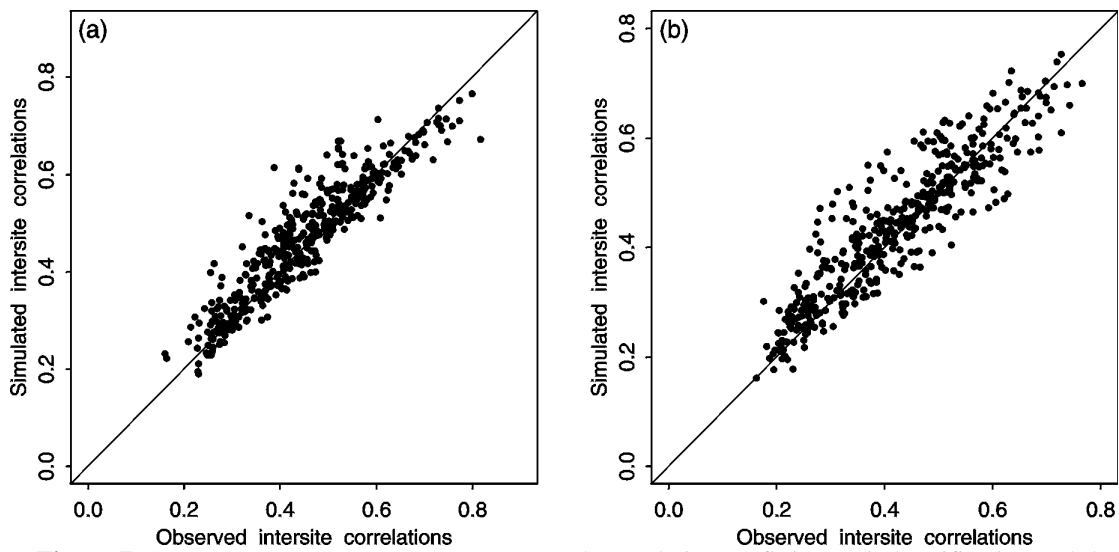


Figure 7: Summer NHMM amounts Spearman rank correlation (a) fitting period verification and (b) out-of-sample validation.

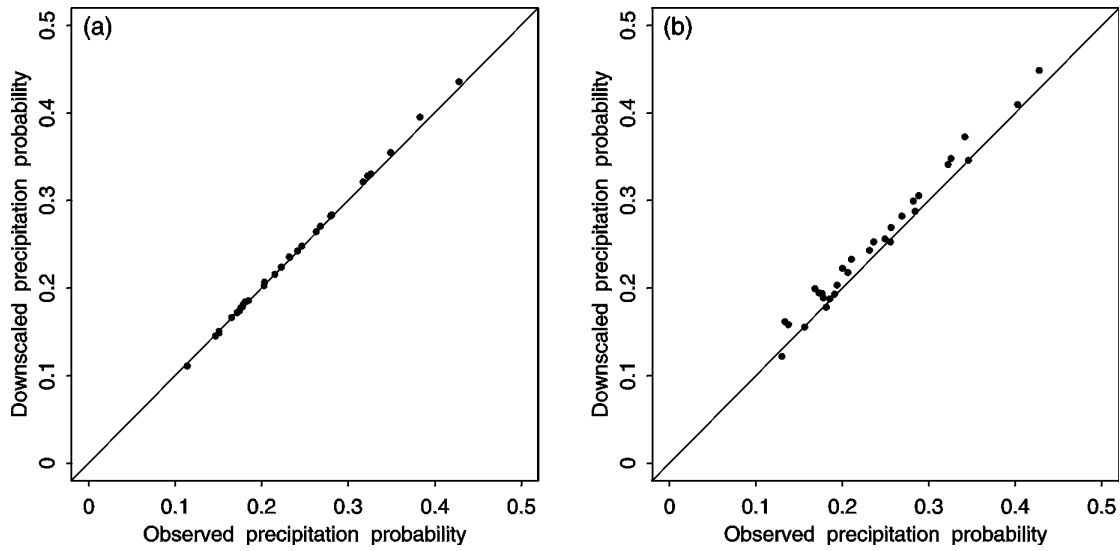


Figure 8: Winter NHMM precipitation probabilities (a) fitting period verification and (b) out-of-sample validation.

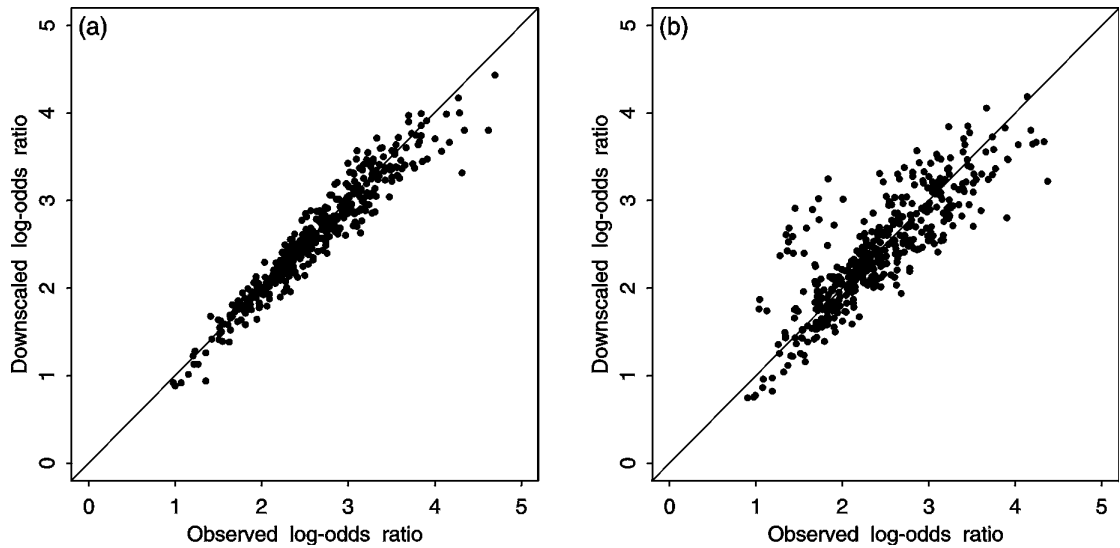


Figure 9: Winter NHMM log-odds ratios (a) fitting period verification and (b) out-of-sample validation.

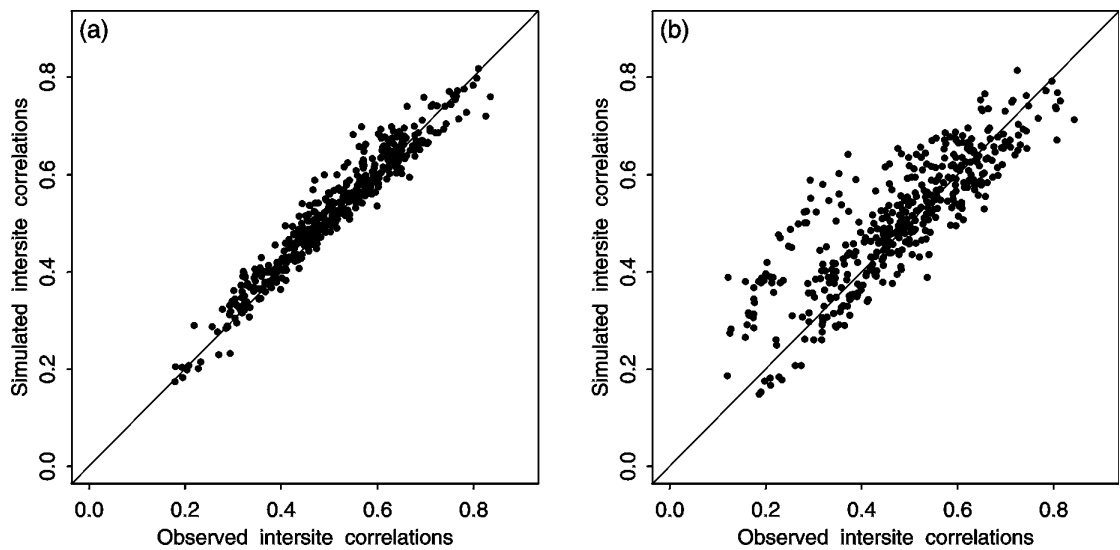


Figure 10: Winter NHMM amounts Spearman rank correlation (a) fitting period verification and (b) out-of-sample validation.



South Eastern Australian **Climate initiative**

Final report for Project 1.4.2

Reanalysis Archive Intercomparison

Principal Investigator: Steve Charles

CSIRO Land and Water, Private Bag 5, Wembley WA 6913,
Steve.Charles@csiro.au, Tel: 08 9333 6795, Fax: 08 9333 6499

Co-Authors:

Guobin Fu

CSIRO Land and Water, Private Bag 5, Wembley WA 6913, Guobin.Fu@csiro.au

Completed: 29 June 2007

Abstract

Reanalysis datasets are global atmospheric datasets created by assimilating observed weather data using state-of-the-art coupled GCMs. There are two datasets commonly used, one created by the National Centers of Environmental Prediction (NCEP) and the National Center for Atmospheric Research (NCAR) in the USA termed ‘NCEP/NCAR Reanalysis’ (Kalnay *et al.* 1996) and one created by the European Centre for Medium Range Weather Forecasting in Europe termed ‘ERA40’ (Uppala *et al.* 2005). There has been significant international research effort in quality controlling, assessing and comparing these datasets. The NCEP/NCAR Reanalysis dataset is used for statistical downscaling model calibration in SEACI Project 1.3.4. Here, the ERA40 fields over the SEACI region are extracted for the variables required to produce the predictor series used in the statistical downscaling models. Comparison of the spatial and temporal properties of the NCEP/NCAR and ERA40 predictor series shows a high degree of agreement. Reanalyses predictors thus provide a baseline for atmospheric conditions over the SEACI region that will be compared to predictors from CSIRO climate model historical runs in subsequent SEACI Projects.

Significant research highlights, breakthroughs and snapshots

Overall, it is evident that the two Reanalyses produce predictor series with a high degree of similarity. As well as giving confidence in the use of both these datasets to understand historical SEACI region atmospheric-rainfall linkages, this also provides a baseline to which historically forced climate model predictor series will be evaluated against.

The extracted ERA40 fields have been used to produce NHMM input predictor sets for the calibrated NHMMs selected in Project 1.3.4. Project 1.4.3 ‘*Comparison of Observed and Reanalyses Downscaled Synoptics and Precipitation*’ will statistically downscale these ERA40 predictor series and compare downscaled weather state and rainfall to those obtained by downscaling the NCEP/NCAR reanalysis predictor series previously extracted.

Statement of results, their interpretation, and practical significance against each objective

Objective 1: Extract atmospheric predictors required by statistical downscaling models from available Reanalyses archives (e.g., ERA40).

ERA40 fields for the 6 by 5 grid over the SEACI region (see Project 1.3.4 Report Figure 2) were extracted for 1958 to 2001 (44 years). The fields investigated were selected based on their use in statistical downscaling model calibration in Project 1.3.4.

Objective 2: Compare NCEP/NCAR and ERA40 predictors used by statistical downscaling models.

The distributions and monthly anomalies of the daily NCEP/NCAR and ERA40 Reanalyses fields were compared. Odd numbered Figures 1 to 11 show the monthly ERA40 anomalies (relative to NCEP/NCAR) of the daily atmospheric predictors used. These show monthly differences between the ERA40 and NCEP/NCAR Reanalyses across the region. They are used here for qualitative comparison, to see where the two reanalyses products deviate. Correspondingly, the quantile-quantile plots comparing the distributions of the daily predictor series are shown in even numbered Figures 2 to 12. These plot the percentiles of the cumulative distributions of the two series against each other. A plot with all points on the one-

to-one line indicates that the two datasets have the same distribution. A ‘U’ shaped plot means that one dataset’s distribution is skewed relative to the other, whereas a ‘S’ shape means that one dataset’s distribution has longer tails than the other. The sea level pressure (SLP) and geopotential height (GPH) fields are very similar between the two reanalysis datasets. The moisture related variables, dew-point temperature depression (DT_d) at the 700 and 850 hPa levels, are also similar with the exception that higher values (indicating drier air) are not as frequent in the ERA40 dataset. It is not possible to say which reanalysis dataset, NCEP/NCAR or ERA40, is the more realistic. It is more a case of assessing the effect of these deviations on statistically downscaled rainfall series, which will be undertaken in Project 1.4.3.

Summary of methods and modifications (with reasons)

- Codes for extracting ERA40 atmospheric fields for the variables (predictors) required for statistical downscaling over south-eastern Australia been developed and tested.
- The extracted ERA40 fields have been compared to the NCEP/NCAR fields. A spatial and temporal multi-variate intercomparison has been undertaken for the predictors over south-eastern Australia that shows good agreement between NCEP/NCAR and ERA40.

Summary of links to other projects

The extraction and assessment of ERA40 statistical downscaling predictors undertaken in this project is a precursor to Project 1.4.3 *Comparison of Observed and Reanalyses Downscaled Synoptics and Precipitation* where the NCEP/NCAR and ERA40 downscaled weather state series will be assessed and compared to observed rainfall trends. Also, the results of this Project will be used in assessing GCM performance in the subsequent Project 1.5.2 *‘Extraction of Predictors from Coupled Climate Model Historical Runs’*.

Publications arising from this project

None to date.

Acknowledgement

The archives of both the NCEP/NCAR and ERA40 Reanalysis data are maintained on CSIRO servers by Mark Collier, CMAR. His assistance is gratefully acknowledged.

Recommendations for changes to work plan from your original table

None

References

- Kalnay, E., M. Kanamitsu, R. Kistler, W. Collins, D. Deaven, L. Gandin, M. Iredell, S. Saha, G. White, J. Woollen, Y. Zhu, A. Leetmaa, R. Reynolds, M. Chelliah, W. Ebisuzaki, W. Higgins, J. Janowiak, K. C. Mo, C. Ropelewski, J. Wang, R. Jenn, and D. Joseph, 1996: The NCEP/NCAR 40-year reanalysis project, *Bulletin of the American Meteorological Society*, **77**, 437-471.
- Uppala, S.M., Kållberg, P.W., Simmons, A.J., Andrae, U., da Costa Bechtold, V., Fiorino, M., Gibson, J.K., Haseler, J., Hernandez, A., Kelly, G.A., Li, X., Onogi, K., Saarinen, S., Sokka, N., Allan, R.P., Andersson, E., Arpe, K., Balmaseda, M.A., Beljaars, A.C.M., van de Berg, L., Bidlot, J., Bormann, N., Caires, S., Chevallier, F., Dethof, A., Dragosavac, M., Fisher, M., Fuentes, M., Hagemann, S., Hólm, E., Hoskins, B.J., Isaksen, L., Janssen, P.A.E.M., Jenne, R., McNally, A.P., Mahfouf, J.-F., Morcrette, J.-J., Rayner, N.A., Saunders, R.W., Simon, P., Sterl, A., Trenberth, K.E., Untch, A., Vasiljevic, D., Viterbo,

P., and Woollen, J. 2005: The ERA-40 re-analysis. *Quart. J. R. Meteorol. Soc.*, 131, 2961-3012.doi:10.1256/qj.04.176

Project Milestone Reporting Table

To be completed prior to commencing the project				Completed at each Milestone date	
Milestone description ¹ (brief) (up to 33% of project activity)	Performance indicators ² (1- 3 dot points)	Completion date ³ xx/xx/xxxx	Budget ⁴ for Milestone (\$) (SEACI contribution)	Progress ⁵ (1- 3 dot points)	Recommended changes to workplan ⁶ (1- 3 dot points)
1. Develop and test codes to extract required predictors from ERA40	Codes working. Fields extracted over south-east Australian region.	1/5/2007	10K	Completed.	None.
2. Compare ERA40 extracted fields to previously extracted NCEP/NCAR fields	Fields compared. Report on comparison (3-5 pages).	30/6/2007	5	Completed. This report is the report on comparison of NNR and ERA40 predictor fields.	None.
3. Extract ERA40 fields for south-east Australian region in format required for NHMM	NHMM input files created.	30/6/2007	5	Completed.	None.

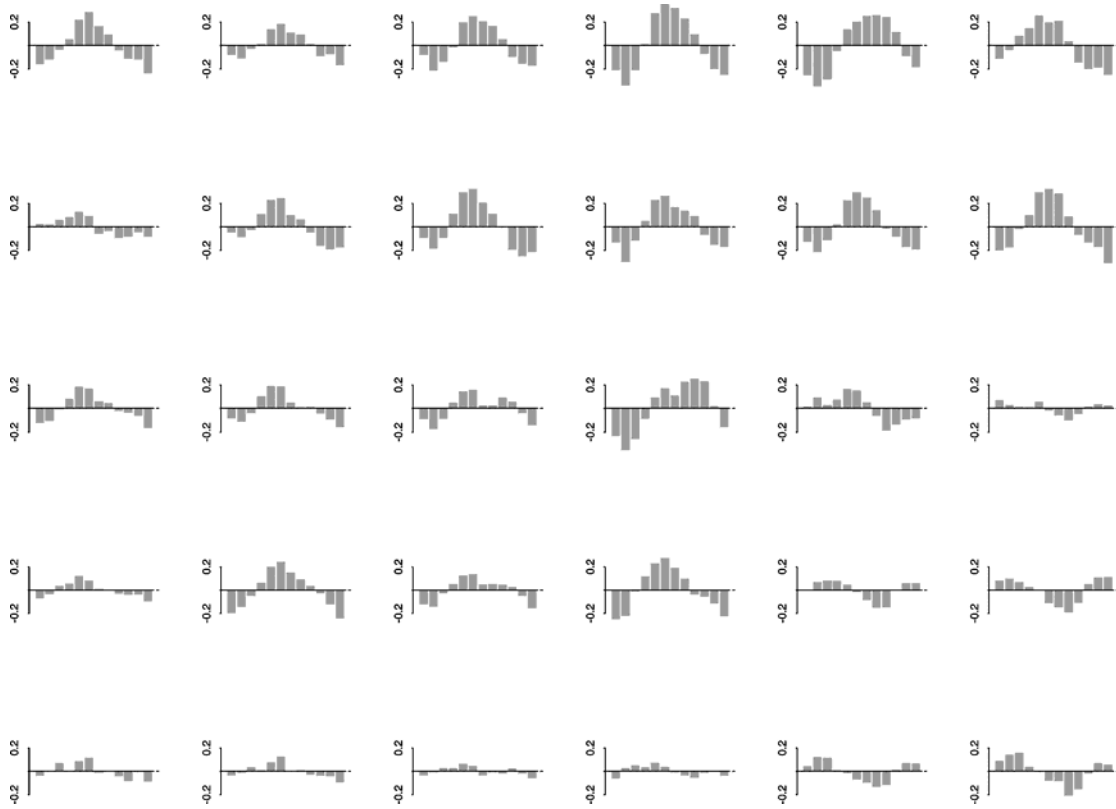


Figure 1. Monthly anomalies of ERA40 SLP (hPa), relative to NCEP/NCAR, for the 6 by 5 grid over south east Australia.

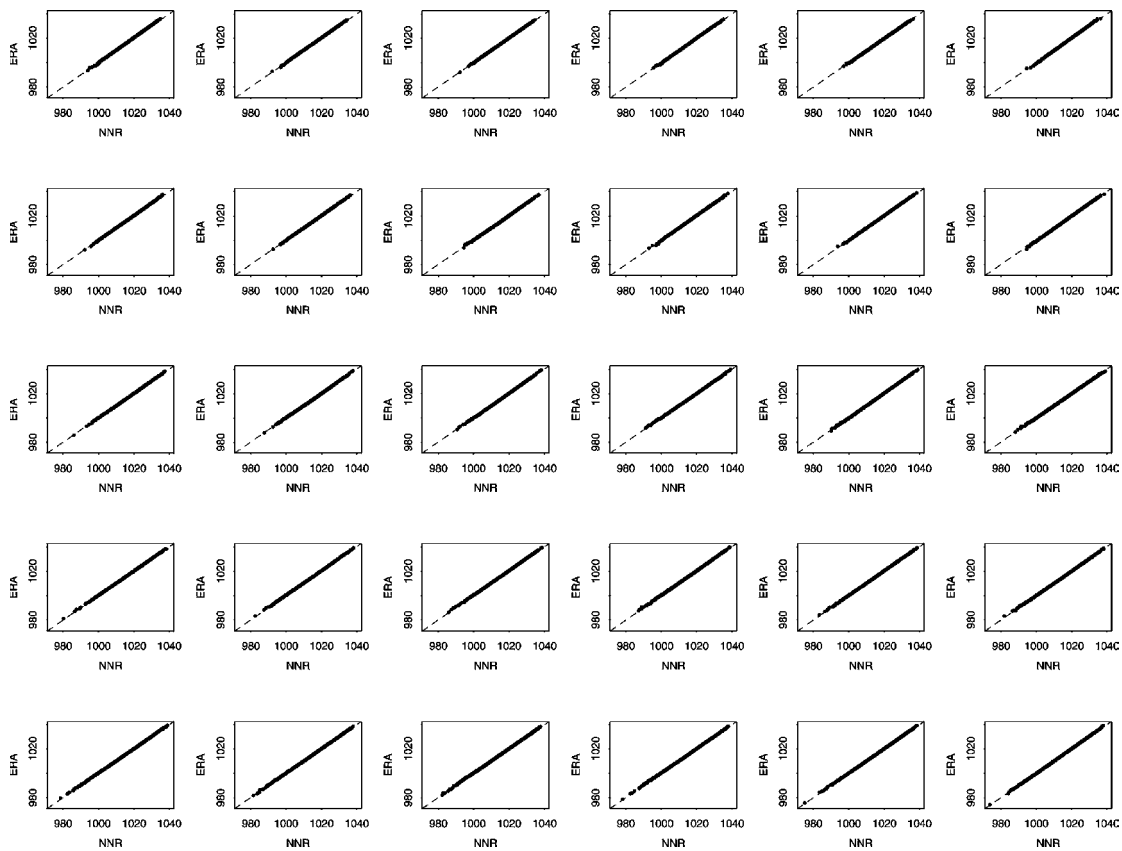


Figure 2. Distribution of daily NCEP/NCAR versus ERA40 SLP (hPa) for the 6 by 5 grid over south east Australia.

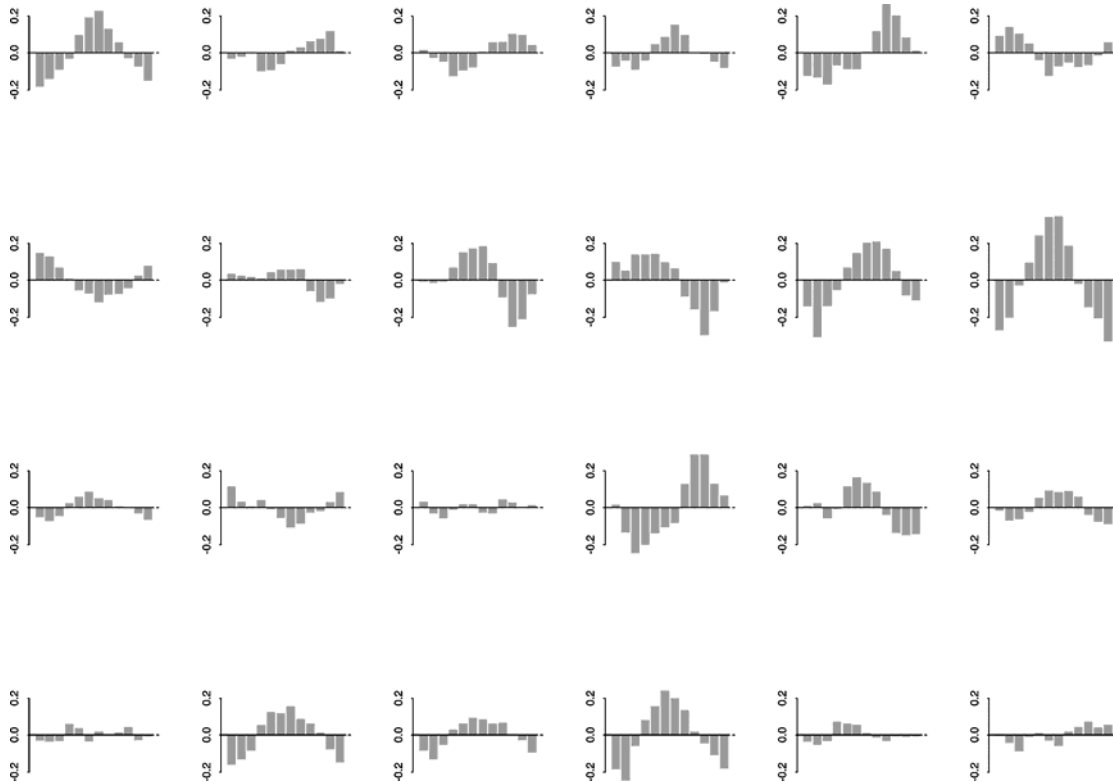


Figure 3. Monthly anomalies of ERA40 North-South SLP gradient (hPa), relative to NCEP/NCAR, for the 6 by 5 grid over south east Australia.

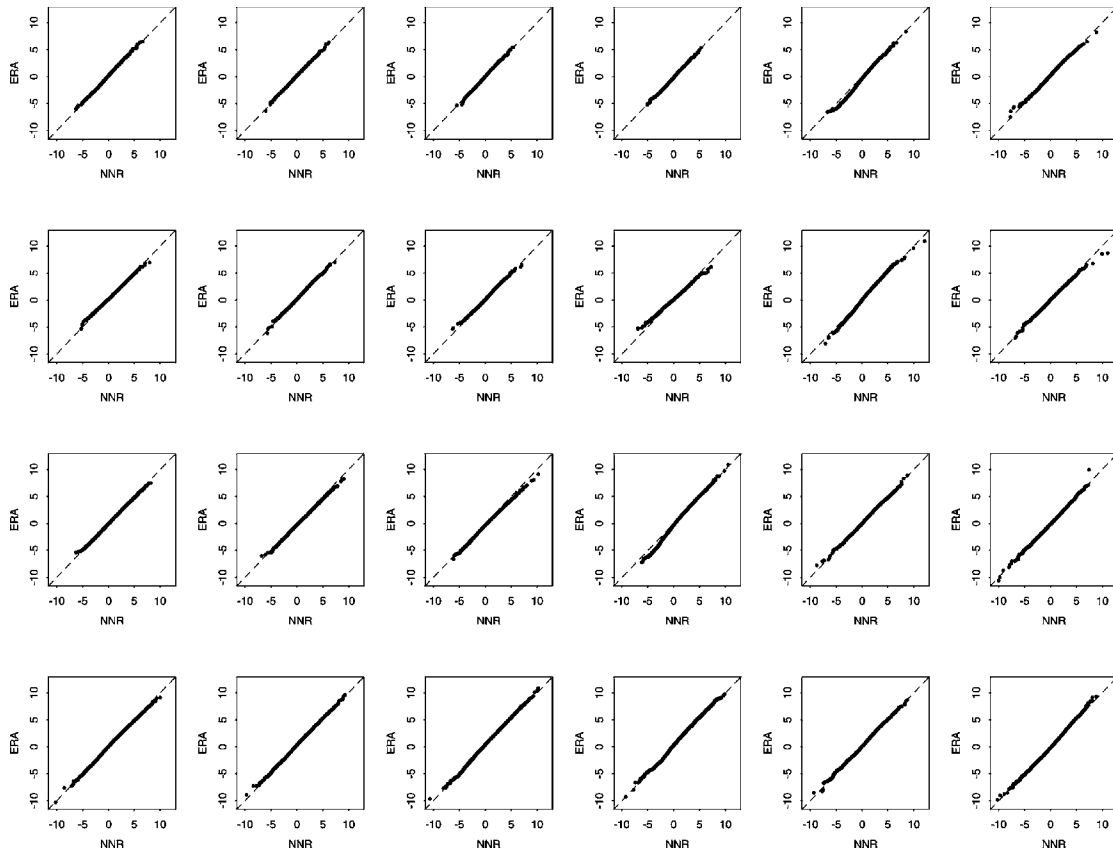


Figure 4. Distribution of daily NCEP/NCAR versus ERA40 North-South SLP gradient (hPa) for the 6 by 5 grid over south east Australia.

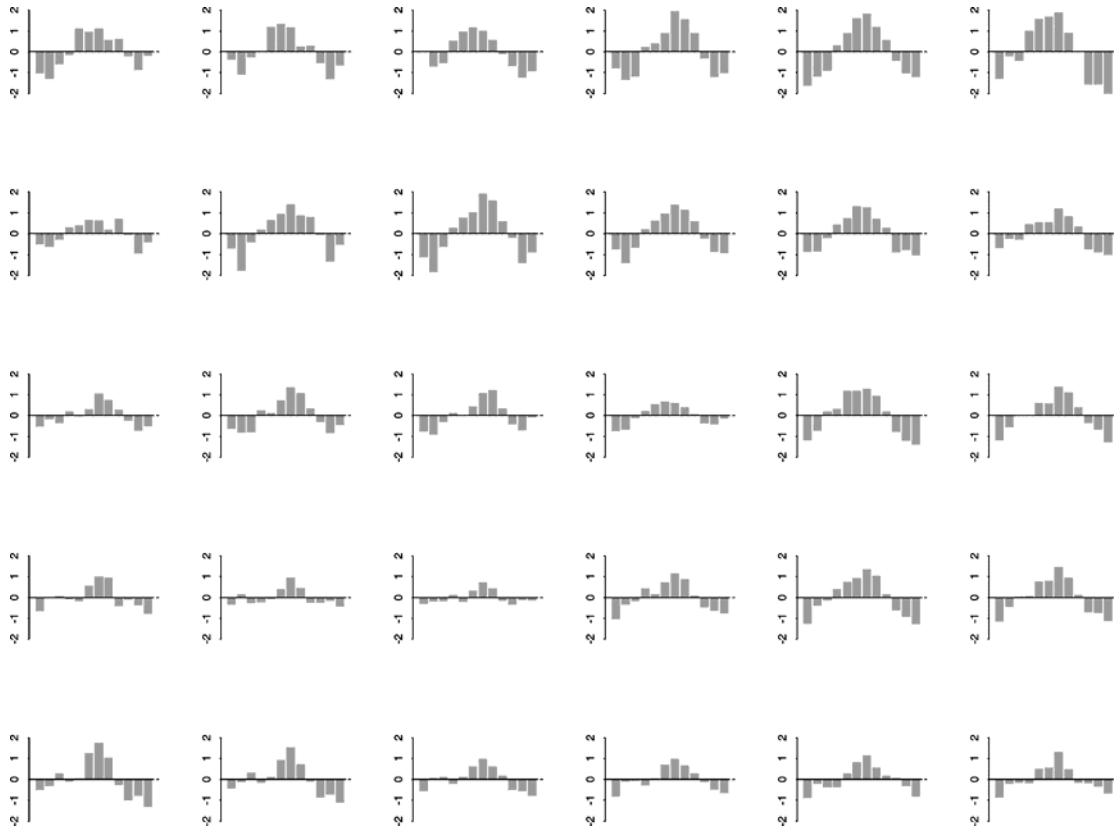


Figure 5. Monthly anomalies of ERA40 DT_{d700} ($^{\circ}C$), relative to NCEP/NCAR, for the 6 by 5 grid over south east Australia.

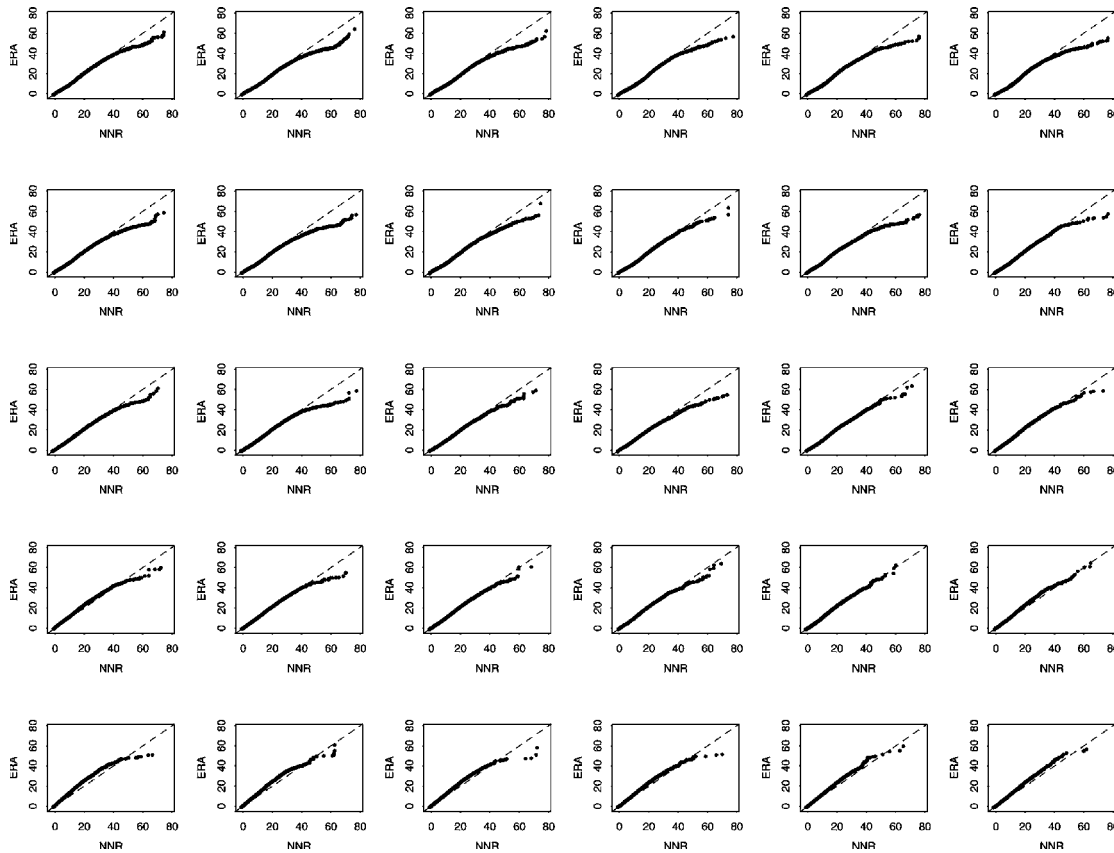


Figure 6. Distribution of daily NCEP/NCAR versus ERA40 DT_{d700} ($^{\circ}C$) for the 6 by 5 grid over south east Australia.

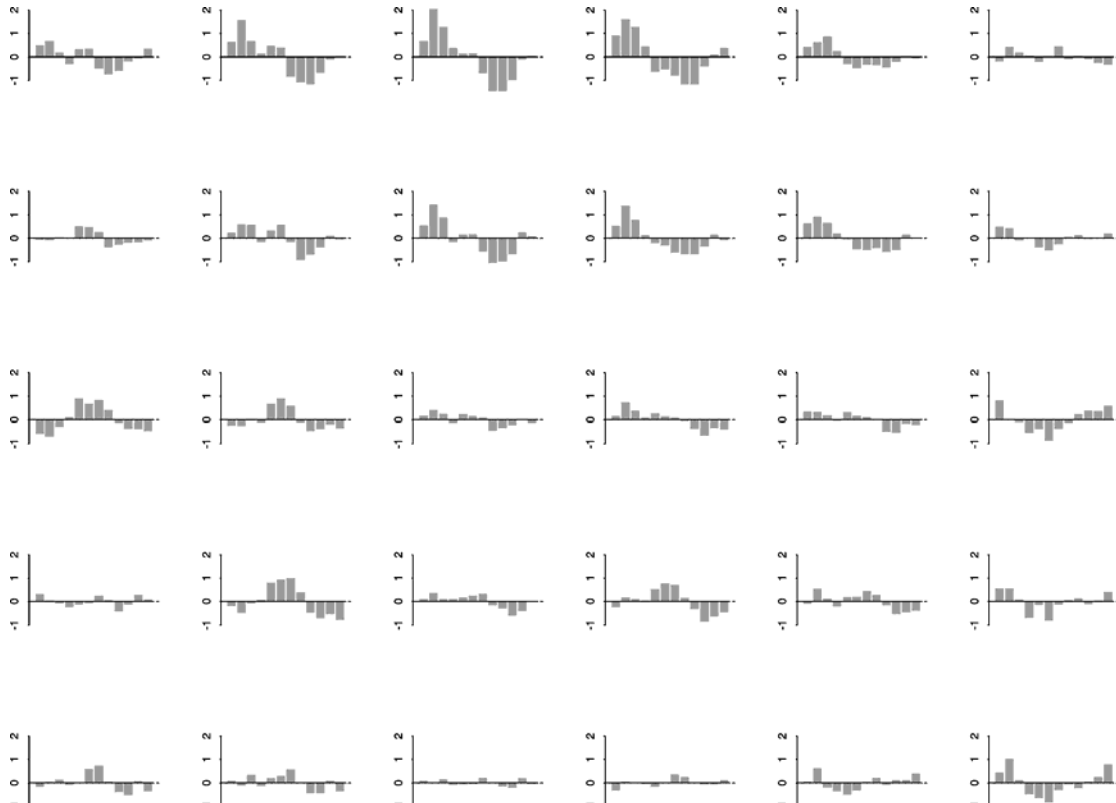


Figure 7. Monthly anomalies of ERA40 DT_{d850} ($^{\circ}C$), relative to NCEP/NCAR, for the 6 by 5 grid over south east Australia.

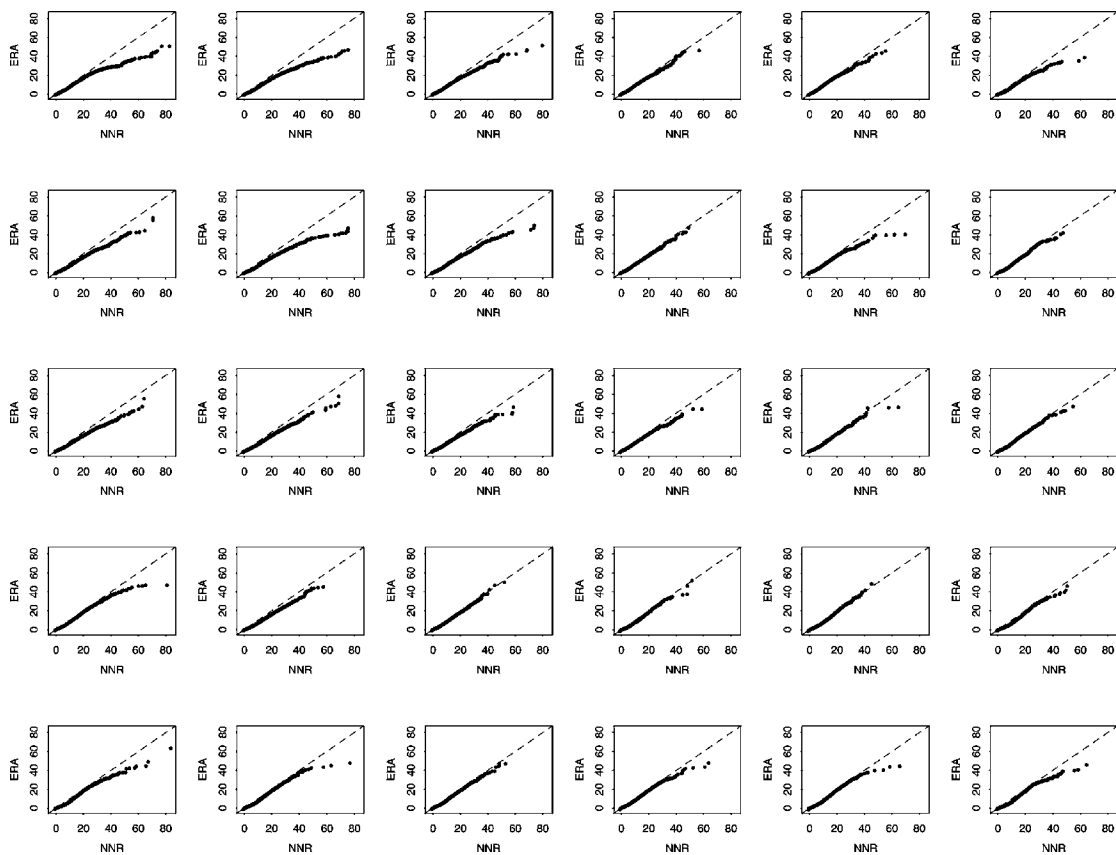


Figure 8. Distribution of daily NCEP/NCAR versus ERA40 DT_{d850} ($^{\circ}C$) for the 6 by 5 grid over south east Australia.

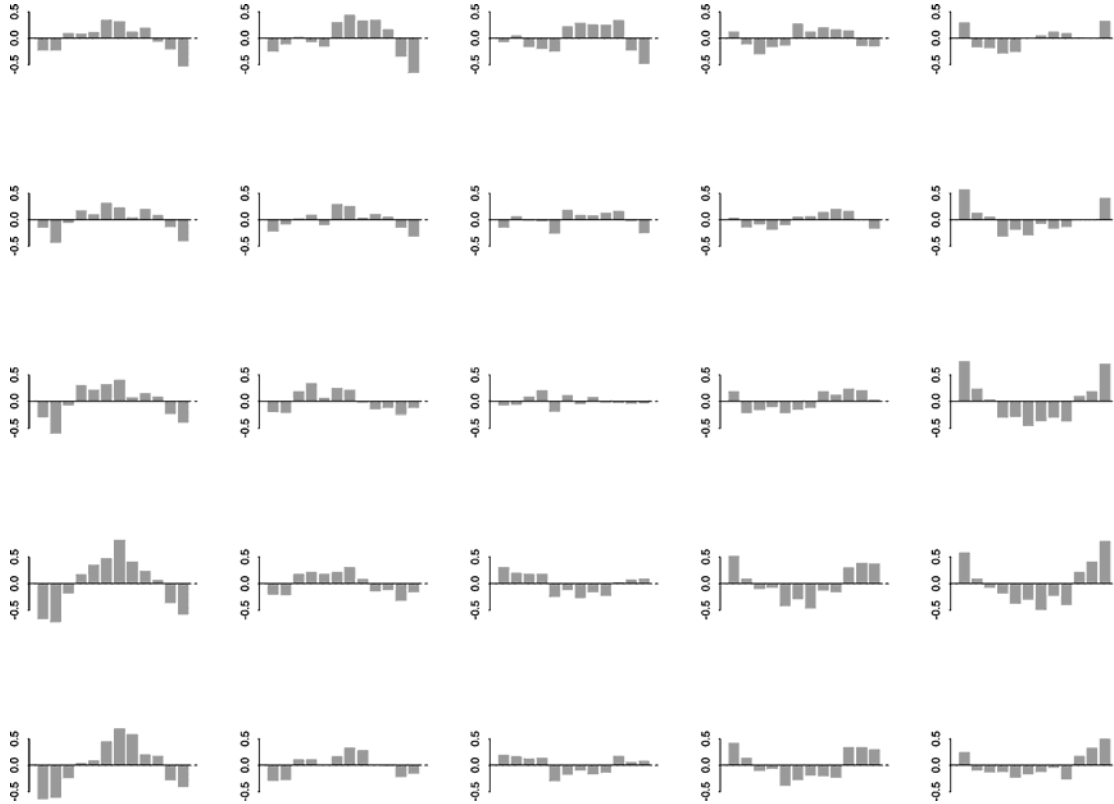


Figure 9. Monthly anomalies of ERA40 East-West GPH500 gradient (m), relative to NCEP/NCAR, for the 6 by 5 grid over south east Australia.

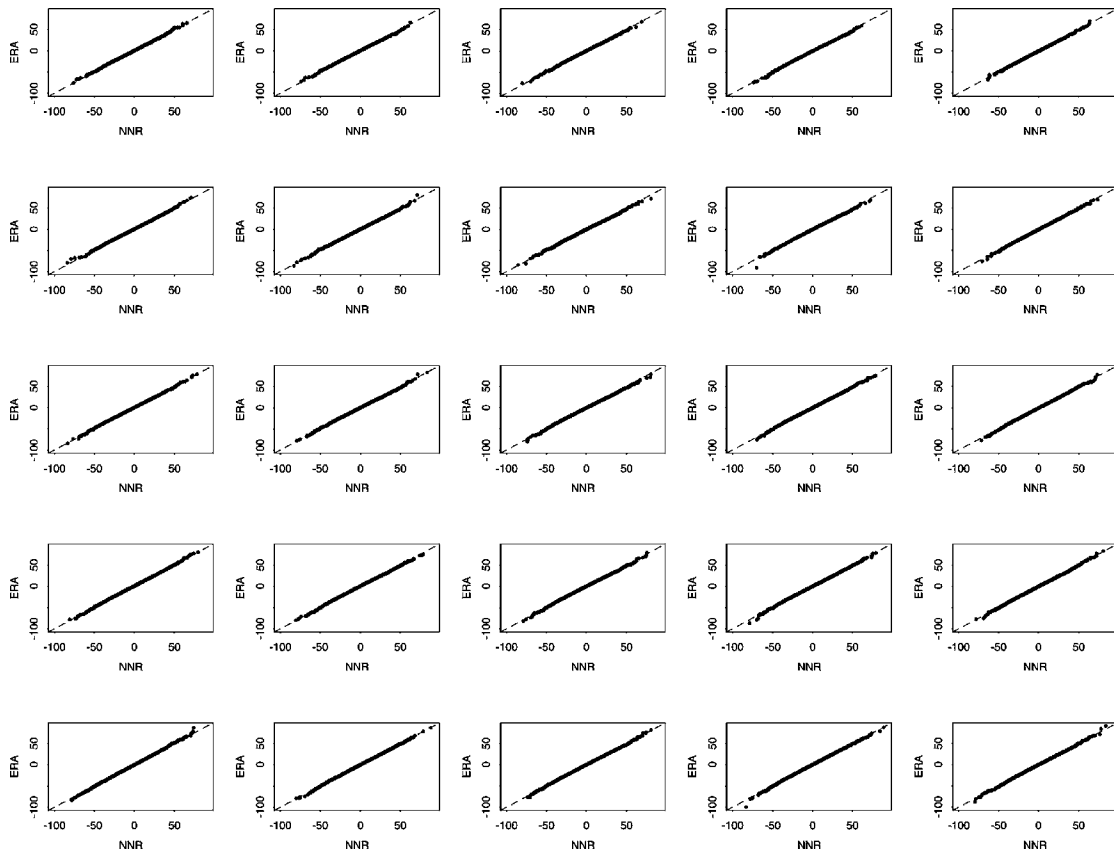


Figure 10. Distribution of daily NCEP/NCAR versus ERA40 East-West GPH500 gradient (m) for the 6 by 5 grid over south east Australia.

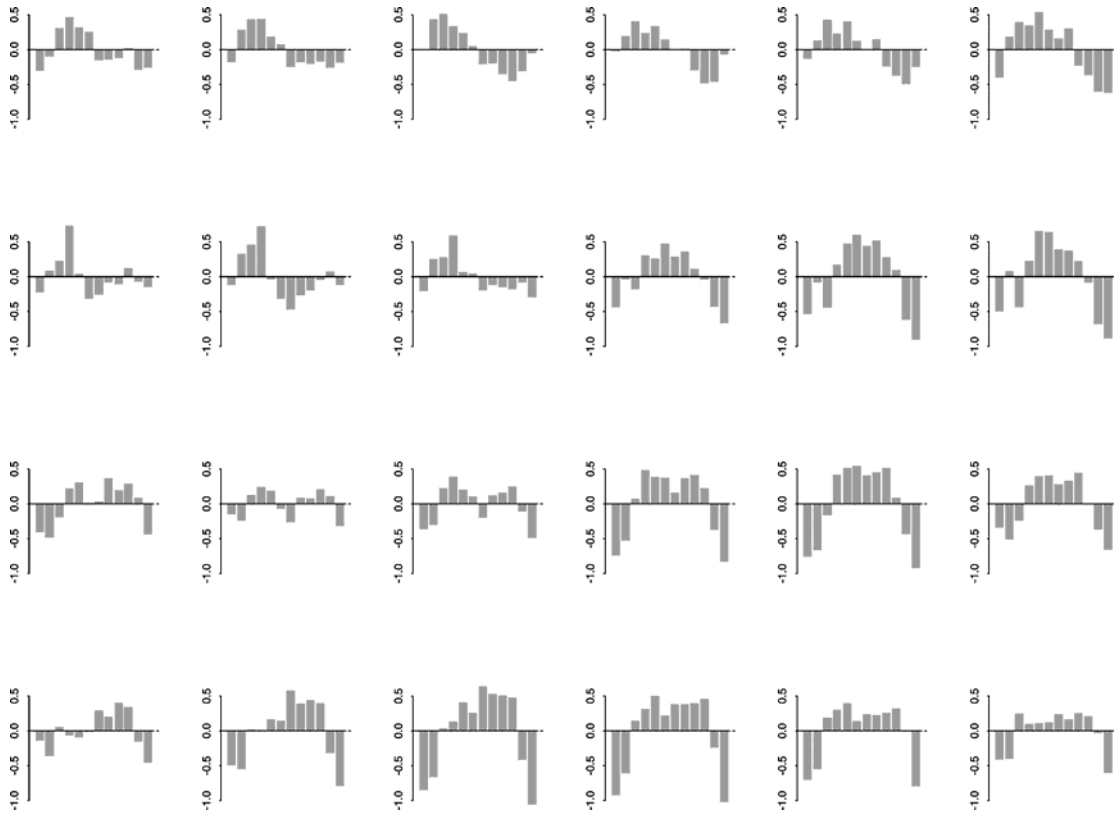


Figure 11. Monthly anomalies of ERA40 North-South GPH700 gradient (m), relative to NCEP/NCAR, for the 6 by 5 grid over south east Australia.

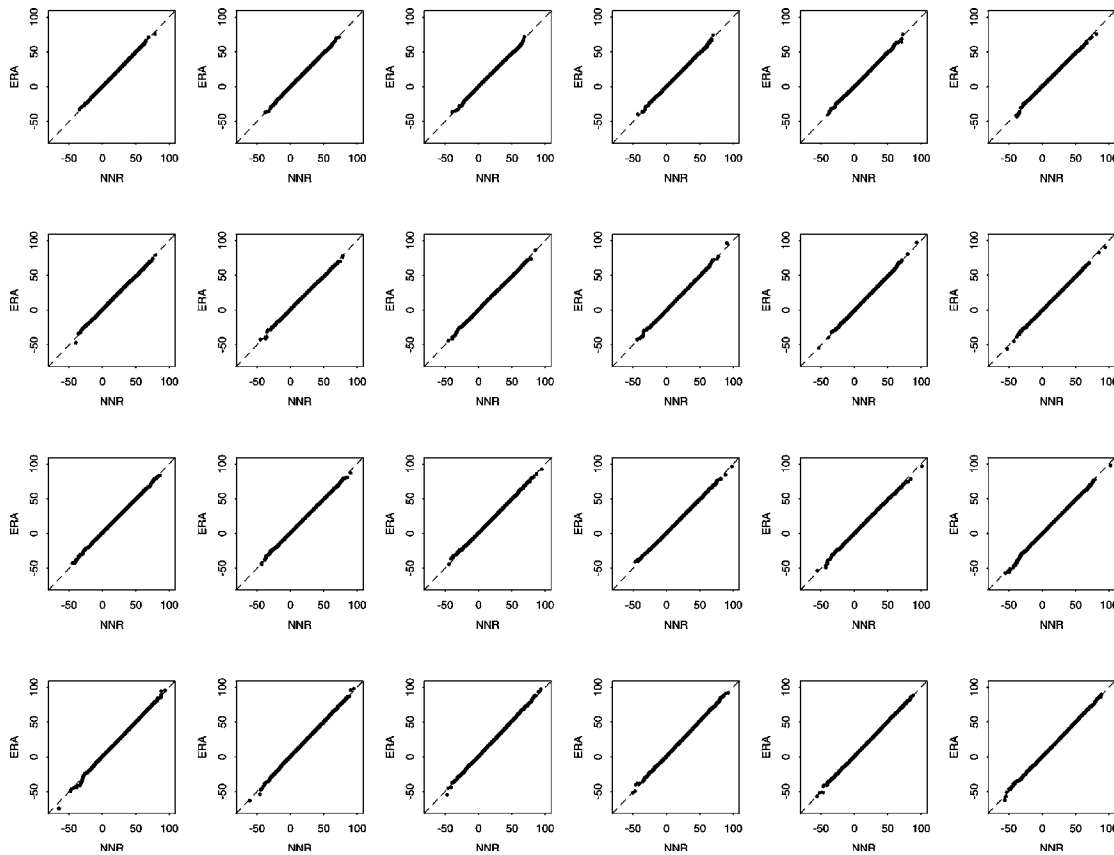


Figure 12. Distribution of daily NCEP/NCAR versus ERA40 North-South GPH700 gradient (m) for the 6 by 5 grid over south east Australia.



South Eastern Australian **Climate initiative**

Final report for Project 2.2.3a

Develop improved regional projection techniques for MDB and the CMA regions of Victoria using multi-model weighted approach

Principal Investigator: Ian Smith

CSIRO Marine and Atmospheric Research, ian.smith@csiro.au, PMB 1, ASPENDALE, VIC, 3195, Ph: 03 9239 4400 Fax: 03 9239 4444

Co-Authors: Ian Watterson Penny Whetton

CSIRO Marine and Atmospheric Research, ian.watterson@csiro.au, penny.whetton@csiro.au PMB 1, Aspendale, VIC, 3195, Ph: 03 9239 4400 Fax: 03 9239 4444

Completed: 30 June 2007

Abstract

In response to stakeholder demands for both less uncertain regional climate change predictions and probabilistic information, new methods have been developed for synthesizing the results from numerous climate model experiments. This report describes a new method for generating probability density functions for scaled warming and net warming for points over south-east Australia. The method allows for weighting of different model results and has been demonstrated using the results from four models. In addition, a method for weighting different model results has also been developed and this is demonstrated using the results for rainfall for the Murray Darling Basin region from 22 models. Project 2.2.3b will demonstrate the results of the application of these new methods to the key regions.

Significant research highlights, breakthroughs and snapshots

- A trial set of probability distributions for DJF temperature change at a grid point in the vicinity of the MDB indicates a mean net warming of about +4.0°C at 2100.
- Results also indicate that severe weighting, based on model performance criteria, can result in a significantly different mean response for MDB rainfall than that based on equal weighting of all model results. Preliminary results indicate the mean response is much drier.
- There is now an increasing recognition amongst the research community of the importance of careful assessment of climate model simulations before their results are used in impacts studies. This was reflected in feedback from a Climate and Hydrology Symposium recently held in Canberra where some of this work was reported.

Statement of results, their interpretation, and practical significance against each objective

Objective 1: To develop new methods for projections for the MDB and the CMA regions of Victoria using a multi-model weighted approach.

The technique for developing probability distributions is sufficiently general to be extended to a larger set of model results and other variables. It will be used to produce a new set of Australia-wide set of projections based on the IPCC Fourth Assessment Report model results.

Objective 2:

To provide information in response to stakeholder feedback which indicate a preference for probabilities.

The results indicate that estimates for the 5% and 95% confidence thresholds for DJF arming at 2100 are about +2.8 °C and +3.2 °C respectively.

They also indicate a potentially significant shift in derived probabilities for rainfall projections. These appear to be much less uncertain than previously shown. This will be further examined as part of Project 2.3.b.

1. Background

Projections at regional scales tend to be accompanied by relatively large uncertainties due to differences in model formulations, resolution, and simulated responses combined with differences in possible future emission scenarios (CSIRO, 2006; Whetton et al, 2005). Model developments, including improved physical parameterizations and the use of higher spatial resolutions, plus more simulations (i.e. the creation of multi-model ensembles) can potentially improve the reliability of regional scale results but it is apparent they will always be accompanied by some level of uncertainty.

Recently, regional rainfall projections produced by Whetton et al. (2005), CSIRO (2006) and Suppiah et al. (2007) used methods similar to those described Giorgi and Mearns (2002) in which a range of model results are sorted according to how well they represent features of the present day climate, but the projections simply presented as ranges of (equally likely) outcomes. Even so, the ranges remained relatively wide, particularly for south-eastern Australia (SEA), and there was not a great deal of difference between these and the previous projections based on fewer models and less stringent criteria (CSIRO, 2001). Stakeholders would like to see uncertainty minimized if possible and/or to have it quantified in a more useful fashion (i.e. generally in the form of probabilities or, more specifically, probability density functions (PDFs)). This is evident from key messages which emerged from a recent survey of focus groups (“2007 climate change projections for Australia: stakeholder feedback”):

- Generally, stakeholders are interested in the best case scenario, the worst case scenario, the most likely scenario and business as usual
- Likelihood is an important factor, so including probabilities is essential
- Stakeholders want to be able to compare 2007 projections with 2001 projections and with observations
- Stakeholders want regional information

For the Third Assessment Report (IPCC, 2001) there were 15 sets of model results available for preparing projections but 23 sets of results were available for the Fourth Assessment Report (AR4) (IPCC, 2007).

In this report we describe and demonstrate a method for generating probabilistic information.

This approach forms the basis of the new CSIRO/BoM climate change projections to be released later this year (Watterson, 2007). In addition we also describe and demonstrate a method for weighting the various model results. Appendices 1 and 2 contain further details of these methods.

2. Generating probabilistic climate change projections

The main aim is to provide a confidence weighting throughout the range of change considered plausible, basing this on the data from simulations by a number of current climate models. For most quantities this means, in effect, a ‘probability density function’ (PDF) for the change variable. Several recent studies have provided such results based on various approaches and assumptions, often of considerable complexity. A new, relatively simple method, has been applied to the results from

four models to produce surface warming projections for a point over south east Australia.

A number of methods for generating a PDF for scaled warming are illustrated in Fig. 1. Allowing for statistical uncertainty, the true value for each model (from multiple runs) is assumed to be from a simple normal PDF centred on the sample value. The uncertainty is determined from that appropriate to differences of two 30-y means, assuming these follow from the interannual standard deviation (SD) field, then scaled. The weighted sum of the four individual distributions is the 'Sum' PDF in Fig 1. (Weights used here are described in Appendix 1.) The normal distribution fitted to this Sum curve is also shown (as Normal). The beta distribution fit to the Sum curve is also shown. The 'Uniform' distribution is between the smallest and largest of the four change ratios. The final curve 'Narrow' is a normal fit to Sum, but with the SD reduced by the square root of the 'effective number of models'. This distribution would be appropriate if one considered the various model results to be a sample from a normal distribution centred on the 'true' change.

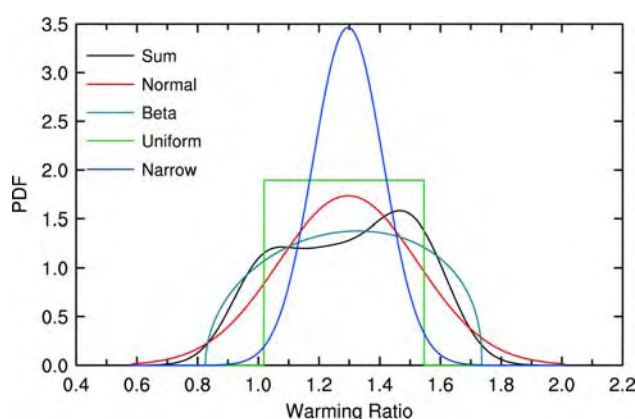


Figure. 1. Probability distribution functions for the warming ratio (local to global average warming) at a point over southeast Australia.

The warming ratio needs to be combined with the actual global mean warming (with its associated uncertainty) to produce a net change. The assumption is made that the scaled local change and the global warming are considered two independent variables. The joint distribution function is simply the product of the two PDFs. Statistics of the net local change can be determined numerically from this joint function.

For the A1B scenario in 2100, a value global average warming of around 3 K (or °C) is suggested by models. If, for simplicity it is assumed to be exactly 3K (i.e. SD=0.0 K), then the joint PDF for the local warming has the same shape as the scaled warming PDF. If the global warming is uncertain with SD=1 K, then the net warming PDFs for the central point are shown in Figure 2. The differences are surprisingly small. The Uniform and Narrow cases give a slightly narrower net warming.

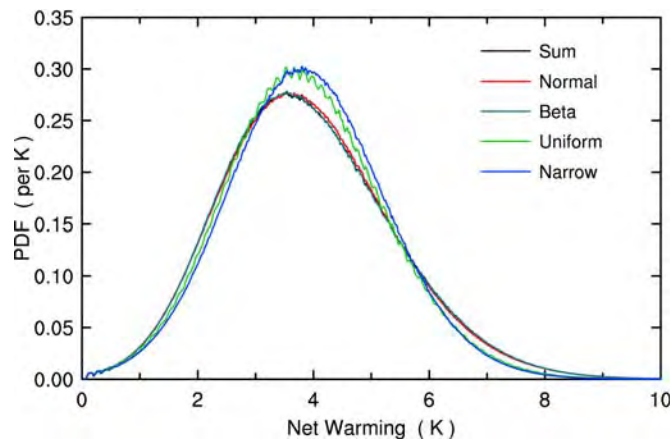


Figure 2. Probability distribution function for net warming at the point calculated from the five warming ratio PDFs and assuming the SD for global warming is 1K.

An intermediate case ($SD=0.2$ K) produces the net warming curves for the central point shown in Fig. 3. The PDFs more closely reflect the differences in Fig. 1.

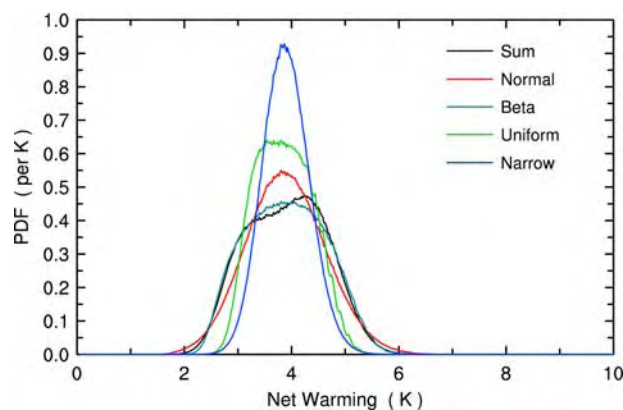


Figure 3. Probability distribution function for net warming at the point calculated from the five warming ratio PDFs and assuming the SD for global warming is 0.2 K.

3. Selecting climate change results based on model performance

Here we describe an assessment of models rainfall results for the Murray Darling Basin (MDB) region. This technique can be used to restrict the number of models contributing to the calculated PDFs described above.

23 AR4 model results (based on the A1B emissions scenario) were assessed. Several approaches were taken to determine the best models performing models with regard to Australia wide annual and seasonal rainfall. A set of best model results were selected as those with above median spatial correlation coefficients and those with below median root mean square errors. In addition to assessing the seasonal mean values, the models were also assessed in terms of their ability to reproduce the seasonal cycle of rainfall at several key locations, including the MDB. Finally, the results from the coarse resolution models were excluded since previous studies have highlighted the importance of horizontal resolution and the representation of topography as crucial to model rainfall.

The details of the full assessment are not shown here but, it is apparent that some simulations are clearly inferior, failing to adequately reproduce either the broad spatial patterns or the quantitative amounts. Of the 22 models, 7 were assessed to provide the best simulations of present day rainfall: (GFDL-Cm2.0, ECHAM5, GISS-AOM, UKMO-HADcm3, MIROC3.2 (hires), GFDL-CM2.1 and UKMO-HADgem1).

Annual and seasonal percentage changes in rainfall for the period 2071-2100 relative to 1971-2000 based on the results using the A1B emissions scenarios (a mid-range scenario) were calculated for each model. These values are shown in Table 1.

Table 1. List of 22 model results for the projected percentage change in rainfall (2071 to 2100) vs (1971-2000). The top 7 selected models are highlighted.

Model	Percentage change in rainfall				
	Annual	Seasonal			
		DJF	MAM	JJA	SON
CSIRO-Mk3	-11.322	4.466	-15.344	-21.270	-30.431
GFDL-CM2.0	-12.410	28.991	3.562	-24.669	-34.333
MRI-CGCM2.3.2	-10.466	-23.397	-21.245	-23.397	-5.572
ECHAM5/MPI	-13.484	-5.725	15.261	-31.692	-32.450
GISS-ER	5.210	20.388	1.922	-17.495	-1.846
FGOALS-G1.0	-4.575	-3.917	-10.238	-5.016	-1.659
MIROC3.2(medres)	20.688	48.390	41.733	-11.238	-0.223
ECHO-G	22.783	59.088	22.942	-16.677	1.451
CCSM3	7.205	12.315	7.876	-10.856	15.790
GISS-AOM	-20.329	-28.843	19.923	-26.280	-29.721
UKMO-Hadcm3	-14.435	-7.082	6.650	-10.674	-40.274
GISS-EH	18.648	23.904	19.404	13.046	13.502
INM-cm3.0	-6.851	7.147	3.022	-19.065	-17.389
MIROC3.2(hires)	-6.016	5.458	6.496	-13.575	-25.254
CGCM3.1(t47)	11.343	6.238	14.308	15.988	8.202
GFDL2.1	-19.963	-1.245	-23.409	-46.104	-12.085
CGCM3.1(t63)	18.705	34.496	14.570	11.931	11.583
BCCR-BCM2	10.103	12.732	37.770	-12.632	5.467
CNRM-CM3	-7.372	7.360	18.003	-36.970	-35.549
IPSL-CM4	-33.637	-19.862	-31.908	-34.185	-52.639
UKMO-HADGEM1	-18.704	8.374	-28.881	-35.057	-30.272
PCM	-5.919	-7.968	-9.864	11.399	-16.497
22-model average	-3.2	8.2	4.2	-16	-14
22-model range	-33 to +23	-24 to +59	-31 to +42	-46 to +16	-53 to +16
Best 7 average	-15	-0.01	-0.06	-27	-29
Best 7 range	-20 to -6	-29 to +8	-29 to +20	-46 to -11	-40 to -12

The important result from this assessment is that the average changes from the best 7 models are more negative than the 22-model averages. Furthermore, this is not purely an artifact of the different sample sizes. T-statistics indicate that the best-7 sample results for rainfall and changes are significantly different to those of the remaining 15 models. For example, the chances that the 7-model average percentage change in annual rainfall (-15%) comes from the same population as the remaining 15 models is close to .001. In other words, the 7-best models form a distinctly different sub-set to

the other models. This is what we would expect if a poor simulation of present day climate is associated with an unreliable prediction of future climate.

These results need to be confirmed and recast into probabilities but it is apparent that the application of this new method paints a somewhat more pessimistic outlook for rainfall over the MDB into the future than previously indicated. We expect that it will be possible (Project 2.2.3b) to refine the projections for this region to better satisfy stakeholder expectations.

4. Summary

- Five different types of scaled warming PDF have been considered. Support for using each of these could be argued, although the uniform distribution, with no weighting of models is clearly outdated. The three other methods of fitting the spread of individual model results produce rather similar net warmings.
- A careful analysis of the performance of IPCC climate models at reproducing features of Australian rainfall has been undertaken. The results suggest that 7 (of the 23 assessed) should be accorded relatively high weightings when preparing PDFs.

The project objectives have been met and these findings will be used to generate the probabilistic information as described under Project 2.2.3b

Summary of methods and modifications (with reasons)

No modifications

Summary of links to other projects

The techniques that have been developed can now be applied to results for temperature and rainfall for the MDB and CMA regions as deliverables for Project 2.2.3b.

Recommendations for changes to work plan from your original table

Nil

Acknowledgements

This work was funded under the South East Australia Climate Initiative and the Australian Climate Change Science Program.

Publications arising from this project

Smith, I.N., Chandler, E., Suppiah, R and Watterson, I.G. (2007) Rainfall Projections: Are they really that uncertain? - results for the Murray Darling Basin. Abstract, Climate and Hydrology Symposium, Canberra, November 2007.

Watterson (2006) Some methods for specifying PDFs. CMAR Technical Note, 14 February, 2006.

Watterson, I.G. (2007) Calculation of probability functions for temperature and precipitation change under global warming. Abstract, Greenhouse2007.

Watterson, I.G. (2007) Calculation of probability density functions for temperature and precipitation change under global warming. Submitted to J.Geophys. Res.

References

Chandler, E. (2007) Reducing uncertainty in model results for Australian rainfall in the 21st century. *Abstract*, AMOS National Conference, Adelaide, February 2007.

CSIRO, 2001. Climate projections for Australia. CSIRO Atmospheric Research, Melbourne, 8 pp. <http://www.dar.csiro.au/publications/projections2001.pdf>

Suppiah, R., K. J. Hennessy, P. H. Whetton, K. McInnes, I Macadam, J. Bathols and J. Ricketts (2007) Australian climate change projections derived from simulations performed for the IPCC 4th Assessment Report. *Aus. Met Mag.* (in press).

Watterson, I. G. (2005) Climate change for the IPCC scenarios simulated by the IPCC multi-model ensemble: results scaled by global mean warming. *Internal report*, 24 May 2005.

Watterson (2006) Some methods for specifying PDFs. *CMAR note*, 14 February, 2006.

Watterson, I.G. (2007a) Simulation of climate and climate change by global models. *SEACI Project 2.1.5a report*, 23 November, 2006.

Watterson (2007b) Calculation of probability functions for temperature and precipitation change under global warming. *Journal of Geophysical Research* (submitted).

Whetton, P.H., McInnes, K.L., Jones, R.N., Hennessy, K.J., Suppiah, R., Page, C.M., Bathols, J., and Durack P. (2005) Climate change projections for Australia for impact assessment and policy application: A review. *CSIRO Technical Paper*. 001, Aspendale, Vic., CSIRO Marine and Atmospheric Research, 34p. http://www.cmar.csiro.au/e-print/open/whettonph_2005a.pdf

Whetton, P. H., Macadam, I., Bathols, J. M., and O'Grady, J. (2007). Assessment of the use of current climate patterns to evaluate regional enhanced greenhouse response patterns of climate models. *Geophysical Research Letters*, 34 (14): L14701, doi:10.1029/2007GL030025

Project Milestone Reporting Table

<p>Develop improved regional projection techniques</p>	<p>Report produced.</p>	<p>30/6/07</p>	<p>70</p>	<p>Techniques for deriving probability functions at grid points over the regions of interest have been developed.</p> <p>The effect of model weighting on the mean response has been demonstrated to be significant and an important component in deriving the probability functions.</p>	<p>None</p>
--	-------------------------	----------------	-----------	---	-------------

Appendix 1

Probabilistic Climate Change Projections for South East Australia: Surface Warming Examples

Ian G. Watterson

1. Introduction

We wish to provide improved methods of projecting climate change for Australia, building on the previous Climate Impact Group (CIG) approach described by Whetton et al. (2005). The main aim is to provide a confidence weighting throughout the range of change considered plausible, basing this on the data from simulations by a number of current climate models. For most quantities this means, in effect, a ‘probability density function’ (PDF) for the change variable. Several recent studies have provided such results based on various approaches and assumptions, often of considerable complexity. A new, relatively simple method, extending that of the CIG, was outlined in my previous note (Watterson, 2006). This is applied to a more realistic case here, to produce surface warming projections over south east Australia (specifically, the domain depicted in Figure 1). The models used and a simple estimation of weighting of them is presented in section 2. (I am able to make use of results prepared for both the SEACI and ACCSP modelling projects here.) Patterns of change (scaled by global mean warming) are considered in Section 3, and probabilistic scaled warming is presented, determined using five approaches. The distributions for net warming under three idealised global mean warming distributions are calculated and presented in Section 4.

2. GCM simulations of climate and climate change for South East Australia

In support of the 2007 Fourth Assessment Report on climate change by the IPCC, a major climate simulation project has been organised by the World Climate Research Program. Some 17 modelling centres from 9 countries have performed simulations of the period 1870-2100 and beyond, using their current climate models. The experiments include prescribed greenhouse gas (GHG) and aerosol changes based on observations to 2000, then following one of three SRES scenarios to 2100, with constant forcing thereafter. Data from some 22 models are currently being considered for the new CSIRO projections. This report considers only four individual models, but briefly compares these to the ‘multi-model mean’ (courtesy Julie Arblaster). The models are listed in Table 1. Preliminary data from the new version of CSIRO’s current model ‘Mk3.5’ are included here. Results from HadGem and GFDL are courtesy of Janice Bathols and Ian Macadam.

Averages for both the full year and the four seasons over the period 1961-1990 have been formed for a number of quantities, including surface air temperature, precipitation and sea-level pressure. These are presented in my upcoming report for SEACI. A simple skill assessment of these quantities is shown in Fig. 2. All four models simulate both the area mean and local values quite well, in comparison to the 0.25° gridded observational data for temperature and precipitation from the Bureau of Meteorology. Data from ERA reanalyses are used as the observational fields for SLP.

Interestingly, the multi-model mean compares slightly better than the individual models, except that HadGem just beats it in two quantities. The ERA rainfall field suffers from well-known problems and scores no better than the models. Some bias may exist from using the averages of daily max and min temperatures as the observational field.

Consideration of an appropriate weighting of models is not the topic of this note. Ideally, this could be based on the (hypothetical) ability of models to simulate the local climate change in a particular field, scaled (or normalised) by the global mean warming. For illustration, we consider here the mean of the seasonal averages in Fig. 2, averaged over the three quantities, as a weight. Dividing by the sum of the four results gives the numbers in Table 1. This rather uniform set of weights will be used for all grid points in the example presented shortly.

Table 1. Models considered in the study, the weight assigned to them and the global mean warming to 2100 under A1B.

Model Name	Origin	Weight	Warming (K)
Mark 3.0	CSIRO Atmospheric Research	0.234	2.21
Mark 3.5	CSIRO Atmospheric Research	0.239	3.43
HadGem	UK Meteorological Office	0.273	3.53
GFDL 2.1	Geophys. Fluid. Dyn. Lab., USA	0.254	2.76
MMM	Multi-Model Mean		2.89

In the multi-model means, the ‘Murray Darling Basin’ regional annual mean change in temperature divided by the global mean is between 1.105 and 1.158 for all SRES scenarios and time periods. Thus, there appears to be little systematic bias in using scaled patterns over the region (see also Watterson, 2005).

Changes from 1976 to 2100 have been determined by linear interpolation between the 1961-90 and 2071-2100 averages. Global mean warmings for this span under the A1B scenario from the models are given in Table 1. (Note that there is no account of control model drift in these values, which would boost the Mk3.0 result to one close to the MMM result.) Maps of the scaled change of temperature for summer (DJF), interpolated to a common 1° grid, are shown in Fig. 1.

The individual model results are determined from land points only (1a to 1d). As described by Watterson et al. (2006) simulations at 0.5° by CCAM show that a sharp drop in warming occurs at coasts, on going from land to ocean. It would seem wise to avoid linear interpolation between land and ocean points as a means of producing values near the real coastline. To assist in producing interpolated values nearer the coast, the model fields are first interpolated to a double grid, using extrapolation to the edges of coastal land squares. The final 1° grid fields are plotted using cell colouring. In fact, the HadGem and (apparently) GFDL models allow squares with fractional surface types. The relatively low values on points that extend beyond the true coast are a result of this. Averaging over the four models (with weights) avoids these values if points with less than four model results are omitted (compare the 1e and 1f maps). A weighted average of results simply interpolated from the full grid is in 1g. The difference over land is rather small in this case, due to the relatively high resolution of the models (2° or better). The simple average over all 22 models, 1h, produces less

abrupt land-sea contrast, partly due to differing and often coarser model grids and coastlines.

3. Distributions for scaled change

In the previous note, a number of methods for generating a PDF for scaled change of a certain quantity at a single point were described. These are illustrated in Fig. 3, using data for warming at the central point of the map, 142°E and 31°S. Allowing for statistical uncertainty, the true value for each model (from multiple runs) is assumed to be from a simple normal PDF centred on the sample value. The uncertainty is determined from that appropriate to differences of two 30-y means, assuming these follow from the interannual standard deviation field, then scaled. The available SD field from Mk3.0 is used for all models here, with the result scaled by 3K. The four sample change ratios here are 1.23, 1.42, 1.02 and 1.55. The common uncertainty SD is 0.11. The weighted sum of the four individual distributions is the ‘Sum’ PDF in Fig 1. The normal distribution fitted to this Sum curve is also shown (as Normal). The range of ratio values allowed here extends from the point where the corresponding cumulative distribution (CDF) is 0.001 to the point where it is 0.999. 1000 values are used to provide close representation of all the curves. These will differ for each grid point –there being no need for them to be common here.

The beta distribution fit to the Sum curve is also shown. Here the end points (two of the four parameters) give the 0.01 and 0.99 values of the CDF of Sum. The steep sides of Sum here lead to sharply dropping sides of Beta. The Uniform distribution is between the smallest and largest of the four change ratios. The choice of second smallest and largest (which would be unwise for four values) would match the original CIG approach.

The final curve ‘Narrow’ is a normal fit to Sum, but with the SD reduced by the square root of the ‘effective N’. This is the number of models, with allowance for uneven weighting, being the inverse of the sum of the squared weights. This distribution would be appropriate if one considered the various model results to be a sample from a normal distribution centred on the ‘true’ change. It would represent a plausible distribution for the ‘true’ value, whose uncertainty will be smaller the more models are used, as in standard statistical theory.

A range of statistics from each of these distributions can be determined. The means match that from the original model results -except in the Uniform case. The SDs vary somewhat, being smallest for Narrow, of course. Percentiles can be readily determined from the CDFs.

Applying the methods to every grid point with four model (land) values produces a map of means that matches 1f (even Uniform is very close). Plotted in Fig. 4 are the 10, 50 and 90 percentiles from all five cases. As anticipated from Fig. 3 the 10 to 90 range is usually smaller for Uniform and Narrow than for the other three.

4. Net warming for 2100

As in the CIG method, the patterns of scaled warming need to be combined with a global mean warming distribution to produce a net change. As described in the

previous note, the assumption is made that the scaled local change 'x' and the global warming 'T' are considered two independent variables. The joint distribution function is simply the product of the two PDFs. Statistics of the net local change can be determined numerically from this joint function.

Consider first the trivial case, where one proposes that the global warming has reached a single specific amount. For the A1B scenario in 2100, a value around 3 K is suggested by the models (Table 1). Suppose for simplicity it is exactly 3K. Then the joint PDF for the local warming is only trivially different from the scaled warming PDF, and all the statistics correspond to those from section 3, with a factor of 3 K. For instance, the maps in Fig. 4 apply to the net case, but with the scale amplified to range from 1.2 K to 6 K.

An idealised PDF that better reflects the uncertainty in global warming in this case, which I used previously, is illustrated in Fig. 5 –the SD=1K case. It is necessary to discretise this normal distribution, and 100 T points seem adequate. Now if the local warming ratio is a single value, say 1, the joint distribution is again simple. The net warming distribution is the same of the global result in Fig. 5.

For the more general case additional calculations are needed. Two methods were used previously. One is a straight forward evaluation of the joint function at each x and T step. This gives 100000 values of probability, each corresponding to a net warming P simply given by xT. Ordering these by P allows a simple conversion to a CDF as a function of P. The second method makes use of the simple form for P, and the separate nature of the joint function. This appears to be computationally more efficient by a factor of about 10.

The net warming PDFs for the central point, determined for the SD=1 global warming case and each scaled case, are shown in Fig. 6. The differences are surprisingly small. The Uniform and Narrow cases give a slightly narrower net warming. Performing the calculation at every grid point leads to the maps shown in Fig. 7. Again, there is very little difference across the five for the 10, 50 and 90 percentiles shown.

The similarity across the five cases is due to the scaled warming PDFs being all relatively narrow, in comparison with the global warming one. A case intermediate between the SD=1 case and the single T case above is for the SD = 0.2 curve shown in Fig. 5. This produces the net warming curves for the central point shown in Fig. 8. The PDFs more closely reflect the differences in Fig. 3.

5. Summary

This note applies the method previously described for generating PDFs for scaled warming and net warming to points over SE Australia. The range of possible results at each point is evident from the maps of 10 and 90 percentile statistics that are generated. The choice of the four models and their weighting used here is only for example purposes.

As previously, five different types of scaled warming PDF are considered. Support for using each of these could be argued, although the uniform distribution, with no weighting of models is clearly outdated. The three other methods of fitting the spread

of individual model results produce rather similar net warmings, in practice. The Beta case has the advantage of allowing a non-zero skewness and a finite range using only four parameters. Given the popularity of Bayesian methods, which (as I understand it) lead to narrowing ranges as the number of models increases, the Narrow case should also be considered. Fortunately, evaluation of all five cases, even for multiple T scenarios, seems quite feasible. Application of the method to a larger set of models and other variables is recommended.

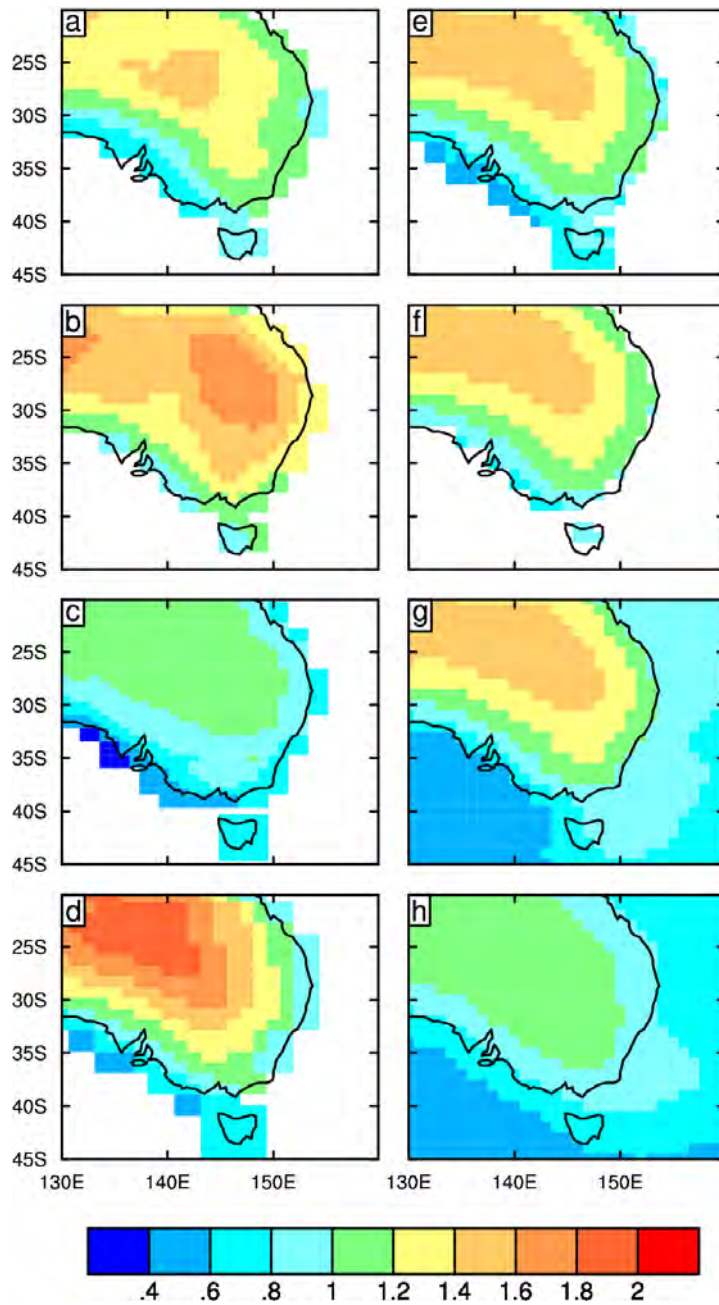


Fig. 1. Change in mean surface air temperature over SEA land divided by global annual mean change for DJF, between years 1976 and 2100, under the A1B scenario, from (a) Mk3.0, (b) Mk3.5, (c) HadGEM, (d) GFDL2.1, (e) weighted mean of one to four models, (f) weighted mean of all four models, (g) weighted mean of four models from land and sea values, and (h) AR4 multi-model mean.

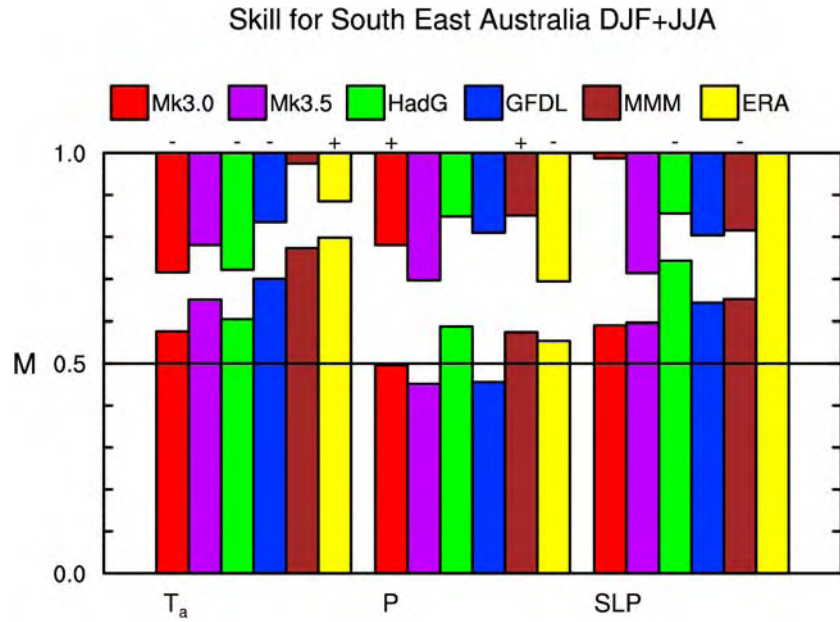


Fig. 2 Histogram representing skill of four models and the MMM in reproducing observational climatological means using data from SEA land for quantities surface air temperature (T_a), precipitation (P) and sea-level pressure (SLP). Bars up from 0 are the M score, bars down from 1 are the M score representing the mean bias over SEA. Both are averaged over the DJF and JJA results. A + or – symbol is shown when the mean bias is of the same sign in both seasons. An additional observational result from ERA40 (1958-2001) is also considered. For SLP, the M score for ERA is unity, as ERA is used as the observed. All data were interpolated to the common BOM grid, and land points in the plotted domain used.

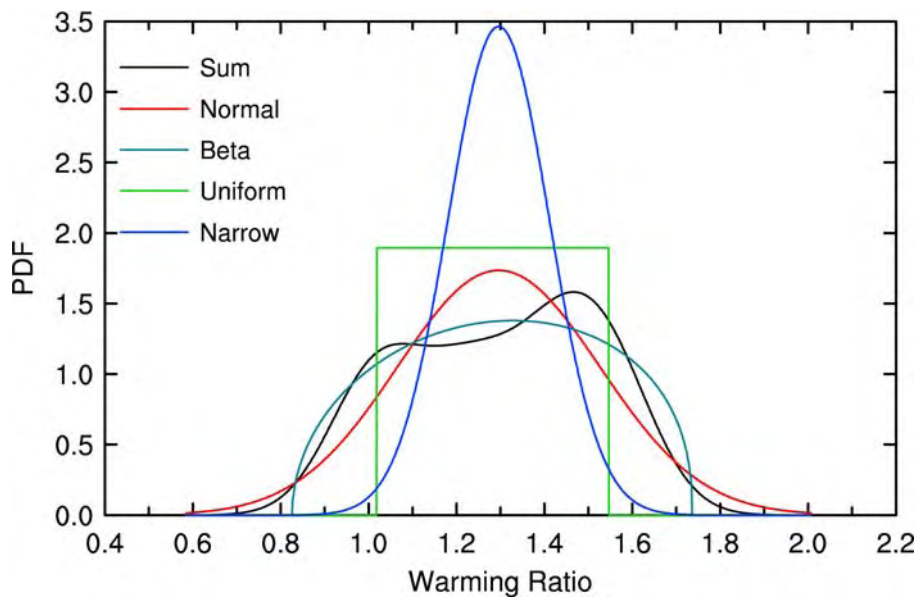


Fig. 3. Probability distribution function for the warming ratio at point 142°E, 31°S calculated from the four models, using five methods, as in key.

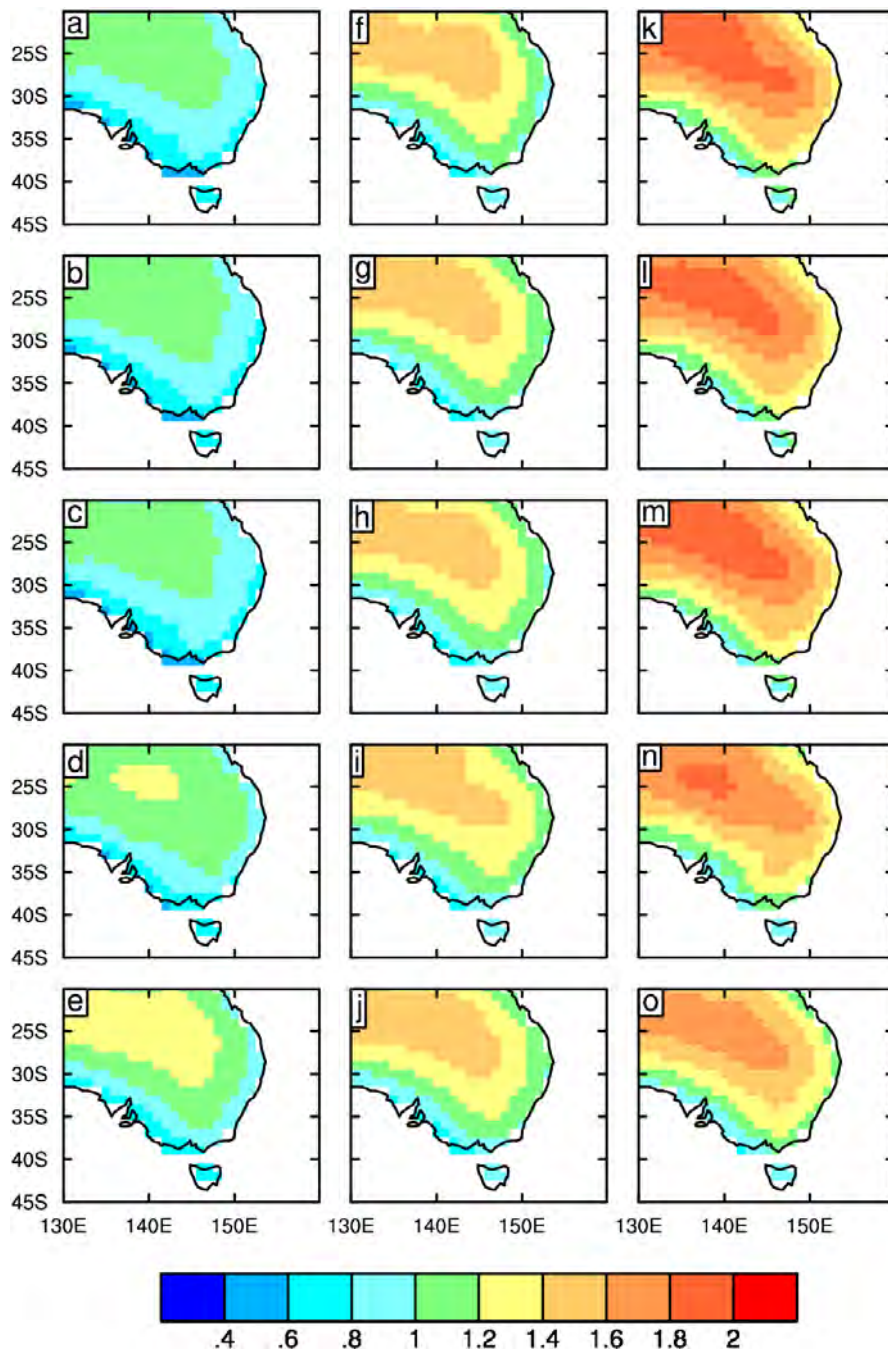


Fig. 4. Maps of percentiles of the warming ratio from all distributions (top to bottom) Sum, Normal, Beta, Uniform, and Narrow: Left column 10%, Middle column 50% and right column 90%.

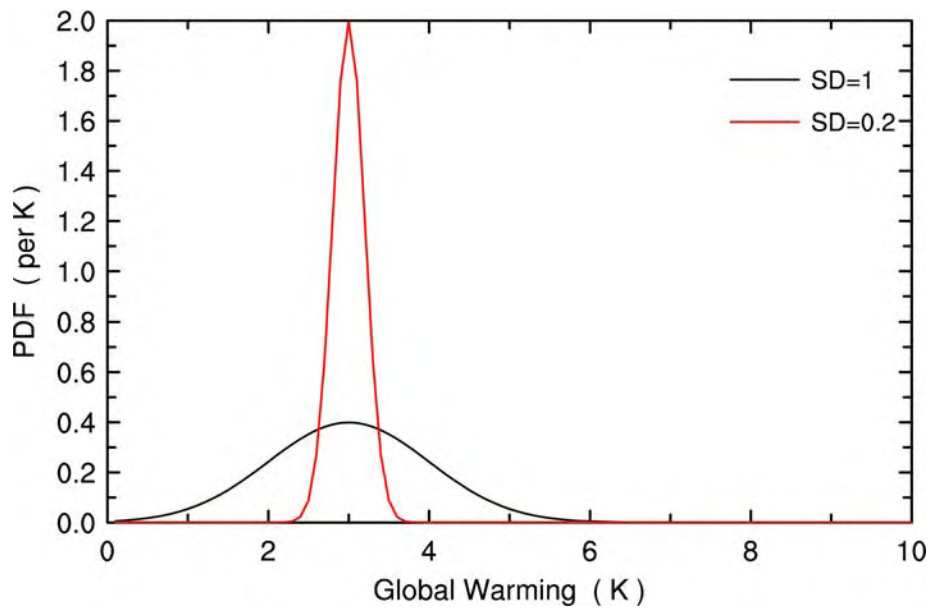


Fig. 5. Idealised distribution of global mean warming, based on the normal distribution with 3 K and SD 1 K or 0.2 K.

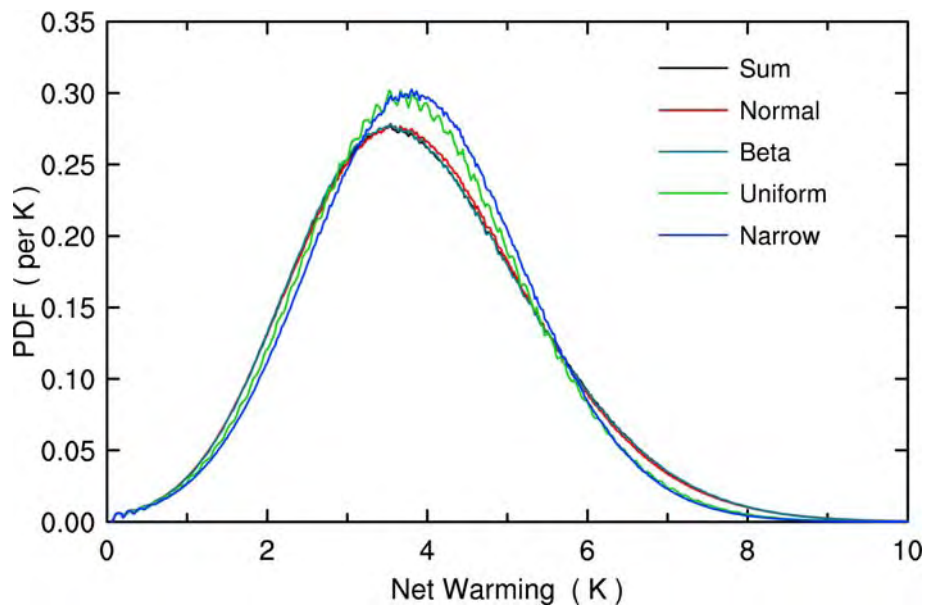


Fig. 6. Probability distribution function for net warming at point 142°E, 31°S calculated from the five ratio PDFs (as in the key) and the SD 1K global warming PDF.

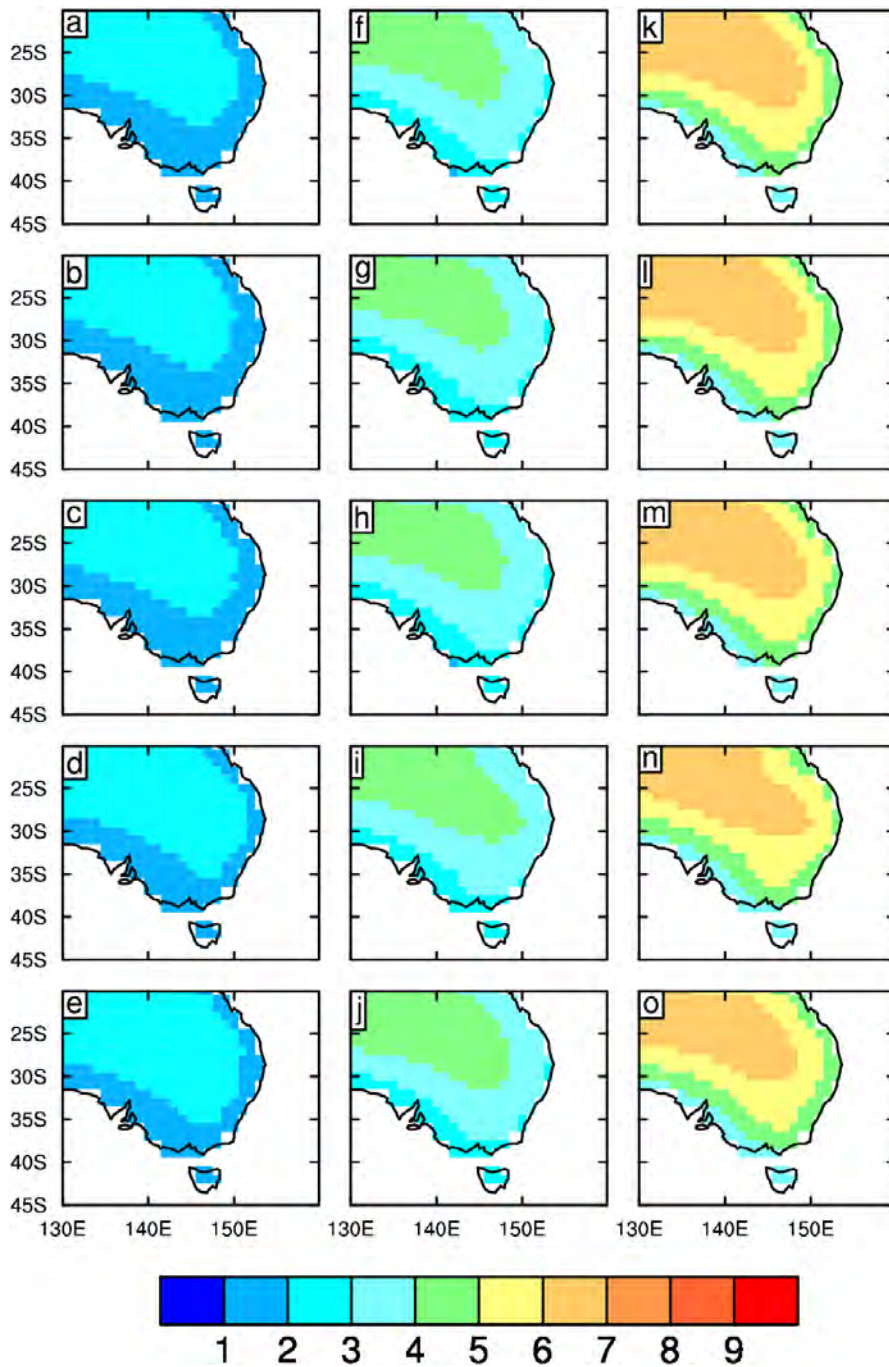


Fig. 7. Maps of percentiles of net warming from all distributions (top to bottom) Sum, Normal, Beta, Uniform, and Narrow: Left column 10%, Middle column 50% and right column 90%.

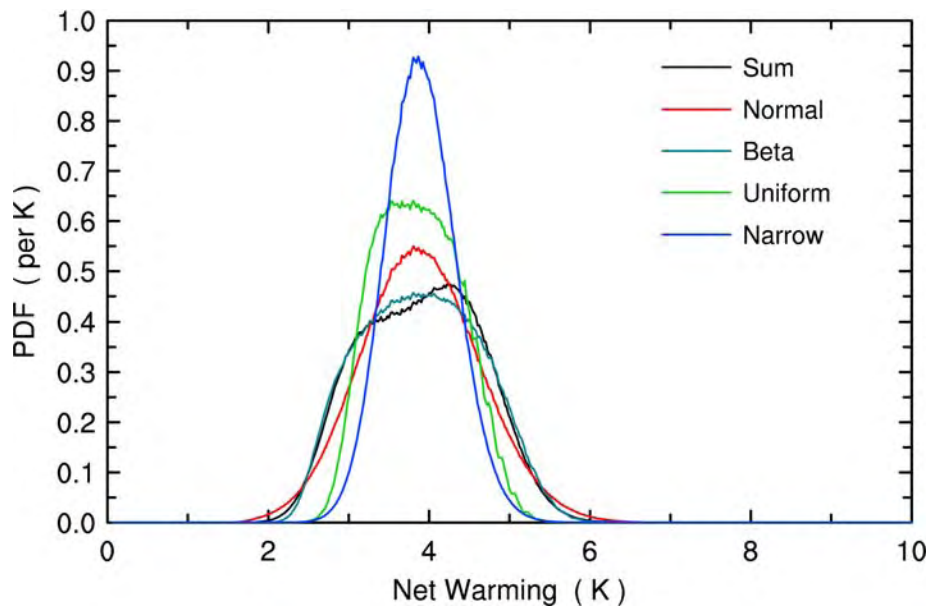


Fig. 8. Probability distribution function for the net warming at point 142°E, 31°S calculated from the five ratio PDFs (as in the key) and the SD 0.2 K global warming PDF.

References

Watterson, I. G. (2006) Some methods for specifying PDFs. *Internal report, dated 14-02-06.*

Watterson, I. G. (2005) Climate change for the IPCC scenarios simulated by the IPCC multi-model ensemble: results scaled by global mean warming. *Internal report, dated 24 May 2005.*

Watterson, I. G., J. McGregor, and K. Nguyen (2006) Influence of winds on changes in extreme temperatures near Australian coasts, as simulated by CCAM. *Abstract for the AMOS National Conference, Adelaide, February 2007*

Whetton et al. (2005) Australian climate change projections for impact assessment and policy application: A review. *CMAR Res. Papr. 1.*

For details on the CSIRO Mk3 and Mk3.5 simulations, see cherax.hpsc.csiro.au/users/dix043/mk3runs/

For the full IPCC dataset, see http://www-pcmdi.llnl.gov/ipcc/about_ipcc.php

Appendix 2

Selecting climate change results based on model performance

Ian Smith and Elise Chandler

It can be argued that weighting models is not ideal since it implies that the results from better performing models can be diluted when combined with the results of poorer performing models. Chandler (2007) provides a preliminary analysis of projections by deliberately ignoring all but the best performing models over the Australian region. Here we describe some further results based on this technique as applied to the MDB region.

Since rainfall is one of the most difficult variables to simulate accurately, we argue that a reliable projection of rainfall must be accompanied by a reasonable simulation of present day rainfall. An assumption here is that a model must, by definition, accurately simulate a number of variables (moisture content, temperatures, winds, pressure etc.) correctly if it is to simulate rainfall correctly. Secondly, we also argue that, because Australia is a continent encompassing a wide range of climate regimes, that a regional projection is more likely to be reliable if the model can capture the variability in space over the wider Australian region. Thirdly, we also argue that, in addition to accurately simulating the means and spatial variability, the ability to simulate the seasonal cycle also provides an important performance measure.

23 AR4 model results (based on the A1B emissions scenario) were assessed. Several approaches were taken to determine the best models performing models. The first of these involved using threshold values for the correlation coefficient and RMSE. Following Suppiah *et al.* (2004), a threshold value of 0.7 chosen as the minimum value for the spatial correlation coefficient. A set of best model results were then selected as those with above median correlation coefficients and those with below median RMS errors. In addition to assessing the seasonal mean values, the models were also assessed in terms of their ability to reproduce the seasonal cycle of rainfall at several key locations, including the MDB. Finally, the results from the coarse resolution models were excluded since previous studies have highlighted the importance of horizontal resolution and the representation of topography as crucial to model rainfall.

The details of the full assessment are not shown here but, it is apparent that some simulations are clearly inferior, failing to adequately reproduce either the broad spatial patterns or the quantitative amounts. In particular, the models IPSL-cm4, BCCR-BCM2, GISS-EH, GISS-AOM, and FGOALS-G1.0 performed poorly in regions of high rainfall (not shown). At the shorter seasonal timescale, spring and autumn were the seasons most difficult to simulate and this proved to highlight the better performing models.

Of the 23 models, 7 were assessed to provide the best simulations of present day rainfall:

GFDL-Cm2.0
ECHAM5
GISS-AOM
UKMO-HADcm3

MIROC3.2 (hires)
GFDL-CM2.1 and
UKMO-HADgem1.

Annual and seasonal percentage changes in rainfall for the region shown in Figure 1 for the period 2071-2100 relative to 1971-2000 based on the results using the A1B emissions scenarios (a mid-range scenario) were calculated for each model. These were then divided by the same model's estimate of global temperature increase over this period to arrive at a percentage change per degree of global warming. These values are shown in Table 1.



Figure 1. Map showing grid points used to define the Murray-Darling river basin.

Table 1. List of 23 model results for the projected percentage change in rainfall (per degree of global warming) over the MDB region. The top 7 selected models are highlighted. The 22-model average shown excludes the results for BCCR-BCM2.

Model	Annual	Percentage change in rainfall				
		Seasonal				SON
		DJF	MAM	JJA	SON	
1 CSIRO-Mk3	-11.322	4.466	-15.344	-21.270	-30.431	
2 GFDL-CM2.0	-12.410	28.991	3.562	-24.669	-34.333	
3 MRI-CGCM2.3.2	-10.466	-23.397	-21.245	-23.397	-5.572	
4 ECHAM5/MPI	-13.484	-5.725	15.261	-31.692	-32.450	
5 GISS-ER	5.210	20.388	1.922	-17.495	-1.846	
7 FGOALS-G1.0	-4.575	-3.917	-10.238	-5.016	-1.659	
8 MIROC3.2(medres)	20.688	48.390	41.733	-11.238	-0.223	
9 ECHO-G	22.783	59.088	22.942	-16.677	1.451	
10 CCSM3	7.205	12.315	7.876	-10.856	15.790	
11 GISS-AOM	-20.329	-28.843	19.923	-26.280	-29.721	
12 UKMO-Hadcm3	-14.435	-7.082	6.650	-10.674	-40.274	
13 GISS-EH	18.648	23.904	19.404	13.046	13.502	
14 INM-cm3.0	-6.851	7.147	3.022	-19.065	-17.389	
15 MIROC3.2(hires)	-6.016	5.458	6.496	-13.575	-25.254	
16 CGCM3.1(t47)	11.343	6.238	14.308	15.988	8.202	
17 GFDL2.1	-19.963	-1.245	-23.409	-46.104	-12.085	
18 CGCM3.1(t63)	18.705	34.496	14.570	11.931	11.583	
19 BCCR-BCM2	40.103	42.732	37.770	-12.632	5.467	
20 CNRM-CM3	-7.372	7.360	18.003	-36.970	-35.549	
21 IPSL-CM4	-33.637	-19.862	-31.908	-34.185	-52.639	
22 UKMO-HADGEM1	-18.704	8.374	-28.881	-35.057	-30.272	
23 PCM	-5.919	-7.968	-9.864	11.399	-16.497	
22-model average	-3.2	8.2	4.2	-16	-14	
22-model range	-33 to +23	-24 to +59	-31 to +42	-46 to +16	-53 to +16	
Best 7 average	-15	-0.01	-0.06	-27	-29	
Best 7 range	-20 to -6	-29 to +8	-29 to +20	-46 to -11	-40 to -12	

The important result from this assessment is that the average changes from the best 7 models are more negative than the 22-model averages. Furthermore, this is not purely an artefact of the different sample sizes. T-statistics indicate that the best-7 sample results for rainfall and changes are significantly different to those of the remaining 15 models. For example, the chances that the 7-model average percentage change in annual rainfall (-15%) comes from the same population as the remaining 15 models is close to .001. In other words, the 7-best models form a distinctly different sub-set to the other models. This is what we would expect if a poor simulation of present day climate is associated with an unreliable prediction of future climate.

These results need to be confirmed and recast into probabilities but it is apparent that the application of this new method paints a somewhat more pessimistic outlook for rainfall over the MDB into the future than previously indicated. We expect that it will be possible (Project 2.2.3b) to refine the projections for this region to better satisfy stakeholder expectations.

References

Chandler, E. (2007) Reducing uncertainty in model results for Australian rainfall in the 21st century. Abstract, AMOS National Conference, Adelaide, February 2007.

CSIRO, 2001. Climate projections for Australia. CSIRO Atmospheric Research, Melbourne, 8 pp. <http://www.dar.csiro.au/publications/projections2001.pdf>

Smith (2007) Regional rainfall projections refining model-based estimates using observed trends. Abstract, IUGG, Perugia, Italy, July 2007.

Suppiah, R., K. J. Hennessy, P. H. Whetton, K. McInnes, I Macadam, J. Bathols and J. Ricketts (2007) Australian climate change projections derived from simulations performed for the IPCC 4th Assessment Report. *Aus. Met Mag.* (accepted).

Watterson (2005) CMAR Research Paper 1.

Watterson, I.G. (2006) Simulation of climate and climate change by global models. SEACI Project 2.1.5a report (23 November, 2006).

Watterson (2007) Calculation of probability functions for temperature and precipitation change under global warming. (submitted to *Journal of Geophysical Research*).

Whetton, P.H., McInnes, K.L., Jones, R.N., Hennessy, K.J., Suppiah, R., Page, C.M., Bathols, J., Durack P. (2005) Climate change projections for Australia for impact assessment and policy application: A review. CSIRO Technical Paper. 001, Aspendale, Vic., CSIRO Marine and Atmospheric Research, 34p. http://www.cmar.csiro.au/e-print/open/whettonph_2005a.pdf

Whetton, P. H., Macadam, I., Bathols, J. M., and O'Grady, J. (2007). Assessment of the use of current climate patterns to evaluate regional enhanced greenhouse response patterns of climate models. *Geophysical Research Letters*, 34 (14): L14701, doi:10.1029/2007GL030025.



South Eastern Australian **Climate initiative**

Final Report Project 3.1.3

**Simulation and potential predictability of SE
Australia rainfall and temperature from the
national dynamical seasonal prediction model**

Principal Investigators: Drs. Harry Hendon, Oscar Alves
and Eunpa Lim

Bureau of Meteorology Research Centre (BMRC), email: hhh@bom.gov.au,
Tel: 03-9669-44120, Fax: 03-9669-4660, GPO Box 1289, Melbourne 3001

Report date: 22 October 2007

Project Abstract

The Predictive Ocean Atmosphere Model for Australia (POAMA) is a state-of-the-art seasonal forecast system based on a coupled ocean/atmosphere model. POAMA was developed by the Bureau of Meteorology Research Centre and CSIRO Marine Research, with support from the Climate Variability in Agriculture Program, a consortium of rural research and development corporations managed by Land and Water Australia.

POAMA is used in real-time by the Bureau to produce an eight-month forecast every day (current forecasts and system information available at <http://poama.bom.gov.au>). One of the special features of POAMA is that it uses the very latest observations from global ocean and atmosphere observing systems, right up to the previous day. The work described here will lead to a detailed assessment of the predictive skill of the POAMA system for south-eastern Australia in simulation and forecast modes, and improved understanding of the key mechanisms and processes that lead to climate variability in the GRDC region.

Project objectives

- Determine the ability of the Bureau's climate/seasonal prediction models to simulate climate variability in south eastern Australia
- Determine potential predictability of climate variability, especially rainfall and surface temperature, in south eastern Australia

Methodology

- Assessment of the simulation skill of POAMA
- Assessment of the potential predictability of the primary modes of climate variability that drive rainfall and temperature in south-eastern Australia by using an ensemble of atmospheric climate model runs (the atmospheric component of POAMA) forced with climatological and observed sea surface temperature variations for the period 1981-2005
- Identification and assessment of the primary modes of climate variability that drive rainfall and temperature in south-eastern Australia using an extended run of the coupled climate version of POAMA and operational hindcasts from POAMA

Summary of the findings

- Analysis of an ensemble of simulations using the atmospheric model of POAMA forced by observed sea surface temperature (SST) variations for the period 1982-2002 indicates the upper limit of predictability for SE Australian rainfall is about 30%. Rainfall is most predictable in autumn-spring. This level of predictability is in line with estimates of observed predictability based on correlations with El Niño indices such as the Nino3 SST index or the Southern Oscillation Index.
- A portion of winter-spring rainfall predictability in the SE stems from sea surface temperature variations in the tropical eastern Indian Ocean. The sensitivity to eastern Indian Ocean SST points to the need to improve observations and initialization in the Indian Ocean in order to improve dynamical seasonal prediction.

- POAMA is found to have skill in predicting the major El Niño-related SST variations as well as some of the east-west SST shifts in individual El Niño events that have large impact on east Australian rainfall. POAMA was also found to simulate the major atmospheric teleconnections driven by El Niño and it captures the observed sensitivity to the east-west shifts of El Niño. Direct prediction of rainfall in SE Australia, however, is hampered by model drift and bias. The ability to predict El Niño and some of its details suggests skilful prediction of regional SE Australian climate might be possible via bridging/downscaling (project 3.2.2)

Methodology and Results

Objective 1: Potential Predictability of SE Australian Rainfall

Introduction

The Bureau of Meteorology routinely makes dynamical seasonal predictions out to 9 month lead time with the POAMA coupled ocean-atmosphere forecast system. POAMA (Predictive Ocean Atmosphere Model for Australia) is an intra-seasonal to inter-annual climate prediction system based on coupled ocean and atmosphere general circulation models. The original focus for POAMA-1 was the prediction of sea surface temperature (SST) anomalies associated with El Niño / La Niña, for which POAMA's predictions are internationally competitive. El Niño/Southern Oscillation (ENSO) is the dominant driver of Australian climate variability (e.g., McBride and Nicholls 1983), thus POAMA's forecasts have great value for anticipating the behavior of El Niño.

The POAMA system is continually evolving and improving, and subsequent versions of POAMA will address problematic bias and drift that hinder direct prediction of regional climate variations, such as rainfall and temperature across continental Australia. However, even assuming model drift and bias can be improved and that increased resolution leads to better regional climate simulation, the degree of predictability of regional climate is unknown. Perfect prediction of the slowly varying surface boundary forcing (primarily tropical sea surface temperatures; SST), which is thought to be the main source of seasonal climate predictability (e.g., Charney and Sukla 1981), will account for only a portion of actual climate variability due to the presence of internal atmospheric noise. Nonetheless, an assessment of the theoretical upper limit of predictability, given perfect knowledge of the slowly varying boundary forcing, will provide an upper bound on the expected skill of the POAMA system.

Methodology

To assess potential predictability of regional climate, we assume perfect knowledge of the slow variation of global tropical SST for the period 1982-2003. Effectively, we replace the ocean model component of POAMA with a prescription of the SST variation that actually occurred. To assess the relative roles of forcing from the Pacific and Indian Oceans SST, we conducted three additional experiments. In "Pacific large", observed SST variations are prescribed in the entire tropical Pacific Ocean, while climatological SST is prescribed elsewhere. In "Pacific small", observed SST is prescribed only in the eastern tropical Pacific Ocean. These two experiments are aimed at elucidating the global teleconnections that are driven by SST variations associated with El Niño/Southern Oscillation (ENSO). The Pacific small runs are aimed at understanding the forcing by SST variations in the main El Niño region of the equatorial eastern Pacific. The Pacific large runs include the SST forcing in the far western Pacific, where anomalies during ENSO tend to be out of phase with those in the eastern Pacific. The role of Indian Ocean SST is highlighted in the Indian experiment, where observed SST variations are prescribed only in the tropical Indian Ocean. In all cases, 8 ensemble members are generated for the period 1982-2003 using slightly different initial conditions and predictability is assessed following Rowell (1998).

Results

Correlation $r_{\text{vprecst, SON}}$

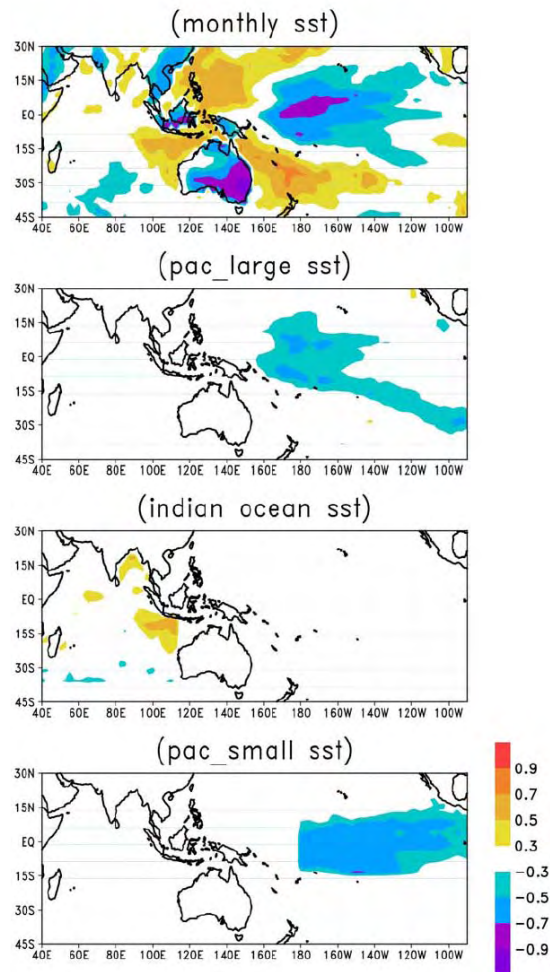


Fig 1. Correlation between simulated SON rainfall in SE Australia (area mean for point south of 32S) and SST for the (top-bottom) the model simulations forced by global SST, Pac large SST, Indian Ocean SST, and Pacific Small SST for the period 1982-2004.

Based on analysis of this suite of “perfect SST” experiments with POAMA seasonal forecasts system, SE Australian rainfall is found to be most predictable in autumn through spring, when up to 30% of the rainfall variance is predictable (Hendon et al. 2007a). That is, if we could perfectly predict global sea surface temperatures, the maximum amount of rainfall variability that we could expect to predict is about 30%. This estimate is an upper limit, as we know that we can never perfectly predict SST. Nonetheless, SST is highly predictable at short lead time. Therefore, 30% predictability should not be viewed as being unattainable. Nonetheless, the potential usefulness of 30% predictability of rainfall needs to be assessed. For instance, predictability of crop yield or stream flow could be assessed based on output from this ensemble of simulations, where both the predictable component and noise component of the climate is known and well sampled.

The estimation of potential predictability of SE Australian rainfall in this study, while highly dependent on the model that was used, is in line with the observed rainfall variance that is accounted for by El Niño, which is the dominant source of interannual variation of SST and of rainfall variability (e.g., McBride and Nicholls 1983; Drosowsky and Chambers 1991). This study also confirms that the atmospheric model of POAMA realistically simulates climate variability over SE Australia that is forced by variations of tropical SST (Hendon et al. 2007a). That is, the sensitivity of simulated rainfall in SE Australia to tropical SST variations is very realistic. Interestingly, this study indicates that a significant portion of the predictable rainfall variability in the SE during spring and winter stems from SST variations in the tropical eastern Indian Ocean (Fig. 1), consistent with observations of rainfall variations associated with the Indian Ocean Dipole (e.g., Nicholls 1989; Meyers et al. 2007). This might appear to be counter to the notion that ENSO is the main driver of rainfall variability during these seasons. However, during ENSO SST anomalies co-vary in the Indian Ocean with those in the equatorial Pacific (Meyers et al. 2007) and it is this co-varying SST in the Indian Ocean that drives a significant portion of the predictable rainfall variations in the SE.

Conclusions

The atmospheric component of POAMA realistically simulates climate variability in SE Australia given perfect knowledge of tropical SST. Improvement of rainfall prediction in the SE from the POAMA system will require improved initialization and simulation of the tropical oceans and in particular the Indian Ocean and reduction in model drift. Currently, model bias and lack of accurate initial oceanic and atmospheric conditions hinder the ability to predict the coupled-state of the Indian Ocean. However, improvements to the POAMA component models should alleviate some of the bias in the Indian Ocean (in particular, the overall cold SST bias and elevation of the thermocline in the eastern Indian Ocean). Furthermore, a new ocean assimilation system is nearing completion and will be part of the POAMA 2 system. This new assimilation scheme, which initializes salinity, temperature and currents, shows great promise for improved initialization of the Indian Ocean. Experiments to assess its impact on predictability of SE Australian climate will continue in Project 3.1.4

Objective 2: Simulation/prediction of primary modes of SE Australia climate variability

Introduction

Assessment of POAMA's ability to simulate the major modes of climate variability that are relevant to SE Australian climate is required to provide a benchmark for future improvements of the forecast systems, such as that anticipated by development of the ACCESS system (e.g., improved spatial resolution, improved physical parameterizations, and reduced model drift). This assessment is also required because the utility of the forecasts from the current version of POAMA is unknown. There is also scope for bridging and downscaling of the forecasts (Project 3.2.2), which is founded on the notion that important climate drivers (primarily ENSO and its teleconnections) are predicted faithfully. The focus of this study is not only on ENSO but also on other tropical sea surface temperature variations such as those in the

equatorial eastern Indian Ocean that are important for SE Australian rainfall (e.g., Nicholls 1989; Meyers et al. 2007). We have also assessed the impact of model drift on these relationships, which should aid future development of the POAMA system.

Methodology

The primary modes of climate variability that drive rainfall variations in SE Australia were assessed in the 25 years of hindcasts (re-forecasts) from the POAMA seasonal forecasting system. In contrast to the model runs used in the first part of this study where SST were prescribed as observed, this second study use the fully coupled system which predicts both atmosphere and ocean conditions. The analysis here is based on a 3 member ensemble of 9-month forecasts for the period 1982-2006. Forecasts are initialized from observed atmospheric and ocean initial states. The atmospheric initial state, together with the land surface condition, is produced by the ALI system (details at <http://poama.bom.gov.au>). The ocean initial condition is provided by the ocean initialization system that piggybacks on the POAMA system. Forecasts are initialized on the first of each month. Three forecasts are made each month from slightly different atmospheric initial conditions but with identical oceanic initial conditions.

Results

We first assess POAMA's ability to simulate the major modes of SST variability that are relevant to Australian climate variability. Foremost is ENSO. However, Wang and Hendon (2007) emphasized that the eastern Australia rainfall is sensitive to the "inter-El Niño" variations of SST as well, which are the east-west shifts of SST anomalies in the central Pacific between different El Niño/La Niña events. For instance, the 1997 El Niño event had SST anomalies shifted well east in the Pacific while the 2002 El Niño was more concentrated in the central Pacific. Wang and Hendon (2007) showed that the springtime drought in 2002 could be accounted for by the westward shift of the El Niño, while the near normal spring in 1997 could be accounted for by the eastward shift.

The skill for prediction of the temporal variation of these leading modes of SST is assessed by the correlation of the predicted and observed El Niño and inter-El Niño patterns of SST variability (Hendon et al 2007b). In general, the ENSO mode is predictable out to at least 6 months, while the "inter-El Niño" variations are predictable for about 4-5 months. At short lead times, the spatial pattern of the SST variations in the forecasts is nearly identical to the observed patterns (Hendon et al. 2007b). At longer lead-times, some important drift in the leading patterns of SST variability occurs. The major drift is the extension of the warm anomaly associated with the El Niño all the way across the Pacific into Indonesia.

We then assessed POAMA's ability to simulate the teleconnection between the leading modes of tropical SST variability and Australian rainfall. The correlation of observed rainfall with the two leading patterns of observed tropical SST for the winter (JJA) season is shown in Fig 2 (middle panels). Correlations are generally negative across eastern Australia (warm SST in the central Pacific is associated with reduced rainfall in eastern Australia). But, rainfall in parts of central eastern Australia is more sensitive to the second mode of SST variation than to ENSO. The SEACI region is equally sensitive (Fig. 3). Similar sensitivity is seen in spring but then the ENSO mode is more dominant (Hendon et al. 2007b)

POAMA's ability to simulate these relationships between rainfall and SST are shown in the panels around the perimeter of Figure 2 (as a function of forecast leadtime) and in Figure 3 for the SEACI region. The impact of model drift on the relationship with the ENSO mode is stunning. For instance, POAMA does a modestly good job representing the negative relationship on the east coast at short lead time (ie. reduced rainfall during El Niño). But, at longer lead-time, POAMA simulates exactly the wrong response (enhanced rainfall in the SE during El Niño). Model drift seems to be less of an issue for the inter-El Niño SST variations. Overall, though, the current version of POAMA appears to do a credible job of simulating the rainfall teleconnections associated with the main modes of SST variability at short lead time, but model drift appears to hinder this simulation at longer lead times.

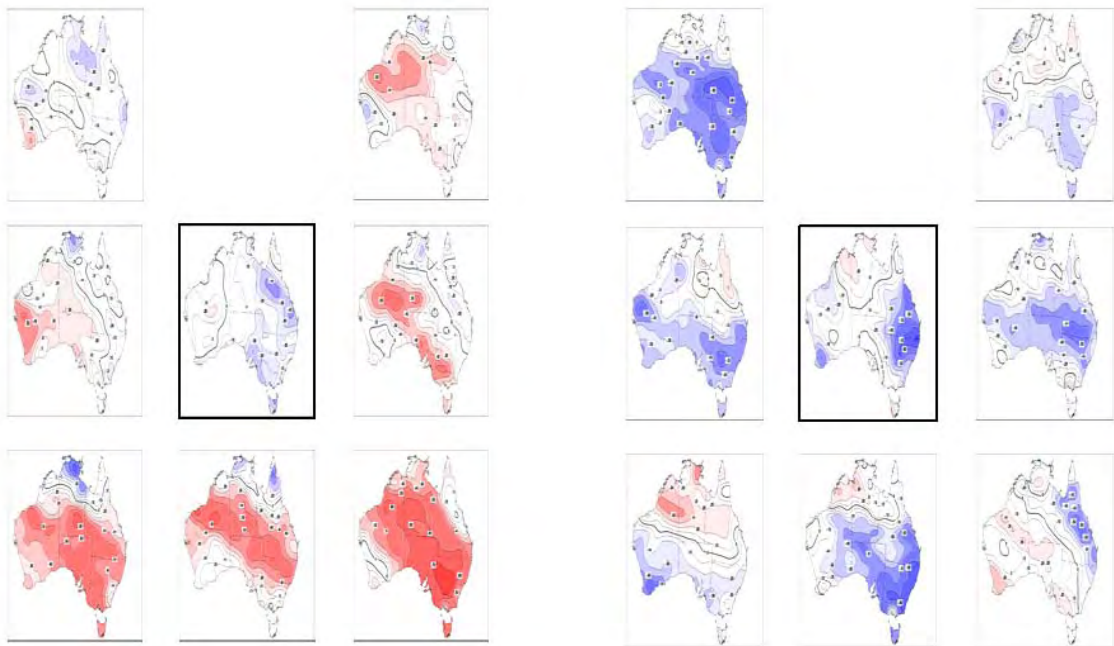


Fig 2. Left panel : Correlation between predicted rainfall and the leading pattern of tropical SST variability (the El Niño mode) for the JJA season from POAMA hindcasts at lead times 0 to 6 months (anticlockwise starting in upper left). Positive (negative) correlations are red (blue). Observed correlation is in center. Right panel: Same but for correlation with the inter-El Niño mode of SST variability:

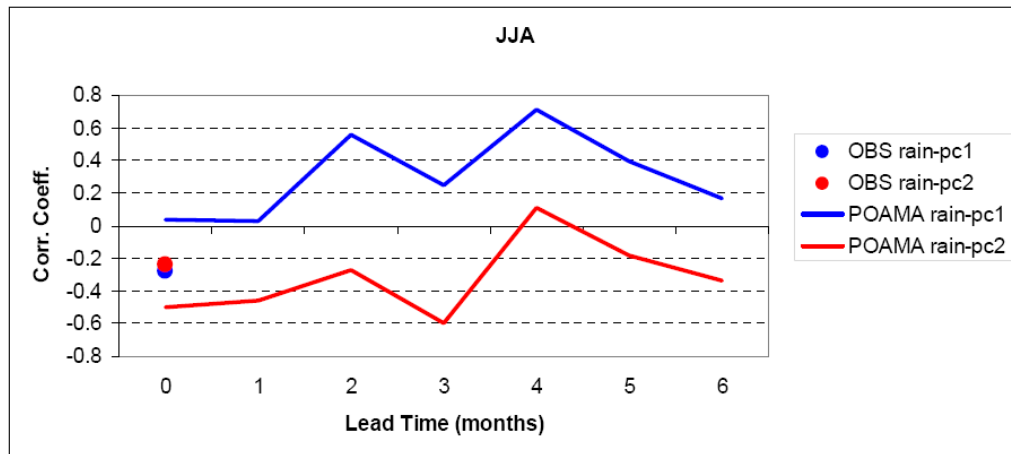


Fig 3. Correlation of SEACI-mean rainfall (landpoints south of 32°S) with leading patterns of SST variability from observations and from POAMA predictions for JJA season

Conclusions

The current version of POAMA (1.5) has skill in predicting tropical SST variations that are important for Australian climate. This includes not only skill in predicting ENSO, but also extends to the important east-west variation of equatorial Pacific SST of individual ENSO events. Eastern Australian rainfall, especially in winter and spring, is sensitive to these east-west variations of SST; hence, POAMA appears to have important predictive capability beyond simply that of the occurrence of El Niño. POAMA also realistically simulates rainfall teleconnections to Australia driven by ENSO and the inter-ENSO variations of SST at short lead time. However, model drift appears to degrade the realism of these teleconnections at longer lead times. There also appears to be an issue with spin up-, whereby the teleconnection is initially too weak, but then strengthens to realistic magnitudes 1-3 months into the forecast.

These results imply that the model drift needs to be remedied and that initialization needs to be scrutinized. One way to alleviate model drift is to “flux correct” in order to maintain a realistic base state. Flux correction should be considered for future versions of POAMA. Improvements to the ocean initialization system are underway, which might remedy some of the apparent initialization shock (spin up) that has been diagnosed here. The impact of the new ocean initialization will be assessed in the coming year as the system becomes available. However, the best approach in the future will be to develop a truly coupled initialization system, whereby the ocean, land surface, and atmosphere are initialized in unison. Support for such a system should be considered in subsequent programs of SEACI.

In conclusion, this analysis provides optimism for future direct utilization of regional climate forecasts from POAMA. In the meantime, these results provide encouragement for development of hybrid statistical-dynamical forecast schemes (Project 3.2.2), whereby predictable components of the climate from POAMA that are relevant for regional SE Australian climate are exploited by statistical techniques to deliver useful regional predictions.

Acknowledgement

This research was supported by the South East Australian Climate Initiative

Publications/Reports (attached in Appendix)

Hendon, H.H., G. Liu, O. Alves, and G. Wang, 2007a: *Assessment of potential predictability of seasonal climate in SE Australia using the Bureau of Meteorology's dynamical seasonal forecast system*. SEACI Technical Report, Milestone 3.1.3.

Hendon, H.H., E. Lim, G. Liu, O. Alves, and G. Wang, 2007b: *Assessment of simulation by POAMA of modes of climate variability that drive rainfall in SE Australia*. SEACI Technical Report, Milestone 3.1.3.

Hendon, H.H., D.W.J. Thompson, and M.C. Wheeler, 2007c: Australian rainfall and temperature variations associated with the Southern Hemisphere Annular Mode. *J. Climate*, **20**, 2452-2467.

Wang, G., and H.H. Hendon, 2007: Sensitivity of Australian rainfall to inter-El Niño variations. *J. Climate*, **20**, 4211-4226.

References

Charney, J. G. and J. Shukla, 1981: [Predictability of monsoons](#). *Monsoon Dynamics*, Editors: Sir James Lighthill and R. P. Pearce, Cambridge University Press, pp. 99-109.

Drosowsky, W. and L. Chambers, 2001: Near-global sea surface temperature anomalies as predictors of Australian seasonal rainfall. *J. Climate*, **14**, 1677–1687.

Jones, D. A. and G. Weymouth, 1997: *An Australian monthly rainfall dataset*. Technical Report 70, Bureau of Meteorology.

McBride, J. L. and N. Nicholls, 1983: Seasonal relationships between Australian rainfall and the Southern Oscillation. *Mon. Wea. Rev.*, **111**, 1998–2004.

Meyers, G., P. McIntosh, L. Pigot, and M. Pook (2007), The years of El Niño, La Niña. and interactions with the tropical Indian Ocean, *J. Climate* (in press).

Nicholls, N., 1989: Sea surface temperatures and Australian winter rainfall. *J. Climate*, **2**, 965–973.

Rowell, D.P., 1998: Assessing potential seasonal predictability with an ensemble of multidecadal GCM simulations. *J. Climate*, **11**, 109–120.

Wang, G., and H.H. Hendon, 2007: Sensitivity of Australian rainfall to inter-El Niño variations. *J. Climate*, **20**, 4211-4226.

Project Milestone Reporting Table

To be completed prior to commencing the project				Completed at each Milestone date	
Milestone description ¹	Performance indicators ²	Completion date ³	Budget ⁴ for Milestone (\$)	Progress ⁵	Recommended changes to workplan ⁶

1. Generate ensemble of simulations with atmospheric component of POAMA forced with observed and climo. SST	Integrations completed and archived	September 2006	35K	8 member ensembles for period 1982-2003 generated using 1) global observed SST, 2) tropical Indian Ocean SST, 3) Tropical Pacific SST, and 4) climatological SST Runs have been archived	none
2. Assess simulation and potential predictability of climate variations in SE Australia in ensemble of forced runs and extended run of coupled version of POAMA	Report produced (4 pages)	Jan 2007	20K	Analysis of potential predictability of regional rainfall completed. Report in preparation.	none

<p>3. Assess simulation of modes of climate variability that drive rainfall and temperature in SE Australia in the POAMA hindcasts</p>	<p>Report produced (4-pages)</p>	<p>June 2007</p>	<p>15K</p>	<p>Seasonal variations of the impact of SAM on regional rainfall diagnosed (Hendon et al. 2007). Sensitivity of regional rainfall to inter-El Niño variations of SST diagnosed (Wang and Hendon 2007). Analysis of the relationship between SE Australian rainfall and regional sea surface temperature variations as a function of season using BAM3 simulations commenced. Drift of ENSO mode in POAMA hindcasts has been assessed and calibration to remove drift has been trialed. Sensitivity of SE Australian rainfall to regional SST variations in BAM3 simulations has been assessed. Ability of POAMA to predict higher order modes of SST variability and associated rainfall variations in eastern Australia has been assessed.</p>	
--	----------------------------------	------------------	------------	---	--

Figures



South Eastern Australian Climate initiative

Final report Project 3.2.2

Review of techniques to bridge/calibrate dynamical seasonal predictions with focus on south eastern Australia

Principal Investigator: Drs. Harry Hendon and Oscar Alves

Bureau of Meteorology Research Centre (BMRC), email: hhh@bom.gov.au,
Tel: 03-9669-4120, Fax: 03-9669-4660, GPO Box 1289, Melbourne 3001

Co-Authors: Drs. Eun-Pa Lim and Guomin Wang

Bureau of Meteorology Research Centre (BMRC), email: e.lim@bom.gov.au,
Tel: 03-9669-4636, Fax: 03-9669-4660, GPO Box 1289, Melbourne 3001

Completed: 16 November 2007

Abstract

The Bureau of Meteorology routinely issues real-time forecasts for tropical sea surface temperature with up to 8 month lead time using the Predictive Ocean Atmosphere Model for Australia (POAMA). Regional climate forecasts from models such as POAMA are hindered by model bias and spatial scale that is too coarse for many applications. Therefore, we have reviewed and investigated the utility of simple statistical schemes for relating regional scale rainfall and temperature to forecasts of climate variables from POAMA.

Statistical-dynamical forecasts capitalize on the components of the climate system for which POAMA provides skilful prediction and which have a strong association with Australian climate. Because statistical post-processing itself cannot generate skill, the dynamical model must have skill in predicting some aspects of the climate. A 3 member ensemble hindcast from POAMA v. 1.5 was examined to determine the predictable components of climate variability that are related to south eastern Australian rainfall variability. The first few dominant modes of tropical Indo-Pacific SST variability, which explain up to 1/2 of Australian rainfall variability (depending on season), are predictable by POAMA at lead time up to 2 seasons. Furthermore, POAMA also demonstrates reasonable skill in directly predicting Australian rainfall at short lead times. Together, these findings suggest the possibility to improve regional forecast skill for Australian rainfall through statistical-dynamical prediction by using POAMA's SST forecast (bridging) or POAMA rainfall forecast (calibration). Preliminary analysis of the POAMA hindcasts indicates skilful prediction for below/above median rainfall for south eastern Australia at lead times out to 2 seasons, and further skill improvement is obtained from statistical-dynamical calibration and bridging. However, skilful prediction by dynamical and statistical-dynamical models varies for different regions in different seasons.

Significant research highlights, breakthroughs and snapshots

- POAMA demonstrates skill in predicting tropical Indo-Pacific SST (lead times to 6-9 months) and Australian rainfall (lead time to ~3 months) with 3 member ensemble hindcasts in 1980-2005.
- Statistical bridging/calibration schemes were developed and found to be able to extend POAMA's forecast skill for south eastern Australian rainfall.
- 10 member ensemble hindcasts from 1980 to 2006 have been generated in order to reduce noise and improve reliability.
- Current Australian rainfall and temperature real-time forecasts are available at POAMA official website : <http://poama.bom.gov.au/>

Statement of results, their interpretation, and practical significance against each objective

- **Project objectives:** Review and identify possible statistical methods to improve direct prediction of rainfall and temperature from the Bureau's dynamical seasonal forecast model (POAMA)

1) Review of statistical-dynamical techniques

The basic approach of all statistical post-processing techniques is to develop relationships between forecasts and verification in a training period, and then to apply the statistical relationship to extend model forecasts for independent periods. In general, there are two ways to design statistical-dynamical prediction schemes: One is to relate forecasts of large-scale features from a dynamical model to regional scale climate variable (statistical bridging - e.g. use tropical SST predicted from POAMA to predict south eastern Australian rainfall based on their observed relationship). The other is to adjust patterns of regional forecasts from the dynamical model against observations in order to remove systematic bias (statistical calibration – e.g. POAMA rainfall forecasts across Australia to observed Australian rainfall). In these methods, predictors (e.g. POAMA SST or POAMA rainfall) must be fields for which the model has predictability, and predictands (e.g. observed rainfall) must have a robust statistical relationship with the predictors.

Common approaches to identifying a statistical relationship of the predictors and predictands include singular value decomposition analysis (SVDA), canonical correlation analysis, or principal component analysis. These techniques expand predictors and predictands in terms of dominant patterns of variability and the time series of those patterns (Bretherton et al. 1992, Ward and Navarra 1997, Feddersen et al. 1999). In this project SVDA was adopted as it provides a direct measure of association between a predictor and a predictand, and its computation is straightforward.

Once the major analysis tool is chosen, the rest of the processes to form a statistical-dynamical prediction scheme are as follows: First the times series of the dominant spatial patterns of the predictor are regressed on the time series of the predictand by a multiple linear regression scheme in a training period. This regression relationship is used to make forecasts of a predictand in an independent period. For more details of the analysis tools and computing processes, refer to Hendon et al. (2007).

2) Identification of predictable climate components by POAMA

According to Wang and Hendon (2007), about 50% of eastern Australian spring rainfall was explained by the leading three spatial patterns (Empirical Orthogonal Function, EOFs) of tropical Indo-Pacific SST in 1982-2002. Wang and Hendon (2007) emphasized that Australian rainfall is not only sensitive to the leading pattern (EOF1) that represents mature ENSO condition, but also to the second and third EOFs which represent east-west shifts of equatorial east Pacific SST that occur in individual El Niño events. Our investigation with an extended observed data record (1980-2006) demonstrated that the temporal variations of the first 4 EOFs of SST can explain up to 50% of the rainfall variability in the south eastern part of the country (SEACI region, 38.5°-33.5°S, 137.5°-152.5°E; Fig. 1).

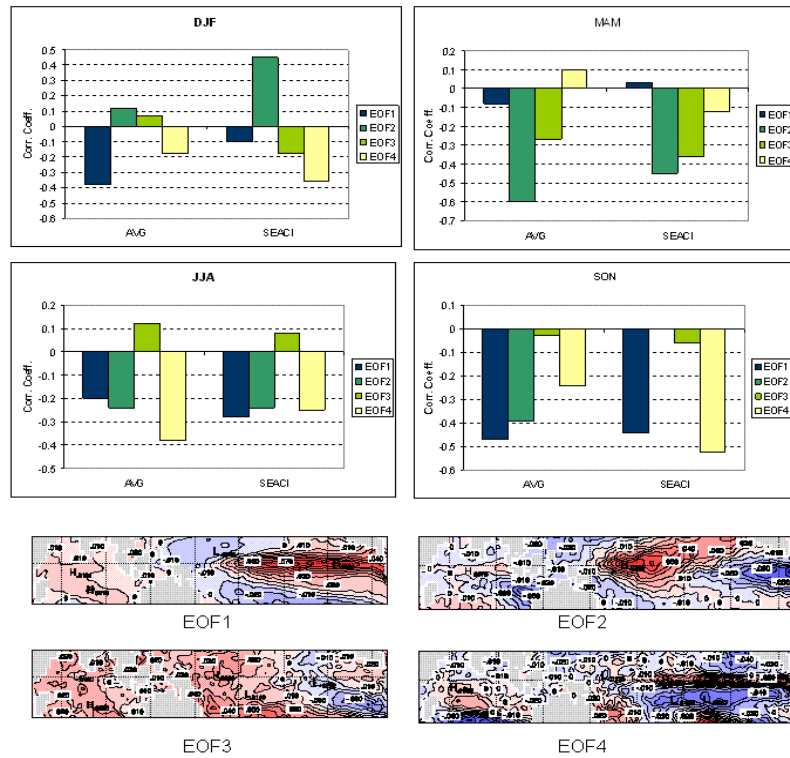


Figure 1: Correlation of observed south eastern Australian rainfall and the time series of the first four leading EOF modes of tropical Indo-Pacific SST variability (histograms). The spatial patterns of the four leading EOF modes of tropical SST are displayed with maps.

Given the observed relationship between the tropical Indo-Pacific SST and Australian rainfall, it is important to address whether POAMA can predict the temporal variations of the leading patterns of tropical SST variability. Our study reveals that the first few EOF time series of SST predicted from POAMA are highly correlated with their observed counterparts with lead times of up to a season (refer to Table A-1 in Appendix for correlation coefficients). POAMA's predictions of the first two dominant modes of SST readily beat persistence in all seasons except for autumn at 3 month lead time. Therefore, POAMA has good skill in predicting not only the occurrence of El Niño/La Niña, but also some of the important variability of SST between ENSO events with lead time of a few months.

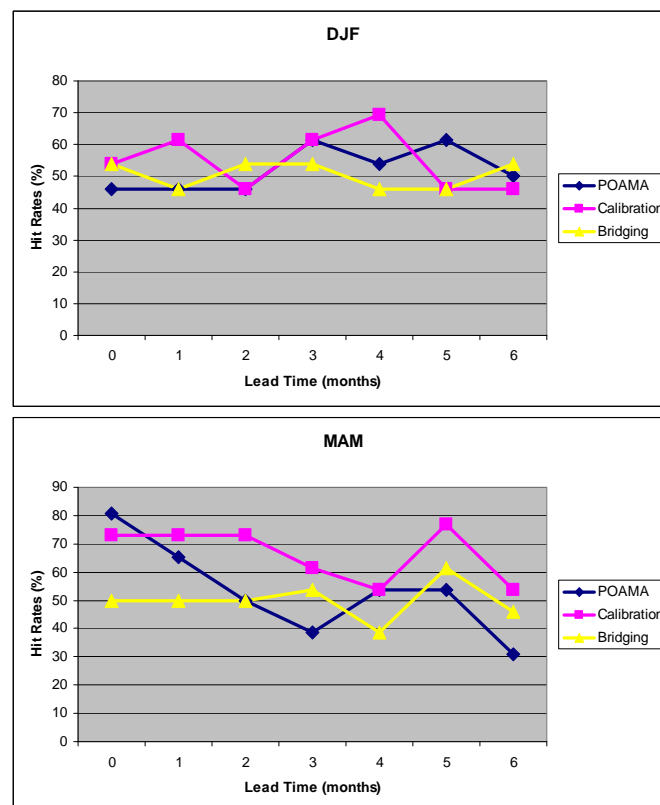
On the other hand, POAMA shows moderate skill in direct prediction of Australian rainfall. The correlation between POAMA's prediction at lead time 0 (lead 0 means, for instance, a forecast for JJA that is initialized on the 1st of June; Lim et al, 2007) and observation for Australian mean rainfall is 0.22, 0.56, 0.39 and 0.48, for summer, autumn, winter, and spring, respectively.

The fact that POAMA is able to predict tropical Indo-Pacific SST variability with good skill and Australian rainfall with moderate skill provides a good base for statistical-dynamical prediction because statistical post-processing itself cannot generate skill: the dynamical model must have skill in predicting some aspects of the climate.

3) Skill assessment of dynamical and statistical-dynamical forecast models

For statistical-dynamical prediction, we regressed the first five SVD mode time series of predicted SST from POAMA onto observed Australian rainfall for statistical bridging. For calibration, we regressed the first five SVD mode time series of predicted rainfall from POAMA onto observed rainfall. The resultant regression relationships were then used in forecast mode by plugging in the respective forecasts of SST or rainfall from POAMA. Because of the short period of hindcasts, we cross-validated the entire processes (leave out a year, develop the relationships, make a forecast for the left out year, and repeat using all years), including recalculation of the SVD modes each iteration.

We measured rainfall prediction skills of dynamical and statistical-dynamical models by hit rates of predicting below/above median rainfall over south eastern Australia (i.e. the percentage of correct forecasts for below/above median rainfall during 26 years in each season). Direct prediction from POAMA shows high skill in autumn and spring rainfall prediction over south eastern Australia but no skill in summer and winter. By contrast, statistical-dynamical schemes results in skilful predictions of south eastern Australia rainfall in summer and winter (Fig. 2). Statistical calibration increases hit rates of prediction of below/above median rainfall in all seasons except for spring, whereas statistical bridging works better in winter than the other two models. As a result, statistical post-processing results in local improvement of skill for the SEACI region. However, it might be achieved at the expense of skill in other areas (see Figure A-1 in Appendix for detailed geographical features of prediction skill).



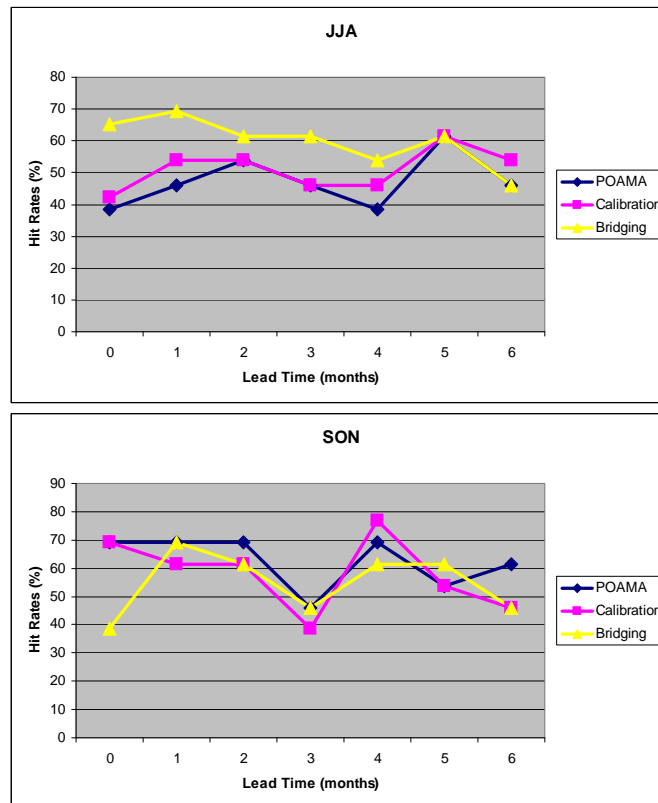


Figure 2: Hit rates (%) of predicting below/above median rainfall averaged over south eastern Australia (SEACI region, 38.5°-33.5°S, 137.5°-152.5°E).

Summary of methods and modifications (with reasons)

- Review literature and practises at other national centres
- Identify the predictable components of the climate system, such as sea surface temperatures (SSTs) in the Nino3 region (150° W to 90° W, 5° S to 5° N), with POAMA hindcasts that can be exploited to improve the prediction of climate variability in south-eastern Australia
- Investigate some simple statistical schemes that exploit the most predictable components of climate in POAMA (e.g., Nino3 SST)

Summary of links to other projects

This project has exploited findings from project 3.1.3 concerning the drivers of climate variability in SE Australia. The results here will feed into 3.1.4 and 3.2.2, where a more comprehensive analysis of climate predictions for SE Australia will be developed and evaluated.

Publications/reports arising from this project

Lim, E.-P. and H. H. Hendon 2007: Dynamical seasonal prediction of tropical Indo-Pacific SST and Australian cool season rainfall (in preparation)

Lim, E.-P. and H. H. Hendon 2007: Seasonal forecasts of Australian rainfall with statistical-dynamical methods (in preparation)

Hendon, H.H., E. Lim, O. Alves, and G. Wang, 2007: *Review of techniques to bridge/calibrate dynamical seasonal predictions with focus on south eastern Australia*. SEACI Technical Report, Milestone 3.2.2.

Lim, E., H.H. Hendon and O. Alves 2007: *Seasonal forecast of the tropical Indo-Pacific SST and Australian rainfall*. SEACI Technical Report, Milestone 3.2.2.

Acknowledgement

This research was supported by the South East Australian Climate Initiative

Recommendations for changes to work plan from your original table

None

References

Alves, O., G.Wang, A. Zhong, M. Smith, F. Tzeitkin, G. Warren, A. Schiller, S. Godfrey, and G. Meyers, 2003: POAMA: Bureau of Meteorology operational coupled model seasonal forecast system. *Science for drought - Proceedings of the National Drought Forum*. Queensland Government, Brisbane.

Bretherton, C. S., C. Smith., and J. M. Wallace, 1992: An intercomparison of methods for finding coupled patterns in climate data. *J. Climate*, **5**, 541–560.

Drosowsky, W. and L. Chambers, 2001: Near-global sea surface temperature anomalies as predictors of Australian seasonal rainfall. *J. Climate*, **14**, 1677–1687.

Feddersen, H., A. Navarra, and M. N. Ward, 1999: Reduction of model systematic error by statistical correction for dynamical seasonal predictions. *J. Climate*, **12**, 1974–1989.

Hendon, H.H., E. Lim, O. Alves, and G. Wang, 2007: *Review of techniques to bridge/calibrate dynamical seasonal predictions with focus on south eastern Australia*. SEACI Technical Report, Milestone 3.2.2.

Jones, D. A. and G. Weymouth, 1997: *An Australian monthly rainfall dataset*. Technical Report 70, Bureau of Meteorology.

Lim, E., H.H. Hendon and O. Alves 2007: *Seasonal forecast of the tropical Indo-Pacific SST and Australian rainfall*. SEACI Technical Report, Milestone 3.2.2.

McBride, J. L. and N. Nicholls, 1983: Seasonal relationships between Australian rainfall and the Southern Oscillation. *Mon. Wea. Rev.*, **111**, 1998–2004.

Nicholls, N., 1989: Sea surface temperatures and Australian winter rainfall. *J. Climate*, **2**, 965–973.

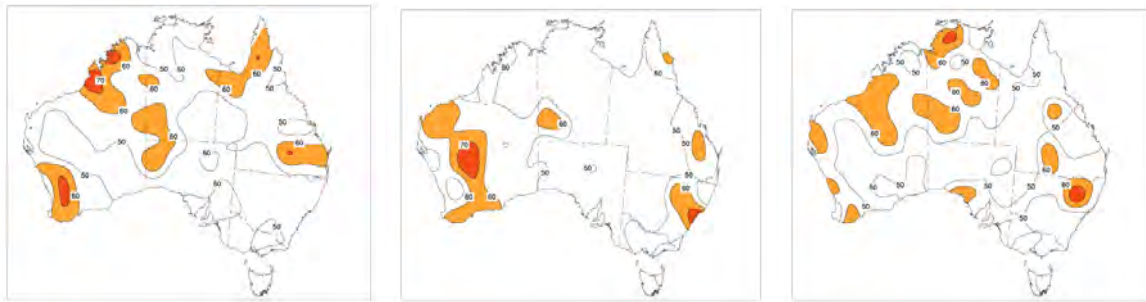
Wang, G., and H.H. Hendon, 2007: Sensitivity of Australian rainfall to inter-El Niño variations. *J. Climate*, **20**, 4211–4226.

Ward, M. N. and A. Navarra, 1997: Pattern analysis of SST-forced variability in ensemble GCM simulations: Examples over Europe and the tropical Pacific. *J. Climate*, **10**, 2210–2220.

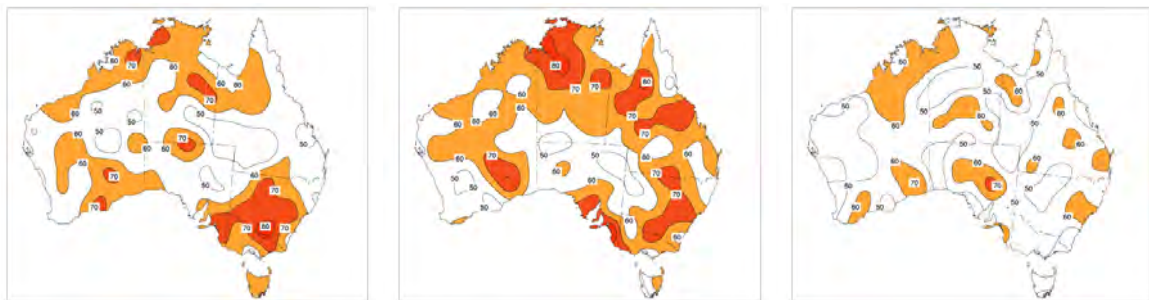
Project Milestone Reporting Table

To be completed prior to commencing the project				Completed at each Milestone date	
Milestone description ¹	Performance indicators ²	Completion date ³	Budget ⁴ for Milestone (\$)	Progress ⁵	Recommended changes to workplan ⁶
1. Review literature on statistical/dynamical prediction and investigate practises at other national centres	Report prepared	December 2006	25K	A technical report on literature review has been completed	None
2. Identify predictable modes of climate variability that can be used to bridge to rainfall and temperature in SE Australia in POAMA hindcasts	Report prepared (as part of Technical report for milestone 3)	March 2007	25K	Sensitivity of rainfall to inter-El Niño SST variations has been diagnosed (paper prepared). POAMA's ability to forecast inter-El Niño SST variations and SE Australian climate has been assessed.	None
3. Investigate some simple statistical schemes that exploit the most predictable components of climate with POAMA	BMRC Technical Report prepared	June 2007	11K	Trial combinations of predictors and predictands have been tested for statistical post-processing.	None

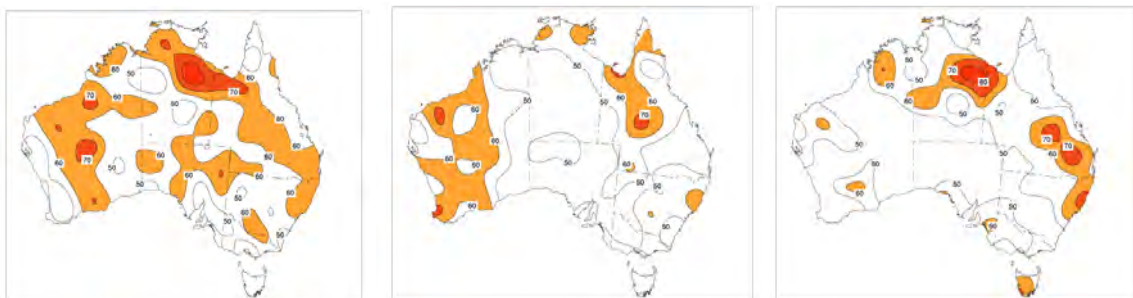
Appendix A



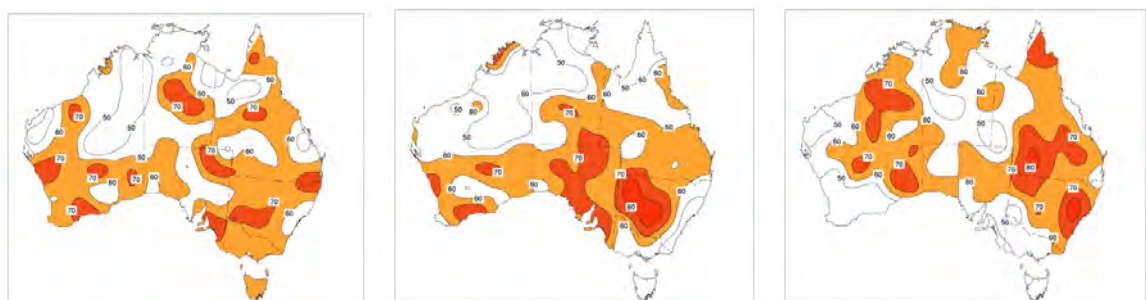
(a) DJF



(b) MAM



(c) JJA



(d) SON

Figure A-1: Hit rates (%) of below/above median rainfall prediction directly from POAMA (left panels), from a statistical calibration scheme (middle panels), and from a statistical bridging scheme (right panels) at lead time 0 month. The contour interval is 10%, and the hit rates greater than 60% are coloured.

Table A-1: Correlation of observed SST EOF time series with the corresponding POAMA SST EOF time series (their spatial domain is the same as shown in Figure 1). Bold numbers are the correlation coefficients statistically significant at the 95% confidence level. (i.e.- coefficients greater than 0.38 are regarded as being statistically significant, given 26 years of sample size).

(a) At lead time 0

correlation		EOF1	EOF2	EOF3	EOF4
DJF	POAMA	0.95	0.88	0.78	0.70
	Persistence	0.98	0.91	0.84	0.76
MAM	POAMA	0.91	0.92	0.81	0.69
	Persistence	0.90	0.90	0.88	0.42
JJA	POAMA	0.90	0.83	0.74	0.65
	Persistence	0.83	0.88	0.89	0.35
SON	POAMA	0.96	0.87	0.54	0.21
	Persistence	0.88	0.82	0.84	0.37

(b) At lead time 3 months

correlation		EOF1	EOF2	EOF3	EOF4
DJF	POAMA	0.88	0.66	0.67	0.50
	Persistence	0.78	0.58	0.62	0.16
MAM	POAMA	0.75	0.73	0.55	0.18
	Persistence	0.80	0.86	0.64	0.29
JJA	POAMA	0.67	0.80	0.54	0.54
	Persistence	0.44	0.69	0.59	0.02
SON	POAMA	0.73	0.76	0.44	0.19
	Persistence	0.40	0.58	0.75	0.06

SEACI publications

The following publications have arisen from work undertaken in the South-Eastern Australian Climate Initiative:





External Publications





Author(s)	Year	Title	Publication	Status	SEACI approval	Location (website)
1. Alory, Wijffels and Meyers Milestone 1.2.1	2007	Observed temperature trends in the Indian Ocean over 1960–1999 and associated mechanisms	<i>Geophysical Research Letters</i> , 34 , L02606, doi:10.1029/2006GL028044	published	No record	
2. Alory, and Meyer Milestone 1.2.1	2007	Warming of the Upper Equatorial Indian Ocean and Changes in the Heat budget (1960-2000)	<i>Journal of Climate</i> .	Draft	With working group and Les Roberts for approval	
3. Chiew Milestone 2.2.1	2007	An overview of methods for estimating climate change impact on runoff	<i>Proceedings of 30th Hydrology and Water Resources Symposium, 4-7 December 2006, Launceston, Tasmania</i>	published	Minute to Wendy seeking approval following working group approval - can't find copy of letter to CSIRO	
4. Hendon, Thompson & Wheeler Milestone	2006	Australian rainfall and surface temperature variations	<i>Journal of Climate</i> .	submitted	Working Group approval for SEACI acknowledgement 11/10/06 – referred to	

3.1.3		associated with the Southern Hemisphere annular mode			Steering Committee but no record of having been considered	
5. Meyers, McIntosh, Pigot and Pook Milestone 1.2.1	2007	The years of El Niño, La Niña and Interactions with the Tropical Indian ocean	<i>Journal of Climate.</i>	submitted	No record	
6. Murphy and Timbal Milestone 1.1.1	2007	A review of recent climate variability and climate change in south eastern Australia.	<i>International Journal of Climate</i>	submitted	Paper is on MDBC folder – can't find whether it was considered	
7. Timbal and Jones Milestone 1.1.2	2007	Future projections of winter rainfall in Southeast Australia using a statistical downscaling technique	<i>Climatic Change</i>	submitted	No record	
8. Timbal & Murphy Milestone 1.1.1	2007	Observed climate change in South-East of Australia and its relation to large-scale modes of variability	<i>International Journal of Climatology</i>	submitted	Minute on MDBC system – not sure if Letter on system dated 5 April 2007	
9. Timbal & Murphy Milestone	2007	Observed climate change in South-East of Australia	<i>BMRC Research Letters</i>	in press	Letter on system dated 5 April 2007	

1.1.1		and its relation to large-scale modes of variability				
10. Rakich, Holbrook and Timbal Milestone 1.1.2	2007	An index to capture moisture transport over eastern Australia	<i>Geophysical Research Letter</i>	submitted	Signed approval on MDBC system	
11. Wang and Hendon Milestone 3.1.3	2006	Sensitivity of Australian Rainfall to Inter-El Niño Variations	<i>Journal of Climate</i>	Submitted	Letter to Paul Holper (unsigned on system) approving 8 Feb 07	
12. Watterso n, McGregor, Nguyen Milestone 2.1.5a	2007	Changes in Extreme Temperatures of Australian Summer Simulated by CCAM, and the Roles of Winds and Land-sea Contrasts	<i>Australia Meteorologic al Magazine</i>	Submitted	Signed approval on MDBC system	

Technical reports


Author(s)	Year	Title	Publication	Status	SEACI approval	File
1. Campbell, E. Milestone 1.5.5		Hierarchical Frameworks for physical – statistical climate models	<i>SEACI technical report milestone 1.5.5</i>		Include in Jan-June 2007 milestone report	 1.5.5 Technical Report_07_18.doc
2. Hendon , Lim Liu, Alves and Wang Milestone 3.1.3	2007	Assessment of simulation by POAMA of modes of climate variability that drives rainfall in SE Australia	<i>SEACI technical Report – Milestone 3.1.3</i>		Include in Jan-June 2007 milestone report	 Report.3.1.3.drivers .hhh.pdf
3. Hendon, Liu, Alves and Wang Milestone 3.1.3		Assessment of potential predictability of seasonal climate in SE Australia using the Bureau of Meteorology's seasonal forecasting system	<i>SEACI technical Report – Milestone 3.1.3</i>		Include in Jan-June 2007 milestone report	 Report.3.1.3.predict ability.hhh.pdf
4. Hendon, Lim , Alves and Wang Milestone	2007	Review of techniques to bridge/calibrate dynamical	<i>SEACI technical Report – Milestone</i>		Include in Jan-June 2007 milestone report	 seaci_report.3.2.2.pdf

3.2.2		seasonal predictions with focus on SE Australia	3.2.2			
5. Lim, Hendon and Alves Milestone 3.2.2	2007	Seasonal forecast of the tropical Indo-Pacific SST and Australian Rainfall	<i>SEACI technical Report – Milestone 3.2.2</i>		Include in Jan-June 2007 milestone report	 MilestoneReport_3.2 .2.reduce.pdf
6. Pook M., J. Dunn, J. Risbey, P. McIntosh and M. Marzloff Milestone 2.1.5a	2006	The Application of an Automatic Synoptic System Identification Algorithm to CSIRO Mark 3 Climate Model Output	<i>SEACI technical Report – Milestone 2.1.5</i>			 D:\My Documents\ Work\Projects\SE.
7. Watterson, I. G Milestone 2.1.5a	2006	Surface hydrology fields simulated by the IPCC multi-model data set	<i>SEACI technical Report – Milestone 2.1.5</i>			 D:\My Documents\ Work\Projects\SE.
8. Watterson, I. G. Milestone 2.1.5a	2006	Probabilistic Climate Change Projections for South East Australia: Surface Warming Examples	<i>SEACI technical Report – Milestone 2.1.5</i>			 D:\My Documents\ Work\Projects\SE.

9. Watterson, I. G. Milestone 2.1.5a	2005	Annular modes in Mk3, and their influence on Australian rainfall and temperatures, in comparison with ENSO	<i>SEACI technical Report – Milestone 2.1.5a</i>			
--------------------------------------	------	--	--	--	--	--

SEACI presentations

Presenter (s)	Year	Title	Conference name	location	SEACI approval	File
1. Bryson Bates		Climate change and Australia's water resources	<i>Greenhouse 2007</i>	http://www.greenhouse2007.com/	Yes – end Sept 07	
2. Bertrand Timbal	2007	Observed climate change in the south-east of Australia: detection and possible attribution	<i>Greenhouse 2007</i>	http://www.greenhouse2007.com/	Yes – end Sept 07	
3. John McGregor	2007	High-resolution dynamical downscaling over Eastern Australia	<i>Greenhouse 2007</i>	http://www.greenhouse2007.com/	Yes – end Sept 07	
4. Freddie Mpelasoka	2007	Runoff projections from different	<i>Greenhouse 2007</i>	http://www.greenhouse2007.com/	Yes – end Sept 07	

		methods of GCM-based climatic scenarios (SEACI)				
5. Ian Smith	2007		<i>Hydrology Symposium</i>			 canberra_2007_2.ppt